Doctoral Thesis

The intrinsic role of CD8α^{-} dendritic cell subset in the initiation of effective humoral immunity

Changsik Shin

Department of Biological Sciences

(Immunology)

Graduate School of UNIST

2016

The intrinsic role of CD8α⁻ dendritic cell subset in the initiation of effective humoral immunity

Changsik Shin

Department of Biological Sciences

(Immunology)

Graduate School of UNIST

The intrinsic role of CD8α$^-$ dendritic cell subset in the initiation of effective humoral immunity

A thesis/dissertation
submitted to the Graduate School of UNIST
in partial fulfillment of the
requirements for the degree of
Doctor of Philosophy

Changsik Shin

12. 16. 2015 of submission

Approved by

Advisor
Yoon-Kyoung Cho

The intrinsic role of CD8α$^-$ dendritic cell subset in the initiation of effective humoral immunity

Changsik Shin

This certifies that the thesis/dissertation of Changsik Shin
is approved.

12. 16. 2015 of submission

Advisor: Yoon-Kyoung Cho

Seongho Ryu

Sebyung Kang

Byoung Heon Kang

Myunggon Ko

Abstract

Dendritic cells (DCs), the most potent antigen presenting cells, have been identified in 1973 by Ralph M. Steinman. DCs. DCs role as an immune initiator as well as regulator, have been intensively studied for their crucial function in regulating cellular and humoral immune responses. Efficiency of human vaccines is mostly dependent on the generation of proper humoral immunity, and recently T follicular helper (Tfh) cells have been identified as a true B cell helper, which significantly advanced our understanding of T cell-dependent B cell humoral immune responses. However, there are still little studies regarding the initial commitment of Tfh cells primed by DCs, particularly by the two major myeloid $CD8\alpha^+$ and $CD8\alpha^-$ DC subsets. In this study, we present the undescribed intrinsic features and roles of the two DC subsets in the induction of Tfh cells and subsequent Tfh cell dependent humoral immune responses. We here demonstrate that the $CD8\alpha^-$ DC subset critically roles in inducing antigen-specific Tfh cells by up-regulated expressions of *Icosl* and *Ox40l* via the non-canonical NF-κB signaling pathway. $CD8\alpha^-$ DCs are able to induce functional Tfh cells regardless of an adjuvant type. Tfh cells initially primed by $CD8\alpha^-$ DCs function as a true B cell helper that results in dramatically enhanced humoral immune responses against various human pathogenic antigens such as *Yersinia pestis* LcrV, HIV Gag, and Hepatitis B surface antigen. In addition, we showed that the localization of $CD8\alpha^-$ DCs in the marginal zone (MZ) bridging channels is closely related to the induction of $CXCR5^+CCR7^{low}$ Tfh cells. We also demonstrated that the major source of IL-6 for inducing Tfh cells is provided from the antigen specifically activated $CD4^+$ T cells primed by $CD8\alpha^-$ DCs, and those secreted by the DC subset seem have a minor role. Moreover, $CD8\alpha^-$ DCs were superior in inducing functional Tfh cells over other antigen presenting cells majorly B cells. In contrast, $CD8\alpha^+$ DCs localized in the T cell enriched region are superior in inducing $CXCR5^{low}CCR7^{high}$ $CD4^+$ T cells responsible for the generation of IFN-γ secreting Th1 cells. Taken together, this study reveals the undescribed intrinsic features and mechanistic role of the $CD8\alpha^-$ DC subset in priming antigen-specific Tfh cell differentiation and thereby provides the potential of investigating $CD8\alpha^-$ DCs to effectively evoke antigen-specific humoral immune responses through the improved therapeutic vaccines.

Table of Contents

List of figures

Abbreviations

APC: antigen presenting cell
ASC: antibody secreting cell
CFSE: Carboxyfluorescein succinimidyl ester
DC: dendritic cell
DCIR2: dendritic cell immunoreceptor
FACS: fluorescence-activated cell sorting
GC: germinal center
HBsAg: hepatitis B surface antigen
HIV: human immunodeficiency virus
i.v.: intravenously
i.p.: intraperitoneally
LPS: lipopolysaccharides
mAb: monoclonal antibody
MACS: magnetic-activated cell sorting
MZ: marginal zone
MHC: major histocompatibility complex
OVA: ovalbumin
OT: ovalbumin-specific transgenic
***P*:** phosphorylation
Poly (I:C): polyinosinic-polycytidylic acid
T: total
Tfh: T follicular helper
Treg: T regulatory
TLR: toll-like receptor
Y. pestis : *Yersinia pestis*
WB: western blot

Chapter 1. Introduction

1.1. Dendritic Cells

1.1.1. History of dendritic cells

The morphology of dendritic cells was initially observed by Paul Langerhans, thus it was initially named as Langerhans cells in the late 19th century. The term dendritic cells was firstly introduced in 1973 by Ralph M. Steinman, who discovered the fundamental and crucial role of DCs in regulating innate and adoptive immune responses and DCs became placed at the center for the control of the complex immune system (Steinman and Cohn, 1973, Banchereau and Steinman, 1998). With his great contributions to the field of dendritic cell specially in its role in inducing adaptive immune responses, he received Albert Lasker Award for Basic Medical Research in 2007 and the Nobel Prize in Physiology or Medicine in 2011.

1.1.2. Dendritic cells role as an immune initiator

Dendritic cells (DCs) have been known as the most potent antigen presenting cells (APCs). Immature DCs uptake foreign antigens in the periphery, process the antigens and then present them in the form of peptide loaded major histocompatibility complex (MHC) on their surface. The antigen-bearing DCs then migrate to secondary lymphoid organs to induce antigen-specific T cell activation, cytotoxic $CD8^+$ or $CD4^+$ helper T cells. These antigen specifically educated T cells then go to the infected areas for pathogen clearance. Therefore, DCs play an important role in the induction of antigen-specific immune responses and thus they are known as an immune initiator (Banchereau and Steinman, 1998) (**Figure 1-1**). DCs do not selectively uptake foreign antigens, which means they uptake self or harmless antigens as well. But they only induce immune stimulatory responses against foreign antigens, and for harmless or self-antigens, they provide immune suppression responses. This phenomenon can be explained by DC maturation process. Foreign antigens but not self or harmless antigens provide DC maturation signal so that immature DCs become matured DCs, ready to educate antigen specific adaptive immune responses. They highly express MHC I and II, co-stimulatory molecules, and produce various cytokines leading to immune stimulation (Banchereau and Steinman, 1998) (**Figure 1-2**). In addition, DCs express toll-like receptors (TLRs) to recognize a variety of microorganism-derived molecular structures to efficiently initiate antigen specific immune responses as an immune initiator (Kaisho and Akira, 2003).

1.1.3. Dendritic cell migration

DCs are nearly located throughout the body to efficiently induce immune responses against harmful pathogens. Immature DCs function as a sentinel randomly walking around in the body to encounter various antigens. The mobility and directionality of immature DCs is reported to be regulated by the concentration of myosin enriched at the rear or front of the DCs (Solanes et al., 2015, Chabaud et al., 2015). Once immature encounter pathogenic antigens, they become matured and foreign antigen loaded mature DCs highly express CCR7 to migrate toward its corresponding chemokine, CCL19 or CCL21, secreted from secondary lymphoid organs where antigen specific T cells are educated by the mature DCs (**Figure 1-3**) (Banchereau and Steinman, 1998, Cyster, 1999, Steinman and Banchereau, 2007, Palucka and Banchereau, 2012). Regarding CCR7 dependent signaling pathways of DC migration, two independent pathways have been reported. Upon CCL19/21 stimulation, DC enhances its directionality via the JNK-c-Jun pathway, and/or its velocity via Rho-associated protein kinases (Iijima et al., 2005, Riol-Blanco et al., 2005).

1.1.4. Dendritic cells as an immune regulator

DCs are important not only to initiate but also to regulate immune responses. During antigen presentation by DCs, naive $CD4^+$ T cells are antigen specifically educated and differentiated into several functional T cell subsets, and each T cell subset induces distinct immune responses (Deenick et al., 2011). For example, IL-12 produced by DCs differentiates naïve $CD4^+$ T cells into IFN- γ producing Th1 cells and they are important for anti-viral infection, and TGF-β is responsible for inducing the regulatory T cells (Treg), important for immune regulation (**Figure 1-4**). Currently, secretory cytokines are known to often determine the fate of various effector $CD4^+$ T cell subsets (Ottenhoff, 2012), however, besides these key cytokines, other factors such as antigen affinity, duration period and co-stimulatory molecules are also considered to be significantly involved in the differentiation of $CD4^+$ helper T cell subsets.

1.1.5. Myeloid dendritic cell subsets

Among the various DC subsets characterized (Shortman and Liu, 2002), two major myeloid/conventional DC subsets in the secondary lymphoid organs are well-defined based on the expression of CD8α and their anatomic locations. $CD8\alpha^+$ DCs express the endocytic receptor, DEC-205, on their surface and are located in the T cell enrich zone within the lymphoid organs. They are known to be specialized in up-taking dying cells (Iyoda et al., 2002) and cross-presentation of non-replicating antigens, leading to cytotoxic $CD8^+$ T cell priming (den Haan et al., 2000). In contrast, $CD8\alpha^-$ DCs, known to specialize in MHC class II presentation (Dudziak et al., 2007), express a distinct uptake receptor, DCIR2, on their surface and they

are enriched in the bridging regions of the marginal zone or interfollicular zone (**Figure 1-5** and **Figure 1-6**) (Iyoda et al., 2002, Dudziak et al., 2007). These two DC subsets can be isolated and they are $CD3^{-}B220^{-}CD11c^{+}CD8\alpha^{+}$ and $CD3^{-}B220^{-}CD11c^{+}CD8\alpha^{-}$ DCs

1.1.6. Dendritic cell subset targeting

Delivering antigens to the distinct DC subset was successfully achieved by utilizing DC targeting strategy. DC targeting strategy by harnessing monoclonal antibodies (mAbs) (Swiggard et al., 1995, Nussenzweig et al., 1982) against endocytic receptors such as DEC-205 and DCIR2 expressed on the two DC subsets enriched our understanding of the functions of these DC subsets in inducing immune responses *in vivo*. Moreover, such targeting antibodies genetically conjugated with various pathogenic antigens have been validated in various disease models to improve vaccine efficacy and to develop novel therapeutics (Trumpfheller et al., 2012, Do et al., 2010).

1.2. T follicular helper cells

1.2.1. Function of T follicular helper cells

T follicular helper (Tfh) cell was firstly observed in human tonsil in 2000 (Breitfeld et al., 2000, Schaerli et al., 2000). Tfh cells, identified as a true B cell helper, express CXCR5 highly, which help them to migrate into the germinal center where they help B cells to differentiate into plasma cells or memory B cells via cytokine or co-stimulation interaction (**Figure 1-7**) (Ma et al., 2012). Then, these B cells would serve for clearance of foreign pathogens and the establishment of long-term humoral immunity. Previous reports demonstrated Tfh cells are closely associated with humoral immunity related diseases such as autoimmunity, humoral immunodeficiency, and T cell lymphomas (Tangye et al., 2013). For example, one previous study showed the enhanced number of human immunodeficiency virus (HIV) -specific Tfh cells in chronic HIV-infected individuals, indicating the significance of Tfh cells responsible for the increased IgG titers seen in these patients (Lindqvist et al., 2012). It has been reported that the Tfh cell development initiates in the inter-follicular region/marginal zone (MZ) bridging channels (Kerfoot et al., 2011), however how Tfh cell differentiation is initially driven is not clearly understood.

1.2.2. Characteristics of T follicular helper cells

Distinct features of Tfh cells have been reported with high expressions of surface markers such as CXCR5, ICOS, PD1, SAP, OX40, low expression of CCR7, key cytokines such as IL-4, IL-6, IL-10, IL-

21, and major transcription factors Bcl-6 and c-Maf, to be distinguished from other effector $CD4^+$ T cells (**Figure 1-7** and **Figure 1-8**) (Reinhardt et al., 2009, King, 2009, Crotty, 2011, Ma et al., 2012). Mutations in CD40L, ICOS, or SH2D1A (SAP) proteins in humans exhibited the reduced frequency of circulating $CD4^+CXCR5^+$ T cells in peripheral blood (Bossaller et al., 2006), and impaired Tfh-like function in X-linked lymphoproliferative patients have been reported to be associated the reduced level of IL-10 secretion from $CD4^+$ T cells (Bossaller et al., 2006, Ma et al., 2005).

1.2.3. Induction of T follicular helper cells

The role of cognate B cells in the induction of Tfh cells was initially validated by several studies. Deficiency of both B cells and various B cell functional molecules, such as CD19, CD40, MHC class II and ICOSL, resulted in the decreased number of Tfh cells (Haynes et al., 2007, Johnston et al., 2009, Akiba et al., 2005, Deenick et al., 2010). In contrast, it has been demonstrated that continuous antigen presentation was sufficient to induce Tfh cell differentiation in B cell-deficient mice (Deenick et al., 2010) suggesting that other antigen-presenting cells (APCs) are essentially involved in Tfh cell differentiation. Moreover, a number of independent studies demonstrated that the induction of Tfh cells arise soon after priming by DCs (Vinuesa and Cyster, 2011, Baumjohann et al., 2011, Goenka et al., 2011, Choi et al., 2011), and thus it appears that cognate B cells are generally required for maintaining Tfh cells, while DCs are necessary to prime naïve $CD4^+$ T cells to differentiate into Tfh cells, especially at the early stage of Bcl6 up-regulation. However, detail mechanisms in the initial differentiation of Tfh cells by DCs were largely unknown. Particularly, the role of the two myeloid/conventional DC subsets in the induction of Tfh cells has not been studied.

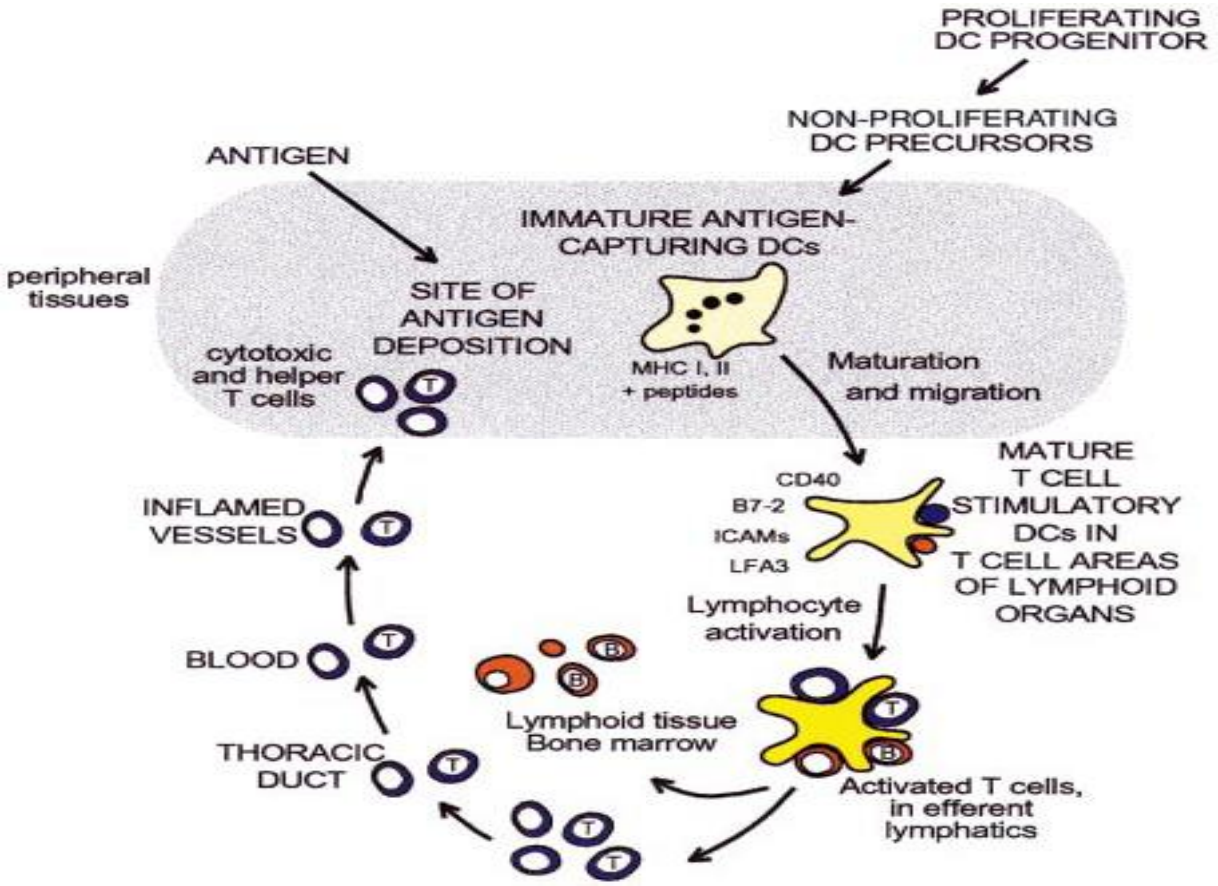

Nature. Rev (1998). 392, 245-252.

Figure 1-1. The migratory role of dendritic cells in inducing adaptive immune responses (Banchereau and Steinman, 1998)

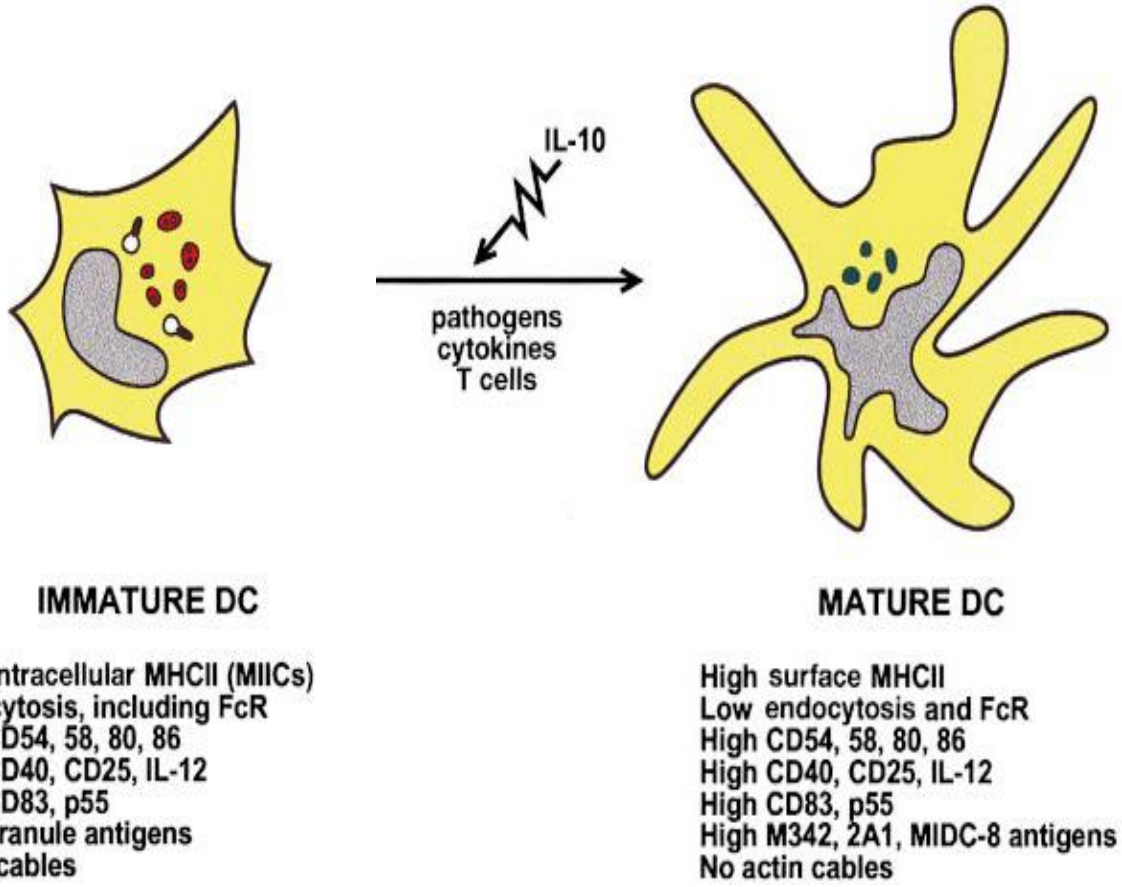

Nature. Rev (1998). 392, 245-252.

Figure 1-2. The features of immature and mature DCs (Banchereau and Steinman, 1998)

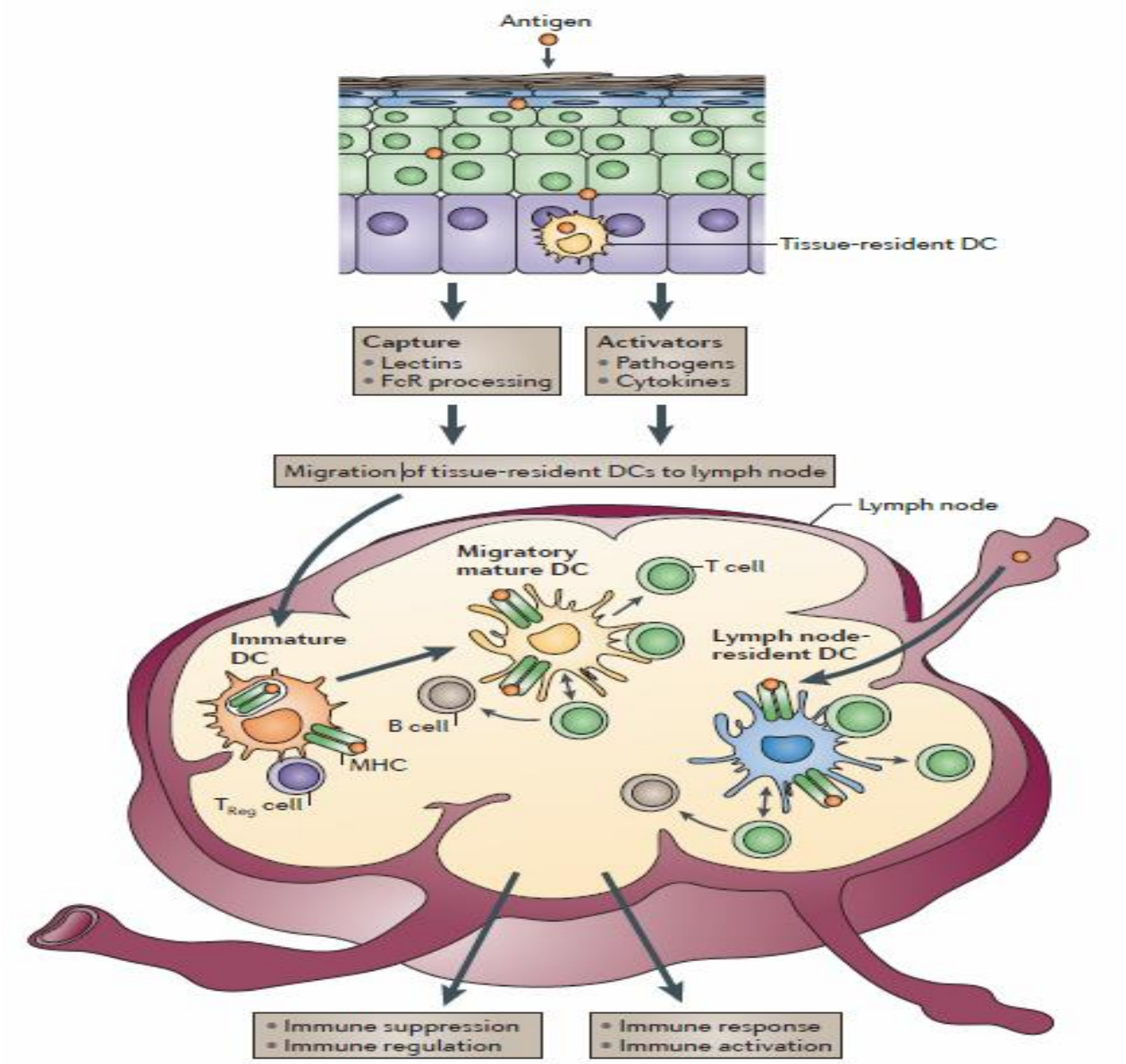

Nature reviews (2012). 12, 265–277

Figure 1-3. Antigen specific T cells are induced by migratory mature DCs (Palucka and Banchereau, 2012)

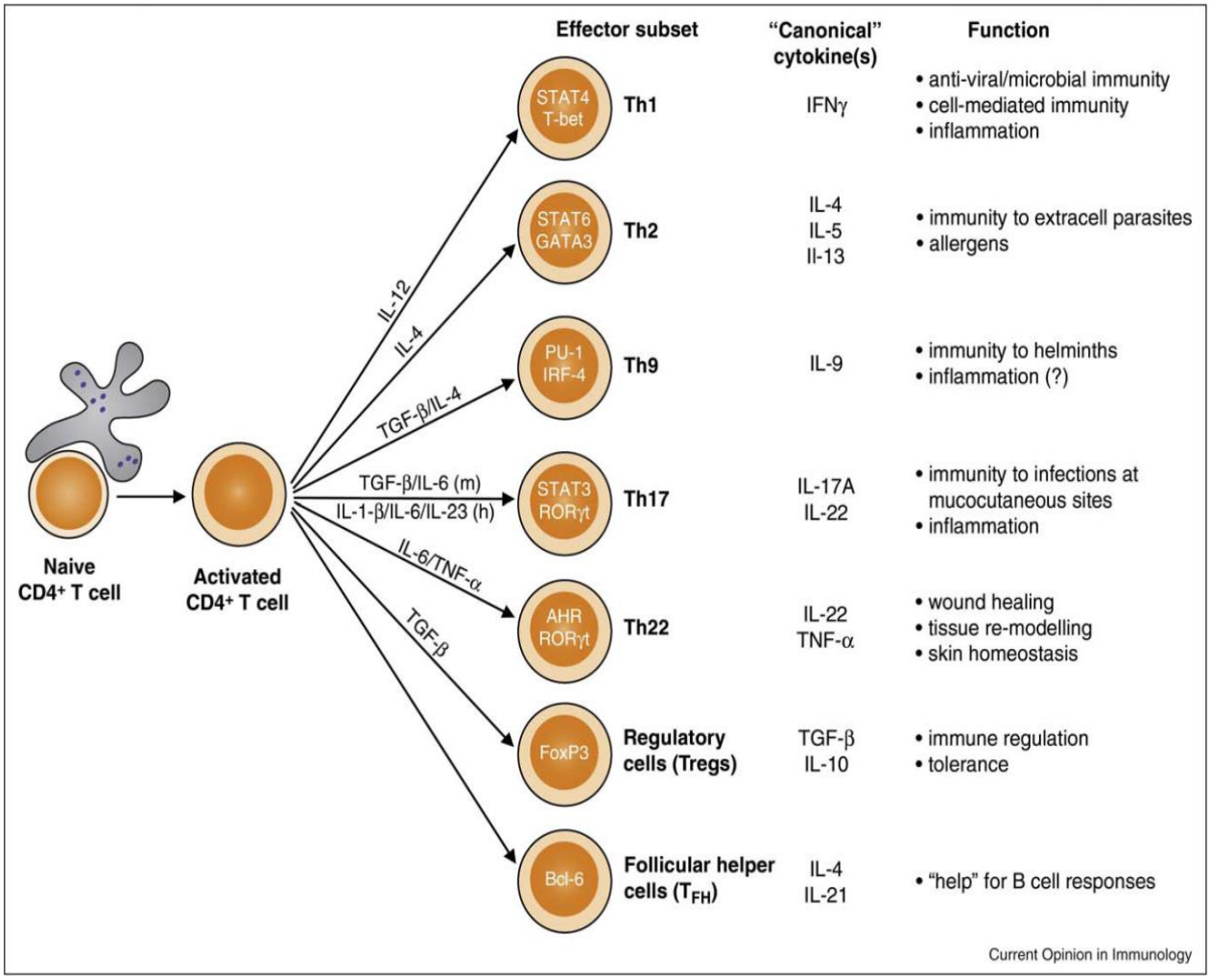

Curr Opin Immunol (2011). 23, 111-118

Figure 1-4. Dendritic cells induce distinct $CD4^+$ T cell subsets (Deenick et al., 2011)

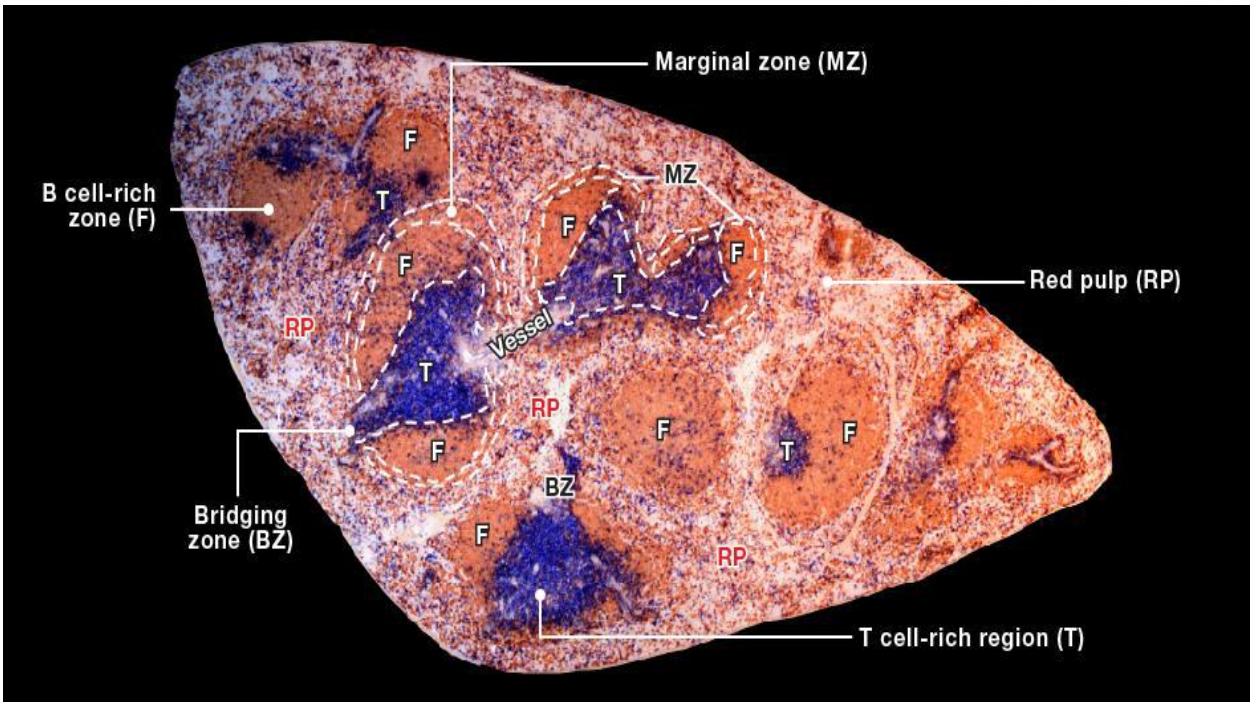

http://www.cell.com/immunity/image-resource-spleen

Figure 1-5. Anatomy of the spleen

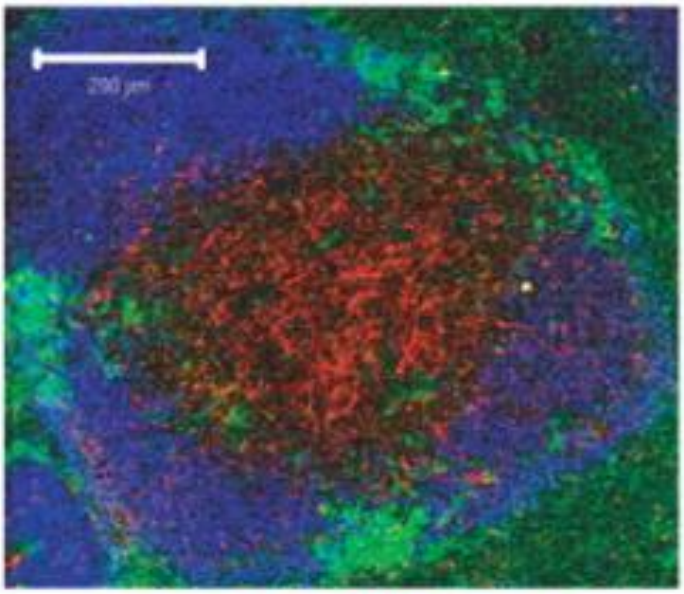

Science (2007). 315, 107-111

Figure 1-6. The locations of myeloid DC subsets in the spleen (Dudziak et al., 2007)

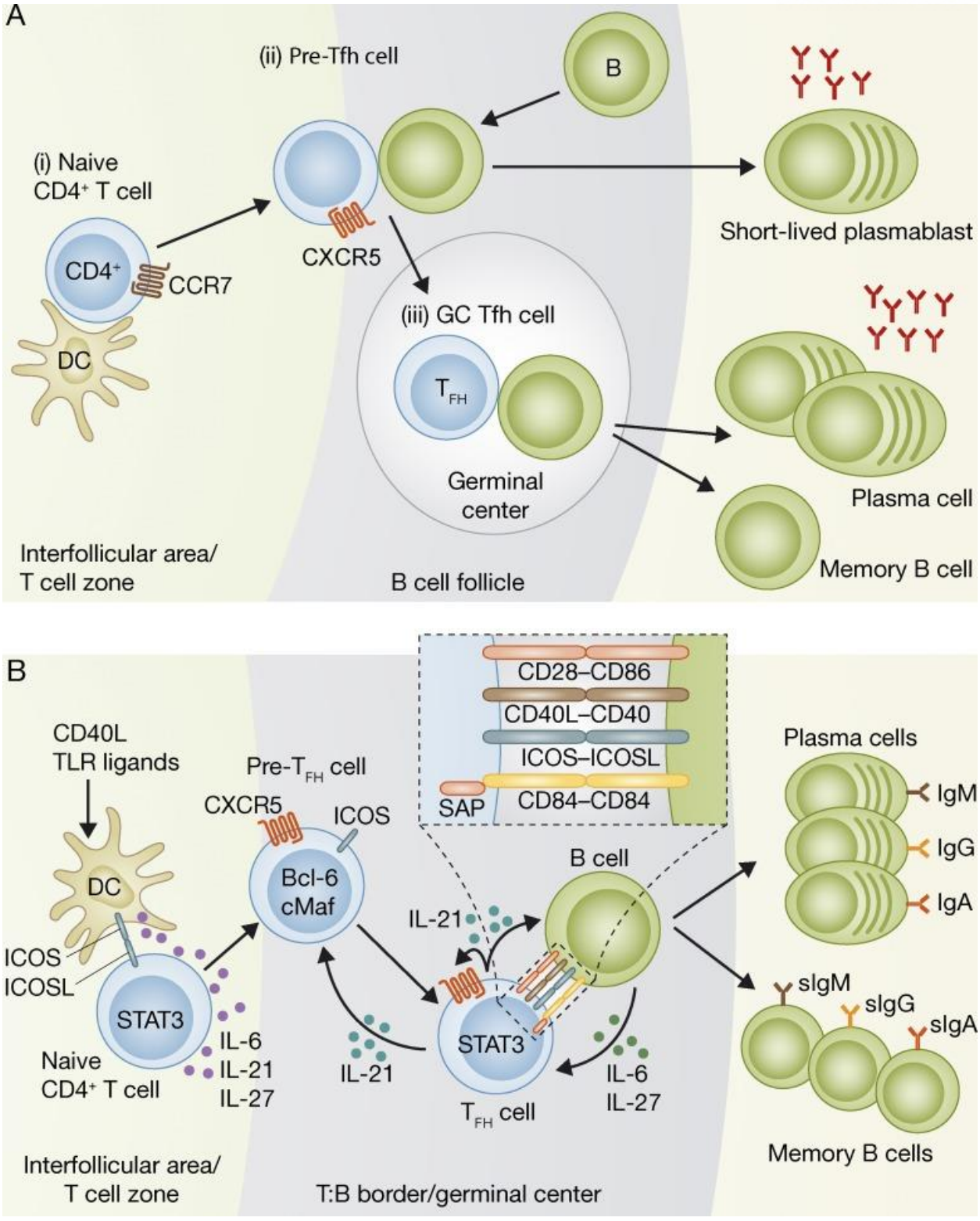

Figure 1-7. Induction of Tfh cells and their function (Ma et al., 2012)

JeM. (2012). 7, 1241-1253

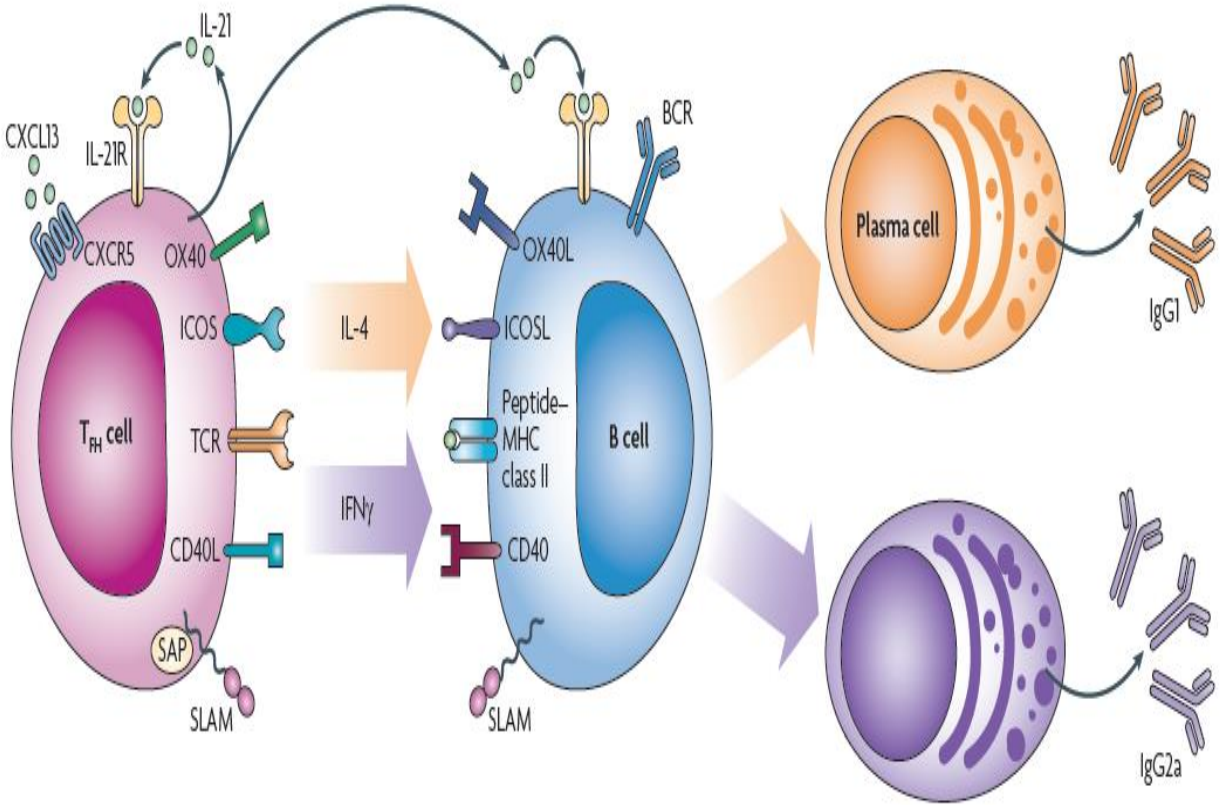

Nature Rev. (2009). 9, 757-766

Figure 1-8. The function of Tfh cells as a true B cell helper (King, 2009)

References

AKIBA, H., TAKEDA, K., KOJIMA, Y., USUI, Y., HARADA, N., YAMAZAKI, T., MA, J., TEZUKA, K., YAGITA, H. & OKUMURA, K. 2005. The role of ICOS in the CXCR5+ follicular B helper T cell maintenance in vivo. *J Immunol,* 175**,** 2340-8.

BANCHEREAU, J. & STEINMAN, R. M. 1998. Dendritic cells and the control of immunity. *Nature,* 392**,** 245-52.

BAUMJOHANN, D., OKADA, T. & ANSEL, K. M. 2011. Cutting Edge: Distinct waves of BCL6 expression during T follicular helper cell development. *J Immunol,* 187**,** 2089-92.

BOSSALLER, L., BURGER, J., DRAEGER, R., GRIMBACHER, B., KNOTH, R., PLEBANI, A., DURANDY, A., BAUMANN, U., SCHLESIER, M., WELCHER, A. A., PETER, H. H. & WARNATZ, K. 2006. ICOS deficiency is associated with a severe reduction of CXCR5+CD4 germinal center Th cells. *J Immunol,* 177**,** 4927-32.

BREITFELD, D., OHL, L., KREMMER, E., ELLWART, J., SALLUSTO, F., LIPP, M. & FORSTER, R. 2000. Follicular B helper T cells express CXC chemokine receptor 5, localize to B cell follicles, and support immunoglobulin production. *J Exp Med,* 192**,** 1545-52.

CHABAUD, M., HEUZE, M. L., BRETOU, M., VARGAS, P., MAIURI, P., SOLANES, P., MAURIN, M., TERRIAC, E., LE BERRE, M., LANKAR, D., PIOLOT, T., ADELSTEIN, R. S., ZHANG, Y., SIXT, M., JACOBELLI, J., BENICHOU, O., VOITURIEZ, R., PIEL, M. & LENNON-DUMENIL, A. M. 2015. Cell migration and antigen capture are antagonistic processes coupled by myosin II in dendritic cells. *Nat Commun,* 6**,** 7526.

CHOI, Y. S., KAGEYAMA, R., ETO, D., ESCOBAR, T. C., JOHNSTON, R. J., MONTICELLI, L., LAO, C. & CROTTY, S. 2011. ICOS receptor instructs T follicular helper cell versus effector cell differentiation via induction of the transcriptional repressor Bcl6. *Immunity,* 34**,** 932-46.

CROTTY, S. 2011. Follicular helper CD4 T cells (TFH). *Annu Rev Immunol,* 29**,** 621-63.

CYSTER, J. G. 1999. Chemokines and cell migration in secondary lymphoid organs. *Science,* 286**,** 2098-102.

DEENICK, E. K., CHAN, A., MA, C. S., GATTO, D., SCHWARTZBERG, P. L., BRINK, R. & TANGYE, S. G. 2010. Follicular helper T cell differentiation requires continuous antigen presentation that is independent of unique B cell signaling. *Immunity,* 33**,** 241-53.

DEENICK, E. K., MA, C. S., BRINK, R. & TANGYE, S. G. 2011. Regulation of T follicular helper cell formation and function by antigen presenting cells. *Curr Opin Immunol,* 23**,** 111-8.

DEN HAAN, J. M., LEHAR, S. M. & BEVAN, M. J. 2000. CD8(+) but not CD8(-) dendritic cells cross-prime cytotoxic T cells in vivo. *J Exp Med,* 192**,** 1685-96.

DO, Y., KOH, H., PARK, C. G., DUDZIAK, D., SEO, P., MEHANDRU, S., CHOI, J. H., CHEONG, C., PARK, S., PERLIN, D. S., POWELL, B. S. & STEINMAN, R. M. 2010. Targeting of LcrV virulence protein from Yersinia pestis to dendritic cells protects mice against pneumonic plague. *Eur J Immunol,* 40**,** 2791-6.

DUDZIAK, D., KAMPHORST, A. O., HEIDKAMP, G. F., BUCHHOLZ, V. R., TRUMPFHELLER, C., YAMAZAKI, S., CHEONG, C., LIU, K., LEE, H. W., PARK, C. G., STEINMAN, R. M. & NUSSENZWEIG, M. C. 2007. Differential antigen processing by dendritic cell subsets in vivo. *Science,* 315**,** 107-11.

GOENKA, R., BARNETT, L. G., SILVER, J. S., O'NEILL, P. J., HUNTER, C. A., CANCRO, M. P. & LAUFER, T. M. 2011. Cutting edge: dendritic cell-restricted antigen presentation initiates the follicular helper T cell program but cannot complete ultimate effector differentiation. *J Immunol,* 187**,** 1091-5.

HAYNES, N. M., ALLEN, C. D., LESLEY, R., ANSEL, K. M., KILLEEN, N. & CYSTER, J. G. 2007. Role of CXCR5 and CCR7 in follicular Th cell positioning and appearance of a programmed cell death gene-1high germinal center-associated subpopulation. *J Immunol,* 179**,** 5099-108.

IIJIMA, N., YANAGAWA, Y., CLINGAN, J. M. & ONOE, K. 2005. CCR7-mediated c-Jun N-terminal kinase activation regulates cell migration in mature dendritic cells. *Int Immunol,* 17**,** 1201-12.

IYODA, T., SHIMOYAMA, S., LIU, K., OMATSU, Y., AKIYAMA, Y., MAEDA, Y., TAKAHARA, K., STEINMAN, R. M. & INABA, K. 2002. The CD8+ dendritic cell subset selectively endocytoses dying cells in culture and in vivo. *J Exp Med,* 195**,** 1289-302.

JOHNSTON, R. J., POHOLEK, A. C., DITORO, D., YUSUF, I., ETO, D., BARNETT, B., DENT, A. L., CRAFT, J. & CROTTY, S. 2009. Bcl6 and Blimp-1 are reciprocal and antagonistic regulators of T follicular helper cell differentiation. *Science,* 325**,** 1006-10.

KAISHO, T. & AKIRA, S. 2003. Regulation of dendritic cell function through Toll-like receptors. *Curr Mol Med,* 3**,** 373-85.

KERFOOT, S. M., YAARI, G., PATEL, J. R., JOHNSON, K. L., GONZALEZ, D. G., KLEINSTEIN, S. H. & HABERMAN, A. M. 2011. Germinal center B cell and T follicular helper cell development initiates in the interfollicular zone. *Immunity,* 34**,** 947-60.

KING, C. 2009. New insights into the differentiation and function of T follicular helper cells. *Nat Rev Immunol,* 9**,** 757-66.

LINDQVIST, M., VAN LUNZEN, J., SOGHOIAN, D. Z., KUHL, B. D., RANASINGHE, S., KRANIAS, G., FLANDERS, M. D., CUTLER, S., YUDANIN, N., MULLER, M. I., DAVIS, I., FARBER, D., HARTJEN, P., HAAG, F., ALTER, G., SCHULZE ZUR WIESCH, J. & STREECK, H. 2012. Expansion of HIV-specific T follicular helper cells in chronic HIV infection. *J Clin Invest,* 122**,** 3271-80.

MA, C. S., DEENICK, E. K., BATTEN, M. & TANGYE, S. G. 2012. The origins, function, and regulation of T follicular helper cells. *J Exp Med,* 209**,** 1241-53.

MA, C. S., HARE, N. J., NICHOLS, K. E., DUPRE, L., ANDOLFI, G., RONCAROLO, M. G., ADELSTEIN, S., HODGKIN, P. D. & TANGYE, S. G. 2005. Impaired humoral immunity in X-linked lymphoproliferative disease is associated with defective IL-10 production by CD4+ T cells. *J Clin Invest,* 115**,** 1049-59.

NUSSENZWEIG, M. C., STEINMAN, R. M., WITMER, M. D. & GUTCHINOV, B. 1982. A monoclonal antibody specific for mouse dendritic cells. *Proc Natl Acad Sci U S A,* 79**,** 161-5.

OTTENHOFF, T. H. 2012. New pathways of protective and pathological host defense to mycobacteria. *Trends Microbiol,* 20**,** 419-28.

PALUCKA, K. & BANCHEREAU, J. 2012. Cancer immunotherapy via dendritic cells. *Nat Rev Cancer,* 12**,** 265-77.

REINHARDT, R. L., LIANG, H. E. & LOCKSLEY, R. M. 2009. Cytokine-secreting follicular T cells shape the antibody repertoire. *Nat Immunol,* 10**,** 385-93.

RIOL-BLANCO, L., SANCHEZ-SANCHEZ, N., TORRES, A., TEJEDOR, A., NARUMIYA, S., CORBI, A. L., SANCHEZ-MATEOS, P. & RODRIGUEZ-FERNANDEZ, J. L. 2005. The chemokine receptor CCR7 activates in dendritic cells two signaling modules that independently regulate chemotaxis and migratory speed. *J Immunol,* 174**,** 4070-80.

SCHAERLI, P., WILLIMANN, K., LANG, A. B., LIPP, M., LOETSCHER, P. & MOSER, B. 2000. CXC chemokine receptor 5 expression defines follicular homing T cells with B cell helper function. *J Exp Med,* 192**,** 1553-62.

SHORTMAN, K. & LIU, Y. J. 2002. Mouse and human dendritic cell subtypes. *Nat Rev Immunol,* 2**,** 151-61.

SOLANES, P., HEUZE, M. L., MAURIN, M., BRETOU, M., LAUTENSCHLAEGER, F., MAIURI, P., TERRIAC, E., THOULOUZE, M. I., LAUNAY, P., PIEL, M., VARGAS, P. & LENNON-DUMENIL, A. M. 2015. Space exploration by dendritic cells requires maintenance of myosin II activity by IP3 receptor 1. *EMBO J,* 34**,** 798-810.

STEINMAN, R. M. & BANCHEREAU, J. 2007. Taking dendritic cells into medicine. *Nature,* 449**,** 419-26.

STEINMAN, R. M. & COHN, Z. A. 1973. Identification of a novel cell type in peripheral lymphoid organs of mice. I. Morphology, quantitation, tissue distribution. *J Exp Med,* 137**,** 1142-62.

SWIGGARD, W. J., MIRZA, A., NUSSENZWEIG, M. C. & STEINMAN, R. M. 1995. DEC-205, a 205-kDa protein abundant on mouse dendritic cells and thymic epithelium that is detected by the monoclonal antibody NLDC-145: purification, characterization, and N-terminal amino acid sequence. *Cell Immunol,* 165**,** 302-11.

TANGYE, S. G., MA, C. S., BRINK, R. & DEENICK, E. K. 2013. The good, the bad and the ugly - TFH cells in human health and disease. *Nat Rev Immunol,* 13**,** 412-26.

TRUMPFHELLER, C., LONGHI, M. P., CASKEY, M., IDOYAGA, J., BOZZACCO, L., KELER, T., SCHLESINGER, S. J. & STEINMAN, R. M. 2012. Dendritic cell-targeted protein vaccines: a novel approach to induce T-cell immunity. *J Intern Med,* 271**,** 183-92.

VINUESA, C. G. & CYSTER, J. G. 2011. How T cells earn the follicular rite of passage. *Immunity,* 35**,** 671-80.

Chapter 2. CD8α$^-$ dendritic cell induces antigen-specific T follicular helper cells generating efficient humoral immune responses

2.1. Introduction

T follicular helper (Tfh) cells, newly identified CD4$^+$ T cell subset, have been recognized as a true B cell helper (Ma et al., 2012, Crotty, 2011). Tfh cells highly express a B cell homing chemokine receptor, CXCR5, which leads their migration to germinal centers (GCs) in a CXCL13-dependent manner where they help cognate B cells to become antibody secreting cells (ASCs), plasma B cells, or memory B cells leading to efficient humoral immunity with long-term memory (Tangye and Tarlinton, 2009, Goodnow et al., 2010). Since the term Tfh cells was firstly introduced (Breitfeld et al., 2000, Schaerli et al., 2000), various studies have provided valuable data to characterize distinct features of Tfh cells such as high expressions of CXCR5, ICOS, PD1, and SAP, key cytokines such as IL-21 and recently IL-4 (Reinhardt et al., 2009) and major transcription factors Bcl6 and c-Maf, to be distinguished from other CD4$^+$ T helper cells (Ma et al., 2012, Crotty, 2011). Given the fact that efficient Tfh cell-dependent humoral immunity as well as long-term humoral memory responses are an essential defensive arm of the vertebrate immune system, it is not surprising that aberrant Tfh cell development or its dysfunctional activity has been known to be closely associated with various human diseases such as autoimmunity, humoral immunodeficiency, and T cell lymphomas (Tangye et al., 2013). Thus, an understanding of the initiation and the regulation of Tfh cells is critical to improve vaccine efficacy as well as to design effective novel therapies.

The role of cognate B cells in the induction of Tfh cells has been validated by several studies. Deficiency of not only B cells but also various B cell functional molecules, such as CD19, CD40, MHC class II and ICOSL, results in the significant decreased number of Tfh cells (Haynes et al., 2007, Johnston et al., 2009, Akiba et al., 2005, Deenick et al., 2010). In addition, interaction between CD4$^+$ T cells and cognate B cells via SAP, a cytoplasmic adaptor protein of the SLAM family, was shown to be critical in inducing Tfh cells (Cannons et al., 2010). In contrast, another study has demonstrated that continuous antigen presentation was sufficient enough to induce Tfh cell differentiation without cognate B cells (Deenick et al., 2010), suggesting that other antigen-presenting cells (APCs) have a major role in Tfh cell differentiation. Moreover, a number of recent studies showed that Tfh cells could arise soon after priming by dendritic cells (DCs) (Vinuesa and Cyster, 2011, Baumjohann et al., 2011, Goenka et al., 2011, Choi et al., 2011), and thus that cognate B cells may be generally required for maintaining functional Tfh cells,

while DCs have a major role in priming Tfh cells, especially at the early stage of Bcl6 up-regulation in Tfh cells.

Although some molecules of DCs have been reported to be critically involved in the induction of Tfh cells (Choi et al., 2011, Fillatreau and Gray, 2003, Cucak et al., 2009), how DCs mechanistically prime naïve $CD4^+$ T cells to become Tfh cells, differently from various $CD4^+$ effector T cell subsets still remain unclear. Particularly, the roles of two distinct $CD8\alpha^+$ and $CD8\alpha^-$ DC subsets in the secondary lymphoid organs in inducing Tfh cells are largely unexplored. Among various DC subsets characterized so far (Shortman and Liu, 2002), two major myeloid DC subsets in the secondary lymphoid organs are well-defined based on the expression of CD8α and their anatomic locations. $CD8\alpha^+$ DCs express the endocytic receptor, DEC-205, and they are located in the T cell enriched zone of the lymphoid organs. They are specialized in up-taking dying cells (Iyoda et al., 2002) and in cross-presentation of non-replicating antigens, leading to cytotoxic $CD8^+$ T cell induction (den Haan et al., 2000). In contrast, $CD8\alpha^-$ DCs, specialized in MHC class II presentation (Dudziak et al., 2007), express a distinct uptake receptor, DCIR2, and they are located in the bridging regions of the marginal zone (Iyoda et al., 2002). A DC targeting strategy by harnessing monoclonal antibodies (mAbs) (Swiggard et al., 1995, Nussenzweig et al., 1982) against various endocytic receptors, e.g. DEC-205 and DCIR2, expressed on the surface of DC subsets enhanced our understanding of the roles of these DC subsets *in vivo*. Moreover, conjugating such DC subset receptor specific targeting antibodies with a wide range of pathogenic antigens has been validated in various disease models to improve vaccine efficacy and to effective deliver novel therapeutic approaches (Trumpfheller et al., 2012, Do et al., 2010).

In this study, we utilized both DC subset-targeting mAbs and DC subset-sorting strategies to study how these two distinct myeloid DC subsets differently prime Tfh cell differentiation by unveiling their underlying mechanisms and signaling pathways. Our data demonstrate that functional Tfh cells are efficiently primed by the $CD8\alpha^-$ DC subset *in vivo* via the enhanced expressions of ICOSL and OX40L on $CD8\alpha^-$ DCs through the non-canonical NF-κB pathway, leading to efficient humoral immune responses against various human pathogenic antigens (Shin et al., 2015).

2.2. Experimental Procedures

Mice

Naïve BALB/c (BC, H-2^d) and C57BL/6 (B6, H-2^b) mice were purchased from Taconic. DO11.10 Thy 1.1, OT-II, RAG-1-deficient, CXCR5 KO, IL-4R KO and IL-12p40 KO mice were purchased from The Jackson Laboratory. IL-21R KO mice were kindly provided from The Rockefeller University (the late Dr. Ralph M. Steinman, New York, NY, USA). SLAM-associated protein or SAP KO mice were generously provided by Dr. Pamela L. Schwartzberg from National Human Genome Research Institute, National Institutes of Health (Bethesda, MD, USA). All mice were properly maintained under specific pathogen-free conditions and used at 6-8 weeks, approved by Ulsan National Institute of Science and Technology Institutional Animal Care and Use Committee (approval number: UNISTIACUC-12-006-A).

Dendritic cell preparation

Total number of splenic dendritic cells was increased by using Fms-like tyrosine 3 ligand (Flt3L) as described (Dudziak et al., 2007). Briefly, 5×10^6 cells of B16Flt3L-melanoma cells were subcutaneously (s.c.) injected to naïve C57BL/6 mice. After 10-14 days, the expanded splenic $CD11c^+$ DCs were isolated with positive magnetic-activated cell sorting (MACS; Miltenyi Biotec, GmbH, Bergisch Gladbach, Germany) and were further sorted into two DC subsets, $CD3^-B220^-CD11c^+CD8\alpha^+$ or $CD3^-B220^-CD11c^+CD8\alpha^-$ DCs by MoFlo XDP (Beckman Coulter, Brea, CA, USA). To analyze intrinsic differences in the two DC subsets, the DCs were stimulated either with 25 μg of poly (I:C) or 100 ng/ml of LPS for 0, 12 or 24 hours. In some experiments, 10 μM of a NIK inhibitor (4H-isoquinoline-1,3-dione, combi-Blocks, San Diego, CA, USA) (Ranuncolo et al., 2012) was treated to the two DC subsets.

$CD4^+$ T cell preparation

OVA-specific transgenic $CD4^+$ T cells from the lymph nodes and the spleen of OT-II or DO11.10 Thy1.1 mice were negatively purified by using hybridoma supernatant cocktails of rat-anti mouse -CD8 (2.43), -MHC class II (T1B120), -Mφ (F4/80), -B220 (RA3-6B2), and -NK cell (NK1.1) antibodies and then depleted with dynabeads sheep anti-rat IgG (Invitrogen, Carlsbad, CA, USA).

Induction of Tfh cells *in vitro*

Naive OVA-specific $CD4^+$ T cells isolated from OT-II mice were co-cultured with purified $CD8\alpha^+$ or $CD8\alpha^-$ DCs (1:10 ratio of DC to T cells) for 1 ~ 6 days in the presence of 25 μg/ml of poly (I:C), 100

ng/ml of LPS, Flagellin or R848 (Invivogen, San Diego, CA, USA) ± 2 μM of OVA peptide (a.a. 323-339) (Genscript, Piscataway Township, NJ, USA). At each indicated time point, activated $V\alpha2^+CD4^+CD44^+$ T cells were isolated, and analyzed for the expression of various surface molecules, transcription factors, and cytokines by flow cytometry, qRT-PCR, and ELISA methods. To block ICOSL or OX40L expressed on the DC subsets, 20 μg/ml of blocking antibodies or their corresponding isotype antibodies were treated when $CD4^+$ T cells were co-cultured with the DC subsets for 3 days.

Induction of Tfh cells *in vivo*

Harvested $CD4^+$ T cells from DO11.10 Thy 1.1 mice were adoptively transferred (3×10^6 cells per mouse) into naïve Thy 1.2^+ BALB/c mice intravenously (i.v.) at day -1. At day 0, PBS, 500 μg of soluble OVA protein (endotoxin-free; Seikagaku Corp, Tokyo, Janpan), or 5 μg of each distinct DC subset targeting monoclonal antibodies (anti-DEC-205 or anti-DCIR2 mAbs) conjugated with OVA protein in the presence of 50 μg of poly (I:C) or LPS were s.c. injected via footpads. At indicated time points, single cells from the lymph nodes or the spleen were harvested and analyzed for the expressions of various molecules by flow cytometry. In some experiments, 100 μg of Isotype, ICOSL, or OX40L blocking mAbs were i.v. injected to the immunized mice at day 0 and 2. Then, 4 days after the immunization, cells were harvested for analysis.

Intracellular staining

Antigen specific Tfh cells were induced *in vivo* as described above. Five days later, single cells were harvested from the lymph nodes or the spleen, and Fcγ receptors were properly blocked with anti-CD16/CD32 antibodies. The cells were then stained with anti-mouse Thy1.1 or DO11.10, CD4, CD44 and CXCR5 for 30 minutes at R.T. Following fixation and permeabilization with a Cytofix/Cytoperm kit (BD Biosciences, San Jose, CA, USA) according to the manufacturer's instructions, the cells were then stained for intracellular Bcl6 or IL-21 along with their corresponding isotypes for 25 minutes at 4 ℃. Data were obtained by flow cytometry. To detect IFN-γ or IL-4 secreting $CD4^+$ T cells, the cells were re-stimulated with 2μM of OVA peptide (323-339) in the presence of 2 μg/ml αCD28 mAbs for 2 hours followed by the treatment of GolgiStop (Invitrogen) for 4 hours.

Production of DC subset-specific targeting antibodies conjugated with various antigens

In this study, we utilized three different proteins conjugated with DC subset-specific targeting antibodies (Do et al., 2010, Trumpfheller et al., 2012). LcrV, HIV gagp24, and OVA proteins were genetically conjugated either to anti-mouse DEC-205 (for $CD8\alpha^+$ DC targeting) mAbs or to anti-mouse DCIR2 (for

$CD8\alpha^-$ DC targeting) mAbs. No significant antigen-specific immune responses were detected with each matched isotype control (data not shown). LcrV and HIV gagp41 proteins were used as described in the previous studies (Do et al., 2010, Trumpfheller et al., 2012). All proteins utilized were free of endotoxin (<0.125 endotoxin units/mg) in a Limulus Amebocyte Lysate assay, QCL-1000 (Bio Whittaker).

***In vivo* immunization with DC subset targeting antibodies**

Mice were intraperitoneally (i.p.) or subcutaneously (s.c.) injected with LcrV- or HIV gagp24-protien conjugated mAbs (5 or 10 μg per mouse) in the hind footpads in the presence of adjuvant (50 μg poly (I:C) +/- 25 μg anti-CD40 antibody per mouse). For some experiments, a priming and boosting strategy was applied where mice were primed and then boosted 4-6 weeks apart with LcrV- or HIV gagp24-protein conjugated targeting mAbs (5 or 10 μg per mouse) in the presence of 50 μg poly (I:C).

Adoptive transfer experiment to RAG-1-deficient mice in the presence of OVA or HBsAg

Naïve OVA-specific $CD4^+$ T cells were activated by each DC subset for 3 days, isolated ($CD4^+CD44^+$ T cells), and then adoptively transferred (2×10^6 cells per mouse) i.v. into RAG-1-deficient mice together with naïve $CD19^+$ B cells (4×10^6 cells per mouse) at day -1 followed by i.p. injection of 500 μg soluble OVA protein in the presence of 50 μg poly (I:C) at day 0. 10 days after the immunization, the RAG-1-deficient mice were boosted i.p. with 500 μg soluble OVA protein and 50 μg poly (I:C). Seven days after the boost, total splenocytes were obtained and ELISPOT assay of anti-OVA ASCs was performed. For HBsAg, naive $CD4^+$ T cells were activated by each DC subset for 3 days with 10 μg/ml HBsAg (LG life sciences, Seoul, south Korea) and 25 μg/ml poly (I:C), isolated, and then adoptively transferred (1×10^6 cells per mouse) i.v. into RAG-1-deficient mice together with sorted naïve $CD19^+$ B cells (4×10^6 cells per mouse) at day -1 followed by i.p. injection of 50 μg HBsAg with 50 μg poly (I:C) at day 0. 10 days after the immunization, the RAG-1-deficient mice were boosted i.p. with 50 μg soluble HBsAg and 50 μg poly (I:C). Seven days after the boost, total splenocytes were obtained and ELISPOT assay of anti-HBs ASCs was performed.

ELISPOT assay for antibody-secreting cells

In order to detect antigen-specific ASCs, ELISPOT plates (Millipore, Billerica, MA, USA) were coated with 5 or 10 μg/ml LcrV, Gagp41, OVA, or HBsAg protein overnight at 4 ℃. After the plates were washed, blocked with RPMI 5% FBS (Gibco, Grand Island, NY, USA) for 1 hour at 37 ℃. Serially diluted cells from the spleen, lymph nodes, or bone marrow were incubated for 6 hours at 37 ℃. The plates were washed and then stained with goat anti-mouse Fc specific IgM, IgG or IgG1 antibody

conjugated with horseradish peroxidase (Southern Biotech, Birmingham, AL, USA) for 2 hours at room temperature. The plates were developed by a peroxidase substrate AEC kit (Vector Laboratories, Burlingame, CA, USA). Visible spots were counted by an ELISPOT reader (Autoimmune Diagnostika GmbH, Straßberg, Germany).

ELISA for serum antibodies and cytokines

High binding ELISA plates (BD Bioscience) were coated with 5 or 10 μg/ml LcrV, Gagp41, OVA, NP_8-BSA, or NP_{30}-BSA protein overnight at 4 ℃. The plates were washed 3 times with PBST (PBS with 0.1% of Tween 20) and then blocked with PBST-BSA 5% for 1 hour at 37 ℃. Serial dilutions of mouse serum were added into the plates and then incubated for 1 hour at 37 ℃. Various secondary goat anti-mouse Fc specific antibodies conjugated with horseradish peroxidase were utilized and developed with o-phenylenediamine (Sigma-Aldrich, St. Louis, MO, USA) tablets at room temperature for 15~20 minutes. Data are presented as log antibody titers with the highest dilution showing OD_{450} >0.1. To detect cytokines in supernatants of the cell culture, we used CBA flex sets (BD Bioscience).

ChIPs

The two DC subsets were treated with or without 25 μg/ml poly (I:C) for 2 hours followed by a ChIP assay using a magna ChIP kit (Millipore). Briefly, the two DC subsets were treated with 37% formaldehyde, 1% in the final solution, for protein-chromatin DNA cross-linking, and then glycine was treated to remove excess formaldehyde. The cells were then sonicated to contain ~500 bp DNA fragments with the Sonic Dismembrator 500 (Fisher Scientific, Waltham, MA, USA). The DNA fragments were precipitated with mouse IgG2a isotype control, anti-moue p52, or anti-acetyl-histone H3 antibodies. The precipitants were treated with 100 μg/ml proteinase K to remove proteins and then incubated for 2 hours at 62 ℃ to reverse cross-linking. Finally, purified DNA was amplified by qPCR (LightCycler 480 SYBR Green I Master, Roche, Clovis, CA, USA). Data were expressed as enrichment related to input.

Immunohistochemistry

Briefly, tissue sections (10 μm) of the spleen were obtained by using Cryotome (Thermo Fisher scientific, thermos, Carlsbad, CA, USA) and then they were fixed with 100% aceton on a slide. To obtain germinal center images, slides were stained with APC anti-mouse IgD (BD Biosciences) and FITC anti-mouse PNA (Vector Laboratories). Then, the stained samples were imaged with FV10i confocal microscope (Olympus, Center Valley, PA, USA).

Flow cytometry

Information on all antibodies used for flow cytometry analysis is listed below. Data were acquired by BD FACS Calibur or BD LSRfortessa, and the data were analyzed by FlowJo software (Tree Star Inc., Ashland, OR, USA), shown on the log scale graph (from 10^1 to 10^4 or 10^5). All data values were obtained after subtracting their corresponding isotype values. MFI stands for Median Fluorescence Intensity.

Antibodies for flow cytometry and FACS

Antigen	Clone	Fluorochrome	Company
DC subset isolation			
CD11c	HL3	PE	BD Biosciences
CD8	53-6.7	APC	BD Biosciences
CD3	145-2C11	FITC	BD Biosciences
B220	RA3-6B2	FITC	BD Biosciences
$CD4^+$ T cell analysis			
Vα2	B20.1	FITC	BD Biosciences
Thy1.1	OX-7	FITC	BD Biosciences
DO11.10	KJ1-26	FITC/PE	BD Biosciences
CD4	RM4-5	APC	BD Biosciences
CD44	IM7	Pe-Cy7/APC-Cy7	BD Biosciences
CXCR5	2G8	PE/Biotin	BD Biosciences
ICOS	7E.17G9	PE/Biotin	BD Biosciences
PD1	RMP1-30	Biotin/APC	eBioscience
Intracellular staining			
Bcl6	K112-91	PE	BD Biosciences
IL-4	11B11	PE	BD Biosciences
IFN-γ	XMG1.2	PE	BD Biosciences
IL-21	mhalx21	PE	eBioscience
DC subsets analysis			
ICOSL	HK5.3	Biotin	eBioscience
OX40L	RM134L	Biotin	eBioscience
PDL1	MIH5	Biotin	eBioscience
PDL2	TY25	Biotin	eBioscience

Antibodies for flow cytometry and FACS

GC B cell analysis			
CD19	1D3	PE	BD Biosciences
IgD	11-26C.2A	APC	BD Biosciences
FAS	Jo2	Pe-cy7	BD Biosciences
GL7	GL7	FITC	BD Biosciences
Streptavidin	Streptavidin	PE/PE-cy7/APC/BV421	BD Biosciences
Isotype control			
Rat IgG2a, κ	R35-95/ RTK2758/2A3	PE/Biotin/ Purified	BD/ BioLegend/Bioxcell
Rat IgG2b, κ	A95-1/ RTK4530/LTF-2	PE/APC/Biotin/purified	BD/ BioLegend/Bioxcell
Mouse IgG1, κ	MOPC-21	PE	BD Biosciences
Functional antibody			
CD40	1C10	purified	BD Biosciences
ICOSL	HK5.3	Functional grade purified	eBioscience, Bioxcell
OX40L	RM134L	Functional grade purified	eBioscience, Bioxcell

Western blot analysis

The two DC subsets were stimulated with or without 25 μg/ml poly (I:C) or 0.5 μg/ml anti-CD40 antibody for 2 hours at 37 ℃ followed by western blot (WB) analysis. WB images were developed with LAS 4000 (GE Healthcare, Cleveland, Ohio, USA). Information on all WB antibodies is listed below.

Antibodies for western blot and chip assay

Antigen	Clone	Application	Company
Western Blot			
Total NIK	polyclonal	WB	Cell Signaling
Phospho-p100	polyclonal	WB	Cell Signaling
Total-p100/p52	polyclonal	WB	Cell Signaling
Total-RelB	C-19	WB	Santa Cruz
Phospho-ERK	polyclonal	WB	Cell Signaling
Total-ERK	137F5	WB	Cell Signaling
Phospho-JNK	polyclonal	WB	Cell Signaling
Total-JNK	37/pan-JNK/SAPK1	WB	BD Biosciences
Phopho-p38	D3F9	WB	Cell Signaling
Total-p38	27/p38α/SAPK2a	WB	BD Biosciences
Beta−actin	AC-15	WB	Ambion
Chip assay			
Mouse IgG2a, κ	G155-178	Chip	BD Biosciences
NFκB p52	c-5	Chip	Santa Cruz
Acetyl Histone H3	polyclonal	Chip	Millipore

qRT-PCR analysis

Total RNA was obtained with Trizol (Invitrogen), and cDNA was synthesized by using a cDNA synthesis kit (NEB, Ipswich, MA, USA). Light Cycler 480 II was utilized to perform a SYBR Green based qPCR experiment. House-keeping genes, *β-actin* and *Gapdh*, were applied for normalization. Information on all primers is listed in below.

Primers for qRT-PCR and chip assay

Genes	Forward	Reverse
qRT-PCR		
ICOS	5'-TGACTGGCTTTGTTAGGG-3'	5'-TGTTAGGTGTTCGTGTTGG-3'
SAP	5'-GTACCACGGCAAAATCAG-3'	5'-GTACACGCCAGGGACAC-3'
Bcl6	5'-CTTCCCACACTGCCATAA−3'	5'-GCATTCTCCCCTACTTTGA−3'
c-maf	5'-CCCTCCTTCTGAGTTCTTCT-3'	5'-GAGTGGCTTTAGTTCATTCTGT-3'
T-bet	5'-TGGAGGTGAATGATGGAG-3'	5'-ATCTCTGCGTTCTGGTAGG-3'
Beta−Actin	5'-TCCTATGTGGGTGACGAG-3'	5'-CTCATTGTAGAAGGTGTGGTG-3'
GAPDH	5'-AAGGACACTGAGCAAGAGAG-3'	5'-GATGGTATTCAAGAGAGTAGGG-3'
Chip Assay		
ICOSL	5'-TGGTGGTGCATAGTTTCCAA−3'	5'-TTCCCCACAACATCTGGAAT-3'
OX40L	5'-CTCTCCCAATGGTCTCCAAA−3'	5'-TTATCATGGAGCCGTCAACA−3'
GAPDH	5'-ACCAGGGAGGGCTGCAGTCC-3'	5'-TCAGTTCGGAGCCCACACGC-3'
CCL2	5'-CTGGAGCTCACATTCCAGC-3'	5'-GGATGTTCTTCCCAGCG-3'

Statistics

Results are expressed as mean ± s.e.m. or mean ± s.d. We used a PRISM 4.0 or EXCEL program (GraphPad Prism, La Jolla, CA, USA) and performed nonparametric Mann-Whitney U test when appropriate. *P* values < 0.05 were considered significant.

2.3. Results

CD8α⁻ DCs augment the generation of Tfh cell-dependent antibody secreting cells

In order to inspect if the two DC subsets have different functions in the generation of Tfh cell-dependent antigen-specific antibody secreting cells (ASCs) *in vivo*, we used distinct DC subset targeting monoclonal antibodies (mAbs) conjugated with LcrV (V) protein from *Yersinia pestis*, anti-DEC-205:V (for targeting $CD8\alpha^+$ DCs) and anti-DCIR2:V (for targeting $CD8\alpha^-$ DCs) conjugated mAbs. We observed significant numbers of anti-V ASCs both in the spleen and the bone marrow harvested from $CD8\alpha^-$ DC targeted groups, while little ASCs were observed from the $CD8\alpha^+$ DC targeted groups (**Figure 2-1A**). The total number of ASCs in the spleen was significantly decreased after 28 days of the immunization, while ASCs in the bone marrow were increased confirming the previously reported fact that long-lived ASCs live in the bone marrow (Slifka et al., 1995). Similar phenomenon was observed by using a different mouse strain (**Figure 2-1B**), demonstrating that the increased number of ASCs by targeting $CD8\alpha^-$ DCs is not limited to a particular MHC haplotype.

We then examined the number of anti-V ASCs in various Tfh cell related KO mice. We observed that anti-V ASCs induced by targeting $CD8\alpha^-$ DCs were dramatically decreased in CXCR5 (Breitfeld et al., 2000)-, SAP (Qi et al., 2008)-, IL-21 (Nurieva et al., 2008) receptor (R)-KO mice (**Figure 2-1C**), but such decreases were not detected in IL-12p40- (Mosmann and Coffman, 1989, Ma et al., 2009) or IL-4R (Kaplan et al., 1996)-KO mice (**Figure 2-1D**). Taken together, these data clearly demonstrated that $CD8\alpha^-$ DCs enhance the generation of Tfh cell-dependent antigen-specific ASCs.

CD8α⁻ DCs specialize in inducing antigen-specific Tfh cells *in vivo*

To investigate functions of the two DC subsets in the induction of antigen-specific Tfh cells *in vivo*, we employed DC subset targeting strategy through ovalbumin (OVA)-conjugated mAbs and OVA transgenic mice. Five days after the immunization, we observed higher percentages and numbers of $CXCR5^+PD1^+$, $CXCR5^+Bcl6^+$, and $CXCR5^+IL\text{-}21^+$ Tfh cells both in the lymph nodes and the spleen from the $CD8\alpha^-$ DC targeted group (**Figures 2-2A-C**; **Figures 2-3B-D**).

In order to confirm the capability of $CD8\alpha^-$ DCs in inducing Tfh cells *in vivo* under different stimulatory cues, similar experiments were performed with LPS. Again, higher percentages and numbers of $CXCR5^+PD1^+$, $CXCR5^+Bcl6^+$, and $CXCR5^+IL\text{-}21^+$ Tfh cells were induced by $CD8\alpha^-$ DCs both in the lymph nodes and the spleen compared with those induced by $CD8\alpha^+$ DCs (**Figures 2-2D-F**; **Figures 2-4B-D**). We observed no significant difference in the total number of $DO11.10^+CD4^+$ T cells induced by

the two DC subsets in the lymph nodes (**Figure 2-2G**). In the spleen, however, we observed higher total number of DO11.10$^+$CD4$^+$ T cells in the CD8α$^-$ DC targeted group (**Figure 2-3E**; **Figure 2-4E**). Once the numbers of Tfh cells were normalized by the total number of DO11.10$^+$CD4$^+$ T cells in each DC subset targeted group, we still observe greater number of Tfh cells induced in the CD8α$^-$ DC targeted group (**Figure 2-3F**; **Figure 2-4F**). As previously studied (Do et al., 2010), CD8α$^+$ DCs were superior in inducing higher number of IFN-γ$^+$CD4$^+$ T cells regardless of total number of DO11.10$^+$CD4$^+$ T cells (**Figure 2-4G**), while CD8α$^-$ DCs are more potent in inducing IL-4 secreting CD4$^+$ T cells (**Figure 2-4H**). Taken together, our data clearly demonstrate that targeting CD8α$^-$ DCs specialize in inducing antigen-specific Tfh cells *in vivo*.

CD8α$^-$ DCs are superior in inducing Tfh cells *in vitro*

To confirm that our observation on Tfh cells induced *in vivo* is due to intrinsic differences between the two DC subsets, CD8α$^+$ DCs and CD8α$^-$ DCs, and not due to DC subset receptor-specific responses via DC targeting mAbs, the two DC subsets were purified and the induction of antigen-specific Tfh cells by each DC subset was compared *in vitro*. At the indicated time point after the co-culture of OVA-specific OT-II CD4$^+$ T cells with either CD8α$^+$ or CD8α$^-$ DCs, the activated CD44$^+$CD4$^+$ T cells were isolated and then analyzed for Tfh cell-related surface markers, transcription factors, and cytokines. Interestingly, we observed the higher ICOS expression on the CD4$^+$ T cells induced by CD8α$^-$ DCs as early as day 2 followed by the enhanced Bcl6 expression at day 3 (**Figures 2-5A-C**; **Figure 2-6A**), which clearly supports the previously suggested theory on a molecular hierarchy from ICOS to Bcl6 (Choi et al., 2011). The expressions of SAP and c-Maf (Bauquet et al., 2009) were also highly increased in the CD4$^+$ T cells induced by CD8α$^-$ DCs, whereas T-bet, a transcription factor of Th1 cell, was highly identified in those induced by CD8α$^+$ DCs (**Figure 2-5C**; **Figure 2-6A**). Again, such phenomena were not restricted to a particular DC maturation cue, poly (I:C). Data showed that the CD4$^+$ T cells induced by CD8α$^-$ DCs with LPS expressed higher levels of CXCR5 and ICOS (**Figure 2-5D**), Bcl6 (**Figure 2-5E**), and greatly secreted IL-21 (**Figure 2-5F**). Moreover, with Toll-like Receptor 5 (TLR5) (flagellin) and TLR7/8 (R848) stimuli, the CD4$^+$ T cells induced by CD8α$^-$ DCs secreted higher level of IL-21 cytokine compared with that secreted from the CD4$^+$ T cells induced by CD8α$^+$ DCs (**Figure 2-5F**). We observed no significant difference in total CD4$^+$ T cell proliferation induced by the two DC subsets *in vitro* (**Figure 2-6B**).

In order to validate the role of *in vitro* induced Tfh cells as a true B cell helper, the *in vitro* generated DC subset-primed CD4$^+$ T cells were adoptively transferred together with naïve CD19$^+$ B cells into RAG-1-deficient mice. After prime and boost immunizations with soluble OVA protein, we observed higher number of anti-OVA ASCs in the group which received the Tfh cells induced by CD8α$^-$ DCs

(**Figure 2-5G**). Together, these data clearly show that CD8α$^-$ DCs are superior in inducing antigen-specific Tfh cells *in vitro*.

CD8α$^-$ DCs efficiently increase germinal center (GC) formation, reaction, and antibody titers

After we observed the capability of CD8α$^-$ DCs in inducing Tfh cells both *in vitro* and *in vivo*, we examined whether CD8α$^-$ DC induced Tfh cell functions as a true B cell helper. As expected, higher percentage of CD19$^+$IgD$^-$GL7$^+$FAS$^+$ GC B cells was observed in total splenocytes harvested from the CD8α$^-$ DC targeted group under different stimuli cues (**Figures 2-7A** and **B**; **Figures 2-8A** and **B**). Histologically, the formation of PNA$^+$ cells well surrounded by IgD$^+$ cells in the spleen from the CD8α$^-$ DC targeted group was detected, whereas we observed no GC formation in the CD8α$^+$ DC targeted group (**Figure 2-8C**). In addition, the CD8α$^-$ DC targeted group demonstrated higher titers of both anti-OVA IgM and IgG antibodies than those from the CD8α$^+$ DC targeted group (**Figure 2-7C**). Titer level of anti-OVA IgM induced by CD8α$^-$ DCs was much higher than those induced by CD8α$^+$ DCs at day 5, which were isotype-switched to IgG at day 5. In the CD8α$^+$ DC targeted group, isotype-switched anti-OVA IgG was notably identified 7 days after the immunization, but its titer level was still lower than those from the CD8α$^-$ DC targeted group. To further ensure the increased GC reaction in the CD8α$^-$ DC targeted group, we inspected affinity maturation of antibodies using NP-OVA. Briefly, 10 days after the immunization, the mice were re-immunized with 10 μg NP_{16}-OVA. 7 and 14 days after the re-immunization, higher ratio of NP_8 to NP_{30} of anti-OVA IgG antibodies was induced by CD8α$^-$ DCs compared with those induced by both soluble OVA protein and CD8α$^+$ DCs (**Figure 2-7D**). These data strongly demonstrate that the CD8α$^-$ DC subset is an inducer of functional Tfh cells, generating efficient humoral immune responses *in vivo*.

Up-regulated ICOSL and OX40L expressed on CD8α$^-$ DCs play a critical role in inducing Tfh cells

In order to study distinct features between the two DC subsets in the induction of Tfh cells, various Tfh cell related ligands on the DC subsets were compared under poly (I:C) or LPS stimulus. Higher expression levels of ICOSL (Choi et al., 2011) and OX40L (Fillatreau and Gray, 2003) were observed in CD8α$^-$ DCs in the presence of both poly (I:C) (**Figure 2-9A**) and LPS (**Figure 2-9B**), whereas higher expression levels of PDL1 and PDL2 (**Figures 2-10A** and **B**), which are reported to negatively control Tfh-dependent humoral immune responses (Cubas et al., 2013, Hams et al., 2011), were observed in CD8α$^+$ DCs. When ICOSL on the two DC subsets was blocked with anti-ICOSL blocking antibodies during DC-T cell co-culture, the formerly enhanced expressions of CXCR5 and ICOS on the CD4$^+$ T cells primed by CD8α$^-$ DCs were decreased to the level as those induced by CD8α$^+$ DCs (**Figure 2-9C**; **Figure**

2-10C). Interestingly, blocking OX40L on CD8α$^-$ DCs with anti-OX40L blocking antibodies during DC-T cell co-culture also reduced expression levels of both CXCR5 and ICOS as much as those induced by CD8α$^+$ DCs (**Figure 2-9C**; **Figure 2-10C**). To further check the functions of enhanced expressions of ICOSL and OX40L on CD8α$^-$ DCs in inducing Tfh cells *in vivo*, blocking antibodies against ICOSL or OX40L were applied during distinct DC subset targeting. The increased expression of CXCR5 on the CD4$^+$ T cells induced by CD8α$^-$ DCs was decreased by blocking either ICOSL or OX40L (**Figure 2-9D**). Moreover, blocking either ICOSL or OX40L on CD8α$^-$ DCs significantly reduced the number of CXCR5$^+$PD1$^+$, CXCR5$^+$Bcl6$^+$, or CXCR5$^+$IL-21$^+$ Tfh cells primed by CD8α$^-$ DCs both in the lymph node (**Figure 2-9E**) and the spleen (**Figure 2-10D**). Thus, the data clearly demonstrate the critical role of both ICOSL and OX40L signaling in CD8α$^-$ DCs for Tfh cell differentiation.

Increased non-canonical NF-κB signaling pathway in CD8α$^-$ DCs regulates *Icosl* and *Ox40l* gene expressions

Based on the previous study demonstrating that the non-canonical NF-κB signaling pathway regulates high level of ICOSL expression in B cells (Hu et al., 2011) and based on our analysis of the non-canonical NF-κB signaling pathway in the two DC subsets from the published gene array data (Dudziak et al., 2007), we hypothesized that the enhanced expressions of ICOSL and OX40L on CD8α$^-$ DCs are controlled by the non-canonical NF-κB signaling pathway. Interestingly, we observed higher level of NF-κB-inducing kinase (NIK), a signal integrator of the non-canonical NF-κB pathway (Sun, 2011), in CD8α$^-$ DCs even in the absence of stimulation and its expression was further enhanced upon poly (I:C) stimulation, whereas it was barely measurable in CD8α$^+$ DCs (**Figure 2-11A**; **Figure 2-12A**). When anti-CD40 stimulation (Coope et al., 2002), which is reported to elicit strong signals through both the canonical and non-canonical signaling pathways, was given to the two DC subsets, the expression level of NIK was enhanced in the two DC subsets, but its expression level was still higher in CD8α$^-$ DCs (**Figure 2-11A**; **Figure 2-12A**). In addition, we observed greater expression levels of phospho(p)-p100, p52, and RelB in CD8α$^-$ DCs in the absence or presence of stimulation (**Figure 2-11A**; **Figure 2-12A**). In contrast, CD8α$^+$ DCs constitutively expressed higher levels of molecular components involved in the pro-inflammatory MAPK signaling pathway, particularly p-JNK, which was barely detectable in CD8α$^-$ DCs (**Figure 2-11B**; **Figure 2-12A**). To confirm if the promoter of *Icosl* or *Ox40l* links with the non-canonical NF-κB signaling pathway, ChIP experiments were performed. We quantified the enriched DNA obtained from the immunoprecipitates by qPCR using primers spanning the upstream regions of *Icosl* or *Ox40l* (**Figure 2-12B**). Upon poly (I:C) stimulation, we observed that the significant enrichment of p52 was associated with the upstream region of *Icosl* (-3000) or *Ox40l* (-1000) in CD8α$^-$ DCs (**Figure 2-12C**). We used

Gapdh and *Ccl2* genes as negative and positive controls for p52, respectively (**Figure 2-12C**). In addition, when a NIK inhibitor (4H-isoquinoline-1,3-dione) was applied, the formerly increased expressions of ICOSL and OX40L on CD8α$^-$ DCs were significantly decreased (**Figure 2-11D**). Therefore, our findings obviously showed that intrinsically increased non-canonical NF-κB signaling pathway regulates the enhancement of ICOSL and OX40L expressions on CD8α$^-$ DCs.

Employing CD8α$^-$ DCs to improve vaccine-induced humoral immunity

We utilized various human pathogenic antigens such as *Y. pestis* LcrV, human immunodeficiency virus (HIV) Gag, and hepatitis B surface antigen (HBsAg) to validate the increased humoral immune responses delivered by CD8α$^-$ DC-primed Tfh cells in respect to improved vaccine strategy. For each pathogen, effective vaccines are not available and long-term protective humoral responses are required and. Firstly, with V antigen, only CD8α$^-$ DC targeting induced substantial numbers of anti-V IgM ASCs in the lymph nodes, which were effectively isotype-switched to IgG1 (**Figure 12-13A**). In the spleen, we observed similar observation where anti-V IgM ASCs were detected as early as day 3, successfully isotype-switched to IgG1 at day 5, and later migrated into the bone marrow (**Figures 12-13B** and **C**). In contrast, we observed inefficacy of targeting CD8α$^+$ DCs against V antigen in inducing anti-V ASCs in all lymphoid organs analyzed (**Figures 12-13A−C**). Overall we observed higher anti-V antibody titers including IgG2a isotype in the CD8α$^-$ DC targeted group as well (**Figure 12-14A**). In addition, data demonstrating significantly enhanced numbers of anti-V ASCs 6 months after the immunization explain the efficacy of targeting CD8α$^-$ DCs in the induction of long-term humoral immune responses (**Figure 12-13D**).

Secondly, we utilized DC subset targeting antibodies conjugated with HIV Gagp24 (Gag) in order to further validate that increased humoral immune responses induced by CD8α$^-$ DCs are not limited to V protein, and observed consistent enhancement in anti-Gag ASCs and antibody titers from the CD8α$^-$ DC targeted group (**Figure 12-13E**; **Figure 12-14B**). Thirdly, we utilized purified CD8α$^-$ DCs to increase humoral immune responses against HBsAg, the immunogen of hepatitis B vaccine. Data again showed the up-regulated ICOS expression on the CD4$^+$ T cells induced by CD8α$^-$ DCs (**Figure 2-15**) as well as significantly enhanced number of anti-HBsAg ASCs following adoptive transfer of the CD8α$^-$ DC-induced CD4$^+$ T cells with naïve CD19$^+$ B cells into RAG-1-deficient mice (**Figure 2-13F**). These data clearly show the efficacy of the CD8α$^-$ DC subset in inducing effective humoral immune responses via functional Tfh cell priming.

2.4. Discussion

Many studies have reported the importance of DCs in priming Tfh cells, but little is known about detail mechanisms by which DC subset primes the initial commitment of antigen-specific $CD4^+$ T cells into Tfh cells. In this study, our data explain important cellular and molecular mechanisms controlled by $CD8\alpha^-$ DCs to prime Tfh cell differentiation, enhancing Tfh cell dependent humoral immune responses. We also here provide the rationale for targeting the distinct $CD8\alpha^-$ DC subset to provoke efficient humoral immune responses against various human pathogenic antigens.

Our study revealed unexplored intrinsic feature differences between the two DC subsets in priming Tfh cell differentiation. Of particular, our data demonstrate that the highly enhanced non-canonical NF-κB signaling pathway increases the expression levels of ICOSL and OX40L on $CD8\alpha^-$ DCs, thereby launching a molecular mechanism of distinct DC subset-derived Tfh cell differentiation. We observed that such intrinsic features or capability of $CD8\alpha^-$ DCs in inducing Tfh cells are not limited to a specific stimulus. One previous study reported that ICOSL/ICOS signaling during DC-T cell priming instructs Bcl6 expression, leading to increase CXCR5 expression on $CD4^+$ T cells and thus determine the early bifurcation between Tfh cells and other effector Th cell developments (Choi et al., 2011). However, it has not been studied that the distinct $CD8\alpha^-$ DC subset enhances ICOS signals to promote Tfh cell induction. Interestingly, our study also shows that both ICOSL and OX40L molecules expressed on $CD8\alpha^-$ DCs have critical roles in promoting ICOS signals of Tfh cells. Considering one previous study suggesting the important role of OX40L on $CD11c^+$ DCs for $CD4^+$ T cells to migrate into the follicle (Brocker et al., 1999), and another study reporting that OX40 stimulation could overcome the impaired migration of $CD4^+$ T cells into B cell follicles, initially caused by lack of CD40 on DCs (Fillatreau and Gray, 2003), it is conceivable that the increased OX40L expression on $CD8\alpha^-$ DCs may also be importantly involved in such molecular hierarchy from ICOS to Bcl6 to CXCR5, which eventually help the migration of Tfh cells into B cell follicles. Based on the data we presented here that the expressions of ICOSL and OX40L were enhanced through the non-canonical NF-kB signaling pathway in $CD8\alpha^-$ DCs and the blocking of either ICOSL or OX40L critically reduced the ability of $CD8\alpha^-$ DCs in inducing Tfh cells *in vivo*, the Tfh cell induction efficiency by the $CD8\alpha^-$ DC subset is delivered by its bona fide intrinsic property.

Because the $CD4^+$ T cells primed by $CD8\alpha^+$ DCs highly expressed T-bet and a number of previous reports showed the efficacy of targeting $CD8\alpha^+$ DCs in inducing of IFN-γ secreting Th1 cells (Do et al., 2010, Trumpfheller et al., 2012), we hypothesize that the highly activated JNK expression is involved in inducing Th1 rather than in Tfh cell. However, further studies are necessary to confirm if $CD8\alpha^+$ DCs

negatively regulate Tfh dependent-humoral immunity via highly expressed PDL1/L2 molecules and JNK signaling.

Beside the mechanisms we discovered, there are known possibilities such as the differences in antigen processing *in vivo* (Dudziak et al., 2007), prolonged antigen presentation (Deenick et al., 2010, Lahoud et al., 2011), or extrafollicular B cell activation (Chappell et al., 2012) of DC subsets could be involved in Tfh cell differentiation. In addition, as reported by previous studies that $CD14^+$ dermal DCs (Klechevsky et al., 2008), late activator antigen-presenting cells (Yoo et al., 2012), or monocyte-derived DCs (Chakarov and Fazilleau, 2014) have a role in promoting Tfh cell induction, we believe that Tfh cell induction may be dependent on the type of the immune responses or antigen provided. Further investigations are necessary to understand how various DC subsets are involved in inducing Tfh cells interplaying with each other *in vivo* within lymphoid organs, which leads us to better appreciate diverse physiological functions of DC subsets. One previous study showed that DCs were a potent inducer of Bcl6 in naïve $CD4^+$ T cells utilizing peptide-pulsed bone marrow derived DCs, but such DC-restricted peptide immunization was not able to induce potent GCs and induce lower PD1 expression on Tfh cells than the soluble protein immunization (Baumjohann et al., 2011). In addition, when antigens were given to only DCs by using CD11c/$A_ß^b$ mice, there was sufficient initiation of Tfh cell differentiation, but these Tfh cells were not able to produce IL-21, thereby requiring additional helps from cognate B cells for full effector function (Goenka et al., 2011). In contrast, our $CD8\alpha^-$ DC targeting strategy demonstrated that immunization with around 1.6 µg ovalbumin could efficiently induce Tfh cells as well as Tfh cell-dependent humoral immune responses even more than those from the group immunized with 500 µg soluble OVA protein, supporting the efficacy of targeting $CD8\alpha^-$ DCs in inducing fully functional Tfh cells *in vivo*.

The involvement of Tfh cells in human diseases was recently reported. A study demonstrated substantial expansion of HIV-specific Tfh cells in chronic HIV-infected patients explaining hyper-secreted IgG seen in them (Lindqvist et al., 2012). Another study also showed that the expanded Tfh cells in HIV-infected patients provided inefficient help to B cells due to the negative regulatory role of PDL1/L2 molecules (Cubas et al., 2013). Thus, based on recent studies on HIV vaccine by recruiting Tfh cells (Streeck et al., 2013), the understanding of cellular and molecular mechanisms involved in Tfh cell initiation and differentiation is crucial to develop efficient vaccines and to improve therapeutic approaches. Our study clearly supports the value of $CD8\alpha^-$ DCs in enhancing humoral immune responses against various human pathogenic antigens. In particular, we utilized $CD8\alpha^-$ DCs to enhance the number of ASCs specific to HBsAg, the immunogen of currently available hepatitis B. Although the current hepatitis B vaccine is very effective, 5~15% of vaccinated patients fail to develop humoral immune responses (Coursaget et al.,

1986, Hadler et al., 1986). CD8α⁻ DC targeting antibody conjugated with HBsAg would be utilized as an alternative for hepatitis B vaccine non-responders. Additionally, in our previous study, successful protection against virulent *Y. pestis* pneumonic plague was observed as we targeted CD8α⁻ DCs with V protein, of which protection efficacy was mainly delivered via the increased anti-V titers (Do et al., 2010), which strongly supports our current study in designing efficient pneumonic plague vaccine by targeting CD8α⁻ DCs. Therefore, the CD8α⁻ DC subset has great potential to be utilized as a preferential target for developing vaccine efficacy in various humoral immunity related diseases.

In conclusion, our study provide insightful facts on how myeloid DC subsets affect Tfh cell fate; it may not be a purely stochastic event as previously suggested (Deenick et al., 2011, Vinuesa and Cyster, 2011, Ballesteros-Tato and Randall, 2013) but instead, the CD8α⁻ DC subset has a selective force to prime the initial commitment of Tfh cells. Our study revealed unknown mechanisms involved in Tfh cell differentiation by the DC subsets, and we believe that our findings along with future efforts to discover human DC subset counterpart of CD8α⁻ DCs will develop efficient vaccines delivering improved quality and quantity of humoral immune responses.

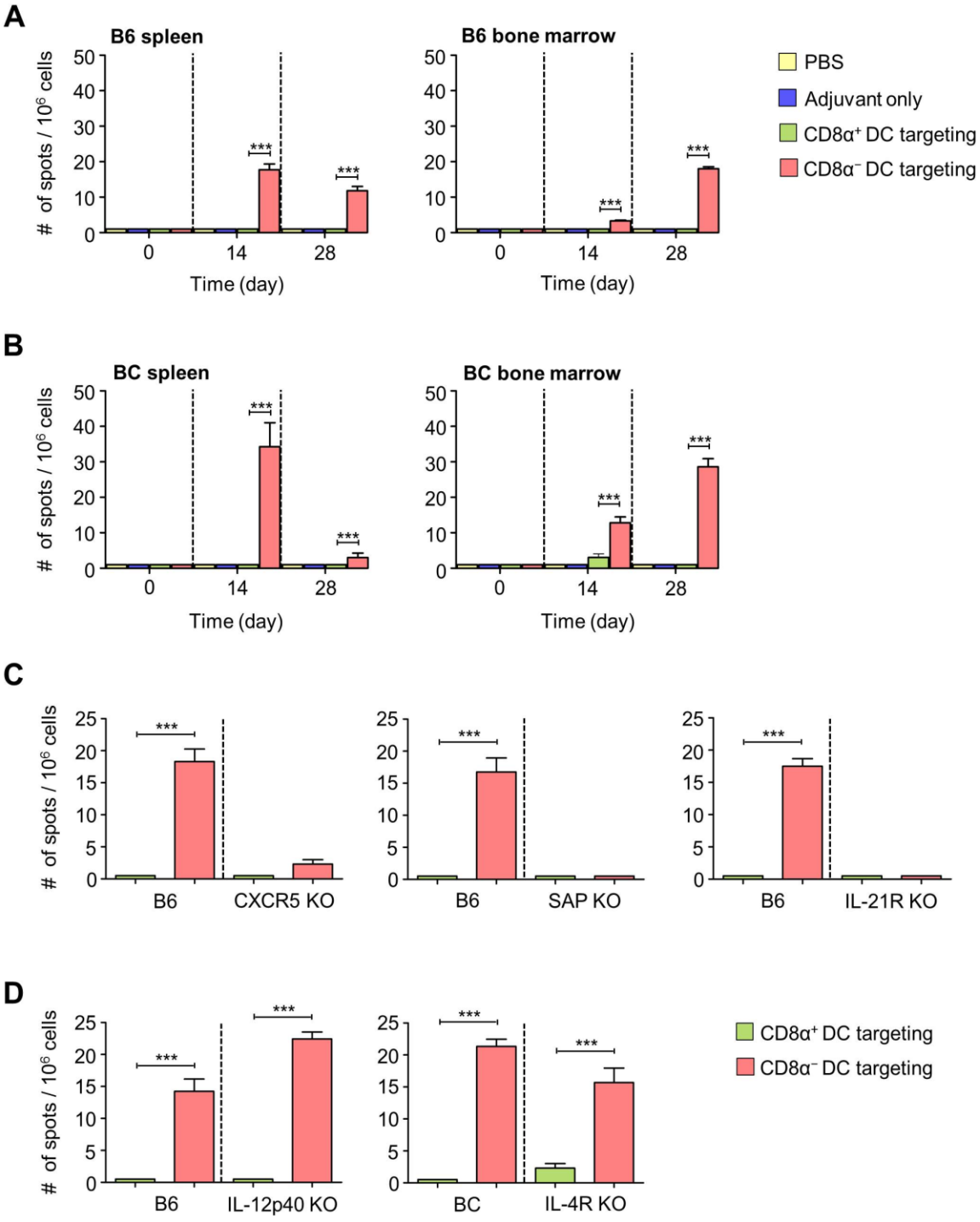

Figure 2-1. CD8α⁻ DCs induce Tfh cell-dependent antibody secreting cells. (**A** and **B**) Naive C57BL6 (B6) (**A**) or BALB/c (BC) (**B**) mice were immunized intraperitoneally (i.p.) with PBS, CD40 monoclonal antibody (mAb) + poly (I:C) (adjuvant only), DEC:V (CD8α$^+$ DC targeting), or DCIR2:V (CD8α$^-$ DC targeting) conjugated mAbs in the presence of CD40 mAb and poly (I:C). At each indicated time point, spleen or bone marrow cells were prepared and anti-V IgG antibody secreting cells (ASCs) were analyzed. (**C** and **D**) CXCR5 KO, SAP KO, IL-21R KO (**C**), IL-12p40 KO, IL-4R KO (**D**), or naïve B6 or BC mice were immunized i.p. with either DEC:V (CD8α$^+$ DC targeting) or DCIR2:V (CD8α$^-$ DC targeting) conjugated mAbs in the presence of CD40 mAb and poly (I:C). Two weeks after the immunization, spleen cells were prepared and anti-V IgG ASCs were analyzed. *** $P < 0.001$. All data represent mean ± s.d. of three or more independent experiments (**A**–**D**, n=3 per group).

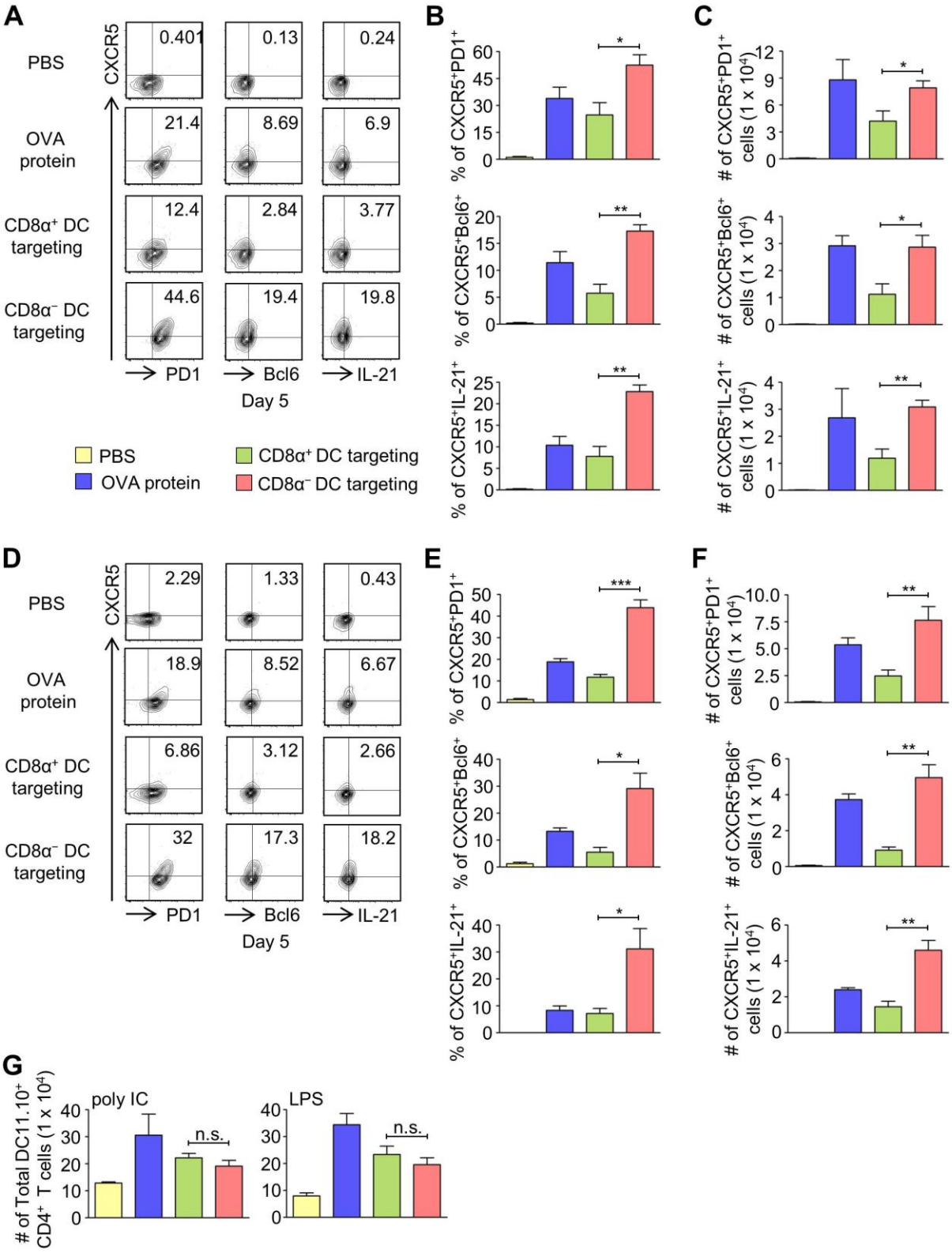

Figure 2-2. CD8α$^-$ DCs efficiently induce Tfh cells *in vivo*. (**A**−**G**) OVA specific DO11.10$^+$Thy1.1$^+$CD4$^+$ T cells were adoptively transferred to naive Thy1.2$^+$ BALB/c mice at day -1, and were immunized subcutaneously (s.c.) with PBS, soluble OVA protein (OVA protein), DEC:OVA (CD8α$^+$ DC targeting), or DCIR2:OVA (CD8α$^-$ DC targeting) conjugated mAbs in the presence of poly (I:C) (**A**−**C**) or LPS (**D**−**F**) at day 0. At each indicated time point after the immunization, lymph node cells were prepared and Tfh cells gated from the DO11.10$^+$CD4$^+$CD44$^+$ T cells were analyzed. (**A** and **D**) Representative FACS plots of CXCR5$^+$PD1$^+$, CXCR5$^+$Bcl6$^+$, or CXCR5$^+$IL-21$^+$ Tfh cells. (**B** and **E**) Percentages (%) of Tfh cells described in (A) and (D), respectively. (**C** and **F**) The number (#) of Tfh cells described in (A) and (D), respectively. (**G**) The total number of DO11.10$^+$CD4$^+$ T cells. Data represent mean ± s.e.m. of three or more independent experiments (**B** and **C**, **E**−**G**). * $P < 0.05$, ** $P < 0.01$, *** $P < 0.001$. (**A**−**G**, n=3-4 per group).

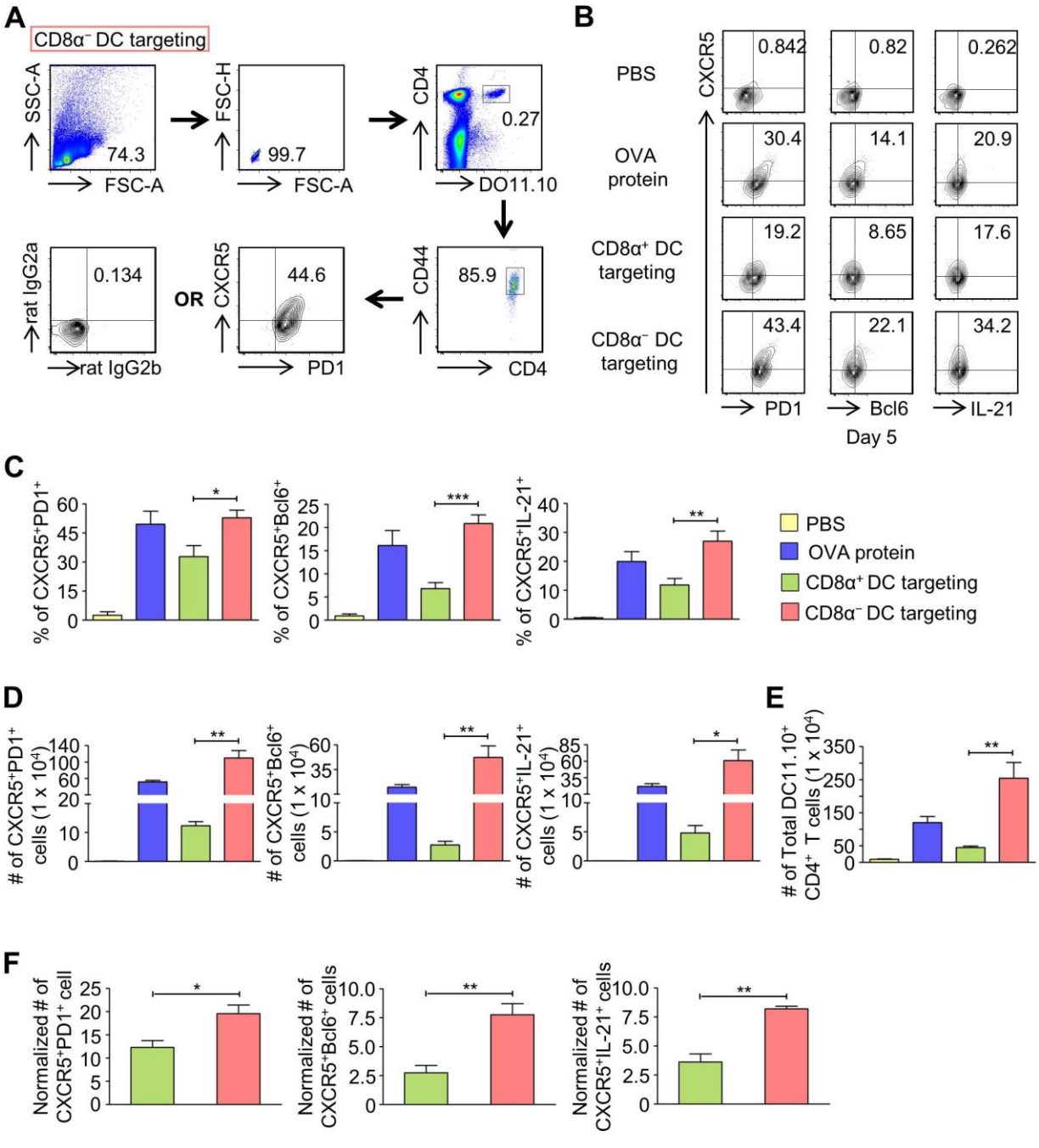

Figure 2-3. Induction of Tfh cells by CD8α$^-$ DCs *in vivo*. (**A**–**F**) OVA specific DO11.10$^+$Thy1.1$^+$CD4$^+$ T cells were adoptively transferred to naive Thy1.2$^+$ BALB/c mice at day -1, and were immunized s.c. with PBS, OVA protein, DEC:OVA (CD8α$^+$ DC targeting), or DCIR2:OVA (CD8α$^-$ DC targeting) conjugated mAbs in the presence of poly (I:C) at day 0. At each indicated time point after the immunization, lymph node (**A**) or spleen cells (**B**–**F**) were prepared and Tfh cells gated from the DO11.10$^+$CD4$^+$CD44$^+$ T cells were analyzed. (**A**) Gating strategy of CXCR5$^+$PD1$^+$ Tfh or isotype control cells analyzed 5 days after the immunization with DCIR2:OVA. (**B**) Representative FACS plots of CXCR5$^+$PD1$^+$, CXCR5$^+$Bcl6$^+$, or CXCR5$^+$IL-21$^+$ Tfh cells. (**C**) Percentages (%) of Tfh cells described in (B). (**D**) The number (#) of Tfh cells described in (B). (**E**) The total number of DO11.10$^+$CD4$^+$ T cells. (**F**) The number of Tfh cells normalized by the total number of DO11.10$^+$CD4$^+$ T cells. Data represent mean ± s.e.m. of three or more independent experiments (**B**–**F**). * $P < 0.05$, ** $P < 0.01$, *** $P < 0.001$. (**A**–**F**, n=3-4 per group).

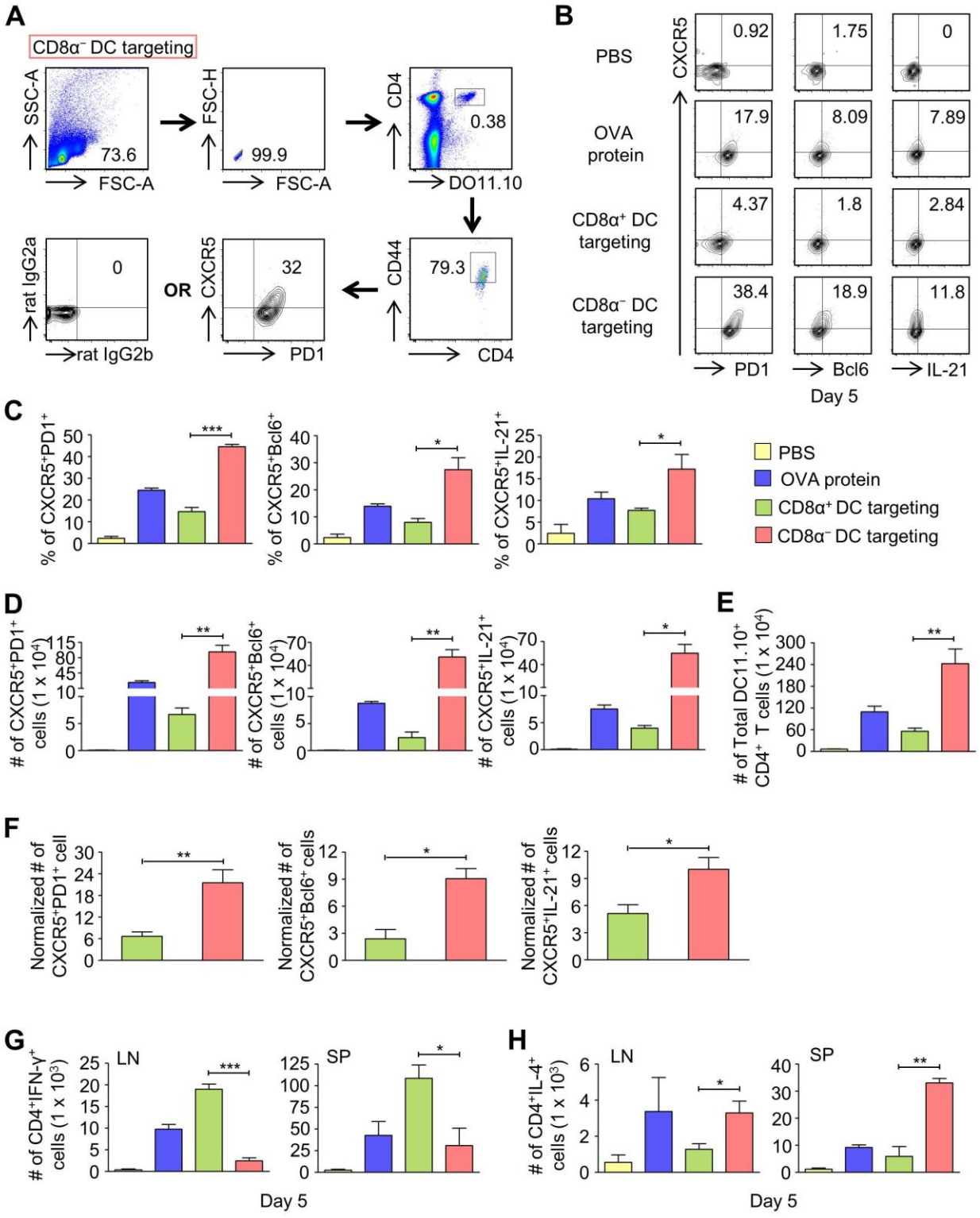

Figure 2-4. Induction of Tfh cells by CD8α⁻ DCs *in vivo*. (**A**–**H**) OVA specific DO11.10$^+$Thy1.1$^+$CD4$^+$ T cells were adoptively transferred to naive Thy1.2$^+$ BALB/c mice at day -1, and were immunized s.c. with PBS, OVA protein, DEC:OVA (CD8α$^+$ DC targeting), or DCIR2:OVA (CD8α$^-$ DC targeting) conjugated mAbs in the presence of LPS at day 0. At each indicated time point after the immunization, lymph node (**A** and **G** and **H**) or spleen cells (**B**–**H**) were prepared and Tfh cells gated from the DO11.10$^+$CD4$^+$CD44$^+$ T cells were analyzed. (**A**) Gating strategy of CXCR5$^+$PD1$^+$ Tfh or isotype control cells analyzed 5 days after the immunization with DCIR2:OVA. (**B**) Representative FACS plots of CXCR5$^+$PD1$^+$, CXCR5$^+$Bcl6$^+$, or CXCR5$^+$IL-21$^+$ Tfh cells. (**C**) Percentages (%) of Tfh cells described in (B). (**D**) The number (#) of Tfh cells described in (B). (**E**) The total number of DO11.10$^+$CD4$^+$ T cells. (**F**) The number of Tfh cells normalized by the total number of DO11.10$^+$CD4$^+$ T cells. (**G** and **H**) The number of CD4$^+$IFN-γ$^+$ (**G**) or CD4$^+$IL-4$^+$ (**H**) T cells obtained either from the lymph nodes (LN) or the spleen (SP). Data represent mean ± s.e.m. of three or more independent experiments (**B**–**H**). * $P < 0.05$, ** $P < 0.01$, *** $P < 0.001$. (**A**–**H**, n=3-4 per group).

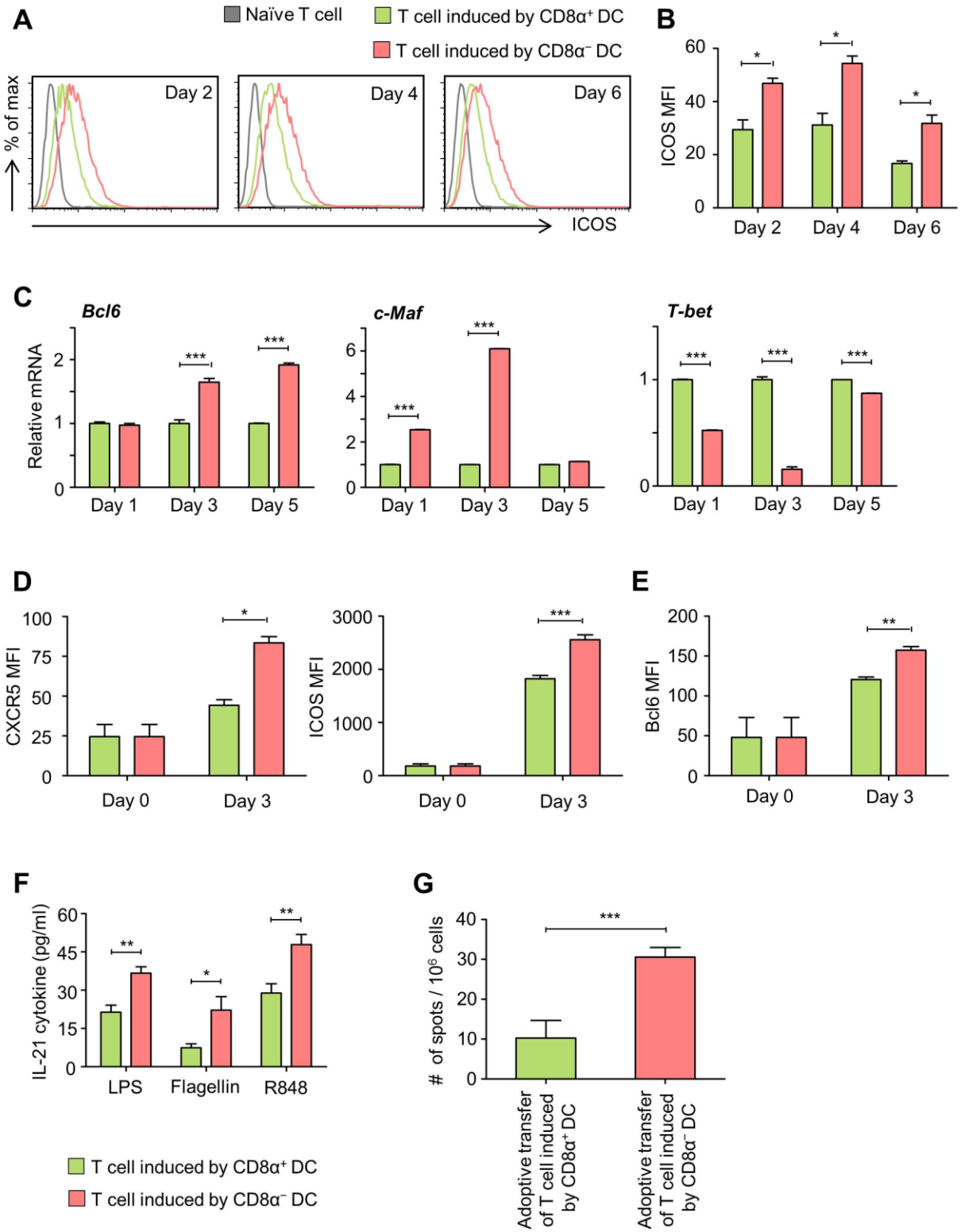

Figure 2-5. CD8α^- DCs induce Tfh cells *in vitro*. (**A**−**G**) OT-II OVA specific Vα2$^+$CD4$^+$ T cells were co-cultured with each DC subset in the presence of OVA peptide (323-339) with poly (I:C) (**A**−**C** and **G**), LPS (**D** and **E**), or LPS, Flagellin or R848 (**F**). At each indicated time point after the co-culture, Vα2$^+$CD4$^+$CD44$^+$ T cells were analyzed. (**A**) Representative histograms of ICOS expression. (**B**) Median fluorescence intensity (MFI) of three independent experiments described in (A), mean ± s.e.m. (**C**) The relative mRNA expression of *Bcl6*, *c-Maf* or *T-bet*. (**D** and **E**) MFI of CXCR5, ICOS (**D**) and Bcl6 (**E**). (**F**) IL-21 production. (**G**) Three days after the co-culture, Vα2$^+$CD4$^+$CD44$^+$ T cells were sorted and adoptively transferred together with naïve CD19$^+$ B cells to RAG-1-deficient mice. Fourteen days after the boost immunization with OVA protein, spleen cells were prepared and anti-IgG ASCs were analyzed (n=2 per group). * $P < 0.05$, ** $P < 0.01$, *** $P < 0.001$. Data represent mean ± s.e.m of three or more (**C**−**F**) or two (**G**) independent experiments.

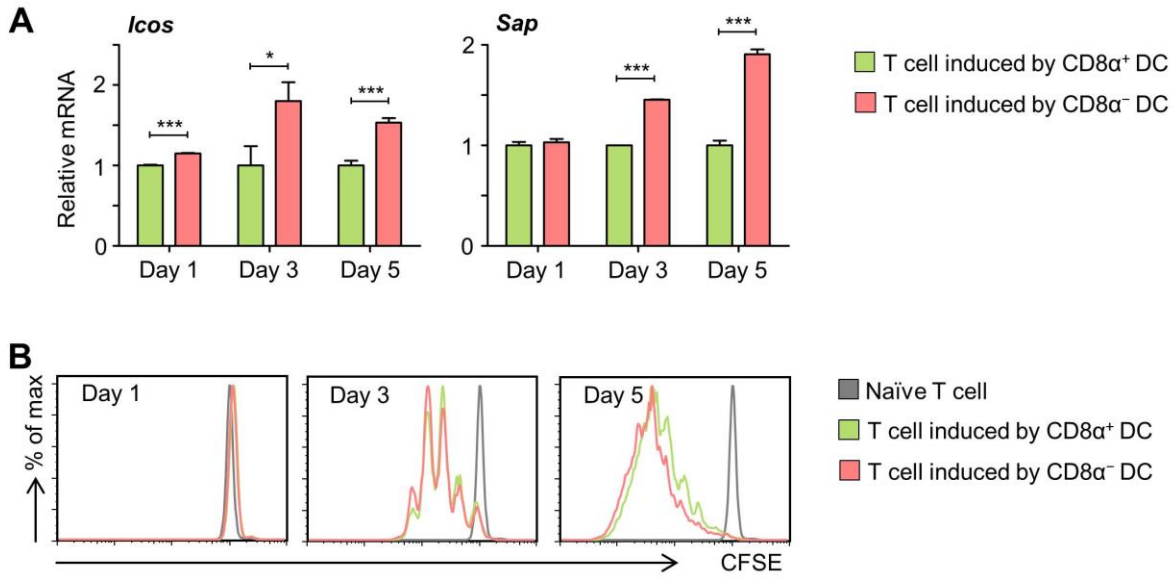

Figure 2-6. Induction of Tfh cells by CD8α⁻ DCs *in vitro*. OT-II OVA specific Vα2$^+$CD4$^+$ T cells were co-cultured with each DC subset in the presence of OVA peptide (323-339) and poly (I:C). At each indicated time point after the co-culture, Vα2$^+$CD4$^+$CD44$^+$ T cells were analyzed. (**A**) Relative mRNA expressions of *Icos* and *Sap*. * $P < 0.05$, *** $P < 0.001$. Data represent mean ± s.e.m. of three independent experiments. (**B**) Proliferation of OT-II OVA specific Vα2$^+$CD4$^+$ T cells analyzed by CFSE dilution assay. Data are representative of three independent experiments.

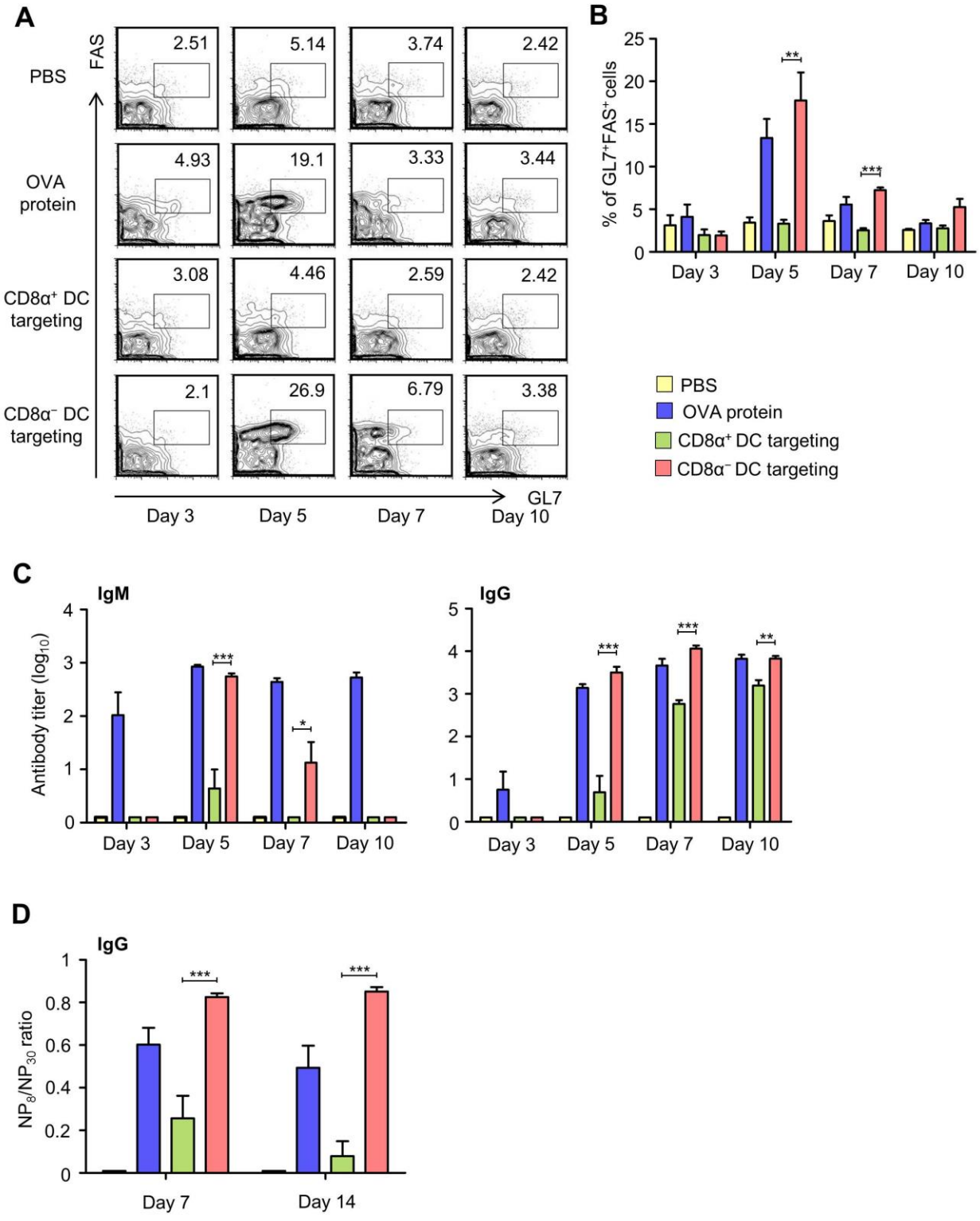

Figure 2-7. CD8α⁻ DCs enhance the formation of GC B cells and antibody titers. (**A**−**D**) OVA specific DO11.10^{+}Thy1.1^{+}CD4^{+} T cells were adoptively transferred to naive Thy1.2^{+} BALB/c mice at day -1, and were immunized s.c. with PBS, OVA protein, DEC:OVA (CD8α^{+} DC targeting), or DCIR2:OVA (CD8α^{-} DC targeting) conjugated mAbs in the presence of poly (I:C) (**A**−**C**) or LPS (**D**) at day 0. At each indicated time point after the immunization, spleen cells (**A** and **B**) or sera (**C** and **D**) were prepared for analysis. (**A**) Representative FACS plots of GL7^{+}FAS^{+} GC B cells gated from CD19^{+}IgD^{-} splenocytes. (**B**) Data represent mean ± s.e.m. of four independent experiments described in (A). (**C**) ELISA analyses of OVA−specific serum IgM or IgG antibodies. (**D**) Ten days after the immunization, each group was re-immunized with NP_{16}-OVA (day 0). ELISA of NP-specific serum IgG antibodies (NP_8/NP_{30}). * $P < 0.05$, ** $P < 0.01$, *** $P < 0.001$. Data represent mean ± s.e.m. of four (**C** and **D**) independent experiments. (**A**−**D**, n=3-4 per group).

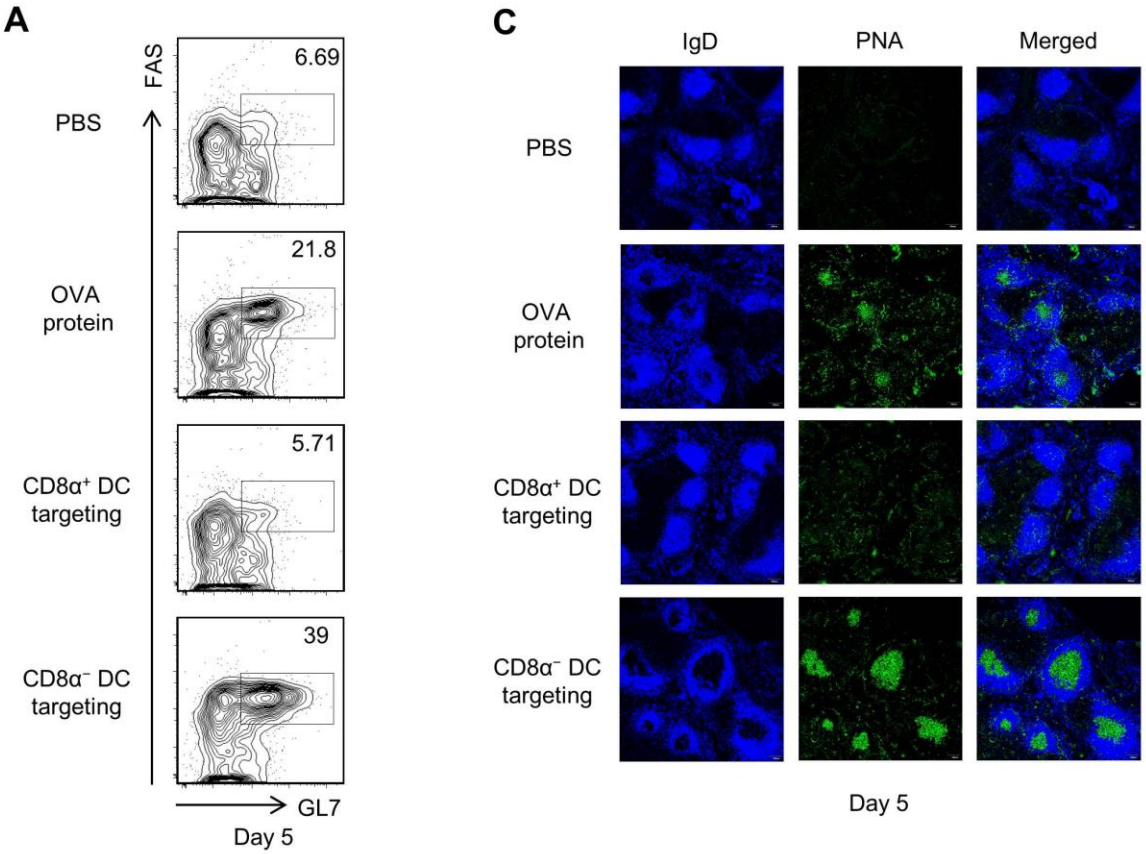

Figure 2-8. GC B cell and Germinal Center formation induced by CD8α$^-$ DCs. (**A**−**C**) OVA specific DO11.10$^+$Thy1.1$^+$CD4$^+$ T cells were adoptively transferred to naive Thy1.2$^+$ BALB/c mice at day -1, and were immunized s.c. with PBS, OVA protein, DEC:OVA (CD8α$^+$ DC targeting), or DCIR2:OVA (CD8α$^-$ DC targeting) conjugated mAbs in the presence of LPS at day 0. 5 days after the immunization, spleen cells were prepared for analysis. (**A**) Representative FACS plots of GL7$^+$FAS$^+$ GC B cells gated from CD19$^+$IgD$^-$ splenocytes. (n=4 per group). (**B**) Data represent mean ± s.e.m. of five independent experiments described in (A). (**C**) Immunohistochemical staining of spleen sections from each indicated group (IgD, blue; PNA, green). Data are representative of three or more independent experiments. (n >10 per group).

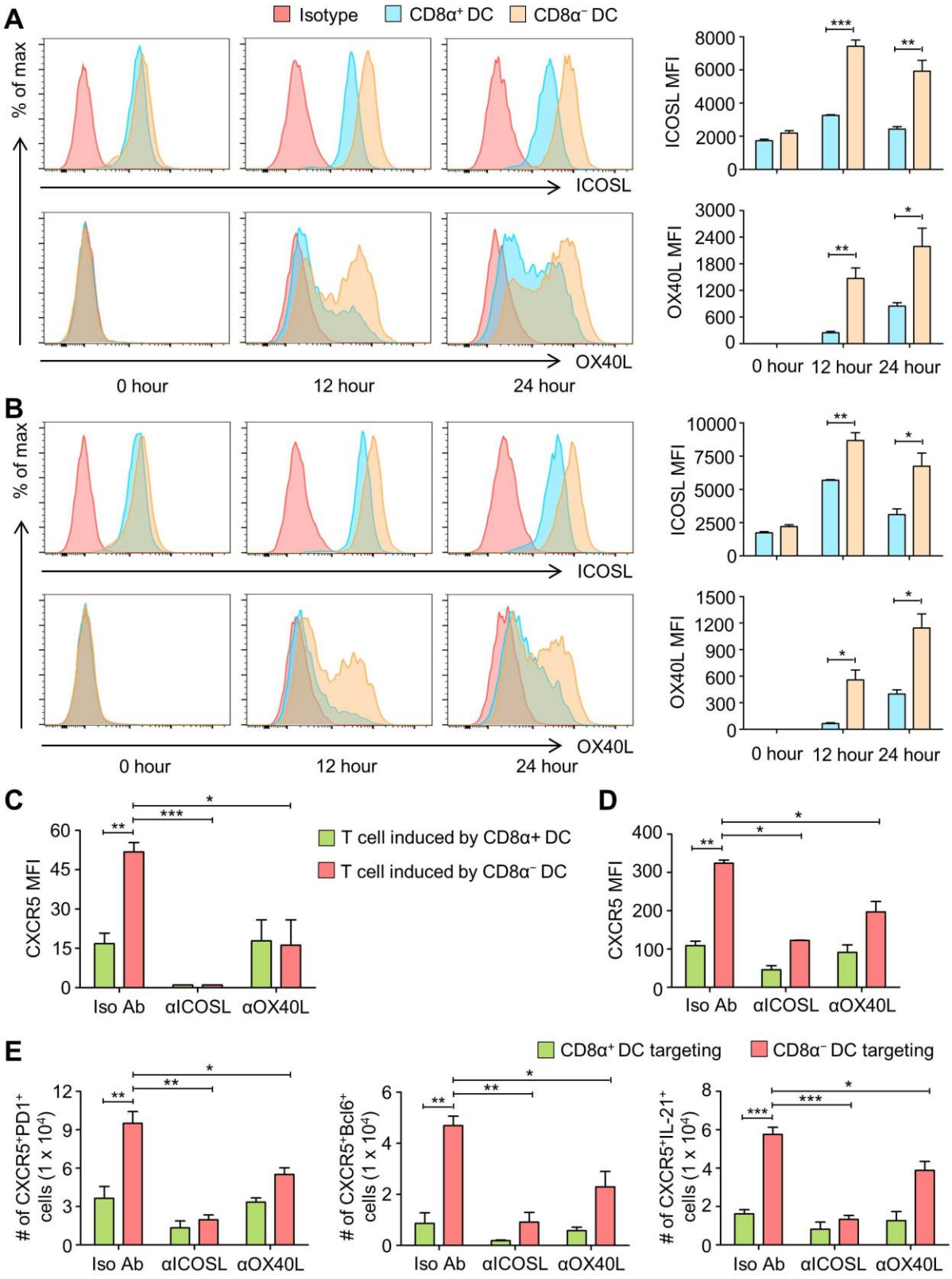

Figure 2-9. **The increased number of Tfh cells was induced by the enhanced expressions of ICOSL and OX40L on CD8α$^-$ DCs.** (**A** and **B**) Sorted DC subsets were stimulated either with poly (I:C) (**A**) or LPS (**B**) for 0, 12, 24 hours *in vitro*. Representative histograms of ICOSL and OX40L. MFIs represent mean ± s.e.m. of three independent experiments. (**C**) OT-II OVA specific Vα2$^+$CD4$^+$ T cells were co-cultured with each DC subset with OVA peptide (323-339) and LPS in the presence of ICOSL or OX40L blocking (αICOSL or αOX40L) mAbs or Isotype mAbs (Iso Ab) for 3 days. MFI of CXCR5 was analyzed from three independent experiments, mean ± s.e.m. (**D** and **E**) OVA specific DO11.10$^+$Thy1.1$^+$CD4$^+$ T cells were adoptively transferred to naive Thy1.2$^+$ BALB/c mice at day -1, and were immunized s.c. with either DEC:OVA (CD8α$^+$ DC targeting) or DCIR2:OVA (CD8α$^-$ DC targeting) conjugated mAbs in the presence of LPS at day 0. ICOSL or OX40L blocking mAbs (αICOSL or αOX40L) or Isotype mAbs (Iso Ab) were injected intravenously (i.v.) to the immunized mice at day 0 and 2. Four days after the immunization, lymph nodes cells were prepared. MFI of CXCR5 (**D**) and the number of CXCR5$^+$PD1$^+$, CXCR5$^+$Bcl61$^+$, or CXCR5$^+$IL-21$^+$ Tfh cells (**E**) were analyzed from three independent experiments, mean ± s.e.m. (n=4 per group). * $P < 0.05$, ** $P < 0.01$, *** $P < 0.001$.

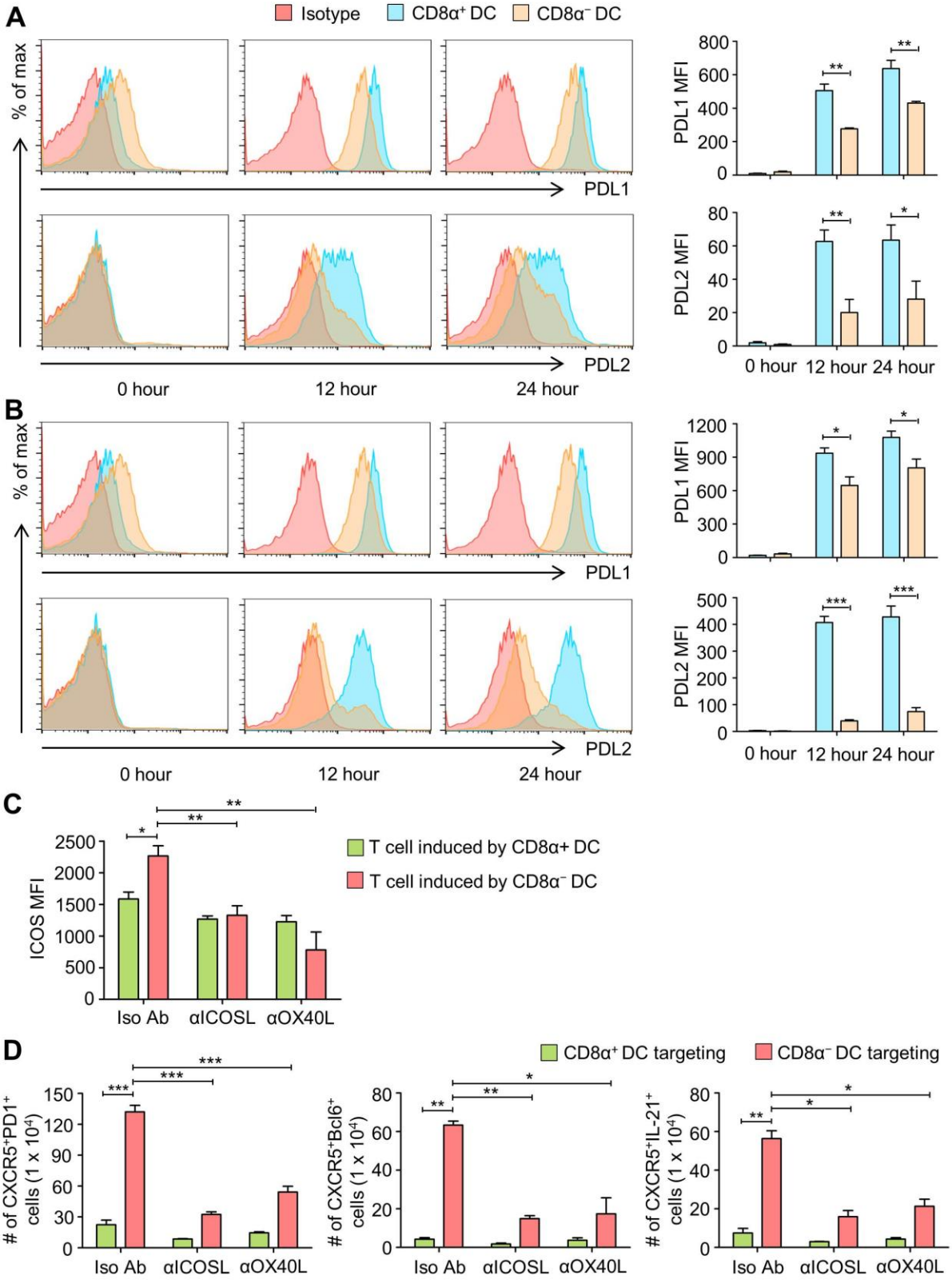

Figure 2-10. Induction of Tfh cells by the enhanced expressions of ICOSL and OX40L on CD8α$^-$ DCs. (**A** and **B**) Sorted DC subsets were stimulated either with poly (I:C) (**A**) or LPS (**B**) for 0, 12, 24 hours *in vitro*. Representative histograms of PDL1 and PDL2. MFIs represent mean ± s.e.m. of three independent experiments. (**C**) OT-II OVA specific Vα2$^+$CD4$^+$ T cells were co-cultured with each DC subset with OVA peptide (323-339) and poly (I:C) in the presence of ICOSL or OX40L blocking (αICOSL or αOX40L) mAbs or Isotype mAbs (Iso Ab) for 3 days. MFI of ICOS was analyzed from three independent experiments, mean ± s.e.m. (**D**) OVA specific DO11.10$^+$Thy1.1$^+$CD4$^+$ T cells were adoptively transferred to naive Thy1.2$^+$ BALB/c mice at day -1, and were immunized s.c. with either DEC:OVA (CD8α$^+$ DC targeting) or DCIR2:OVA (CD8α$^-$ DC targeting) conjugated mAbs in the presence of LPS at day 0. ICOSL or OX40L blocking mAbs (αICOSL or αOX40L) or Isotype mAbs (Iso Ab) were injected intravenously (i.v.) to the immunized mice at day 0 and 2. Four days after the immunization, spleen cells were prepared. The number of CXCR5$^+$PD1$^+$, CXCR5$^+$Bcl61$^+$, or CXCR5$^+$IL-21$^+$ Tfh cells were calculated from two or three independent experiments, mean ± s.e.m. (n=4 per group). * $P < 0.05$, ** $P < 0.01$, *** $P < 0.001$.

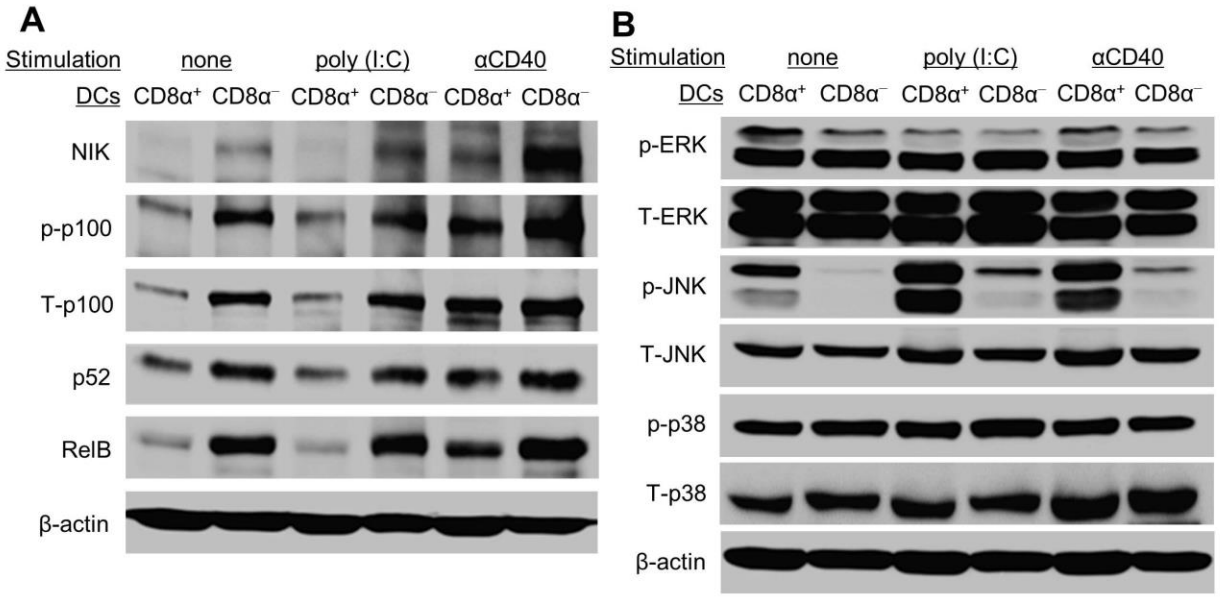

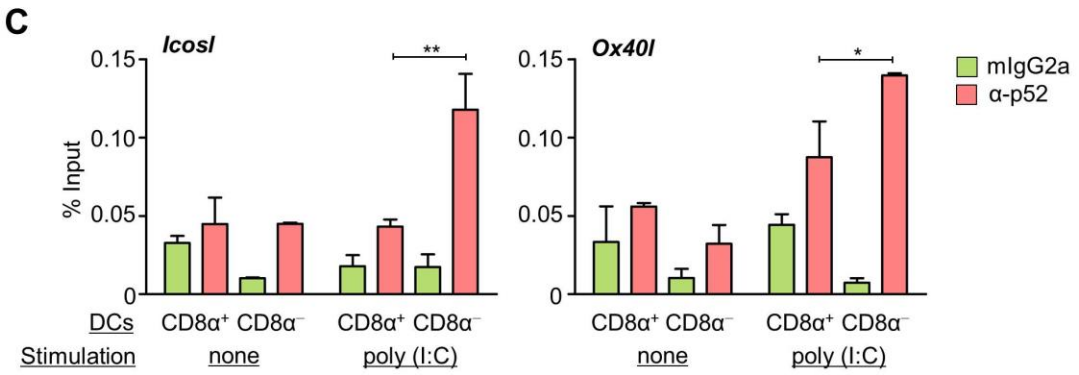

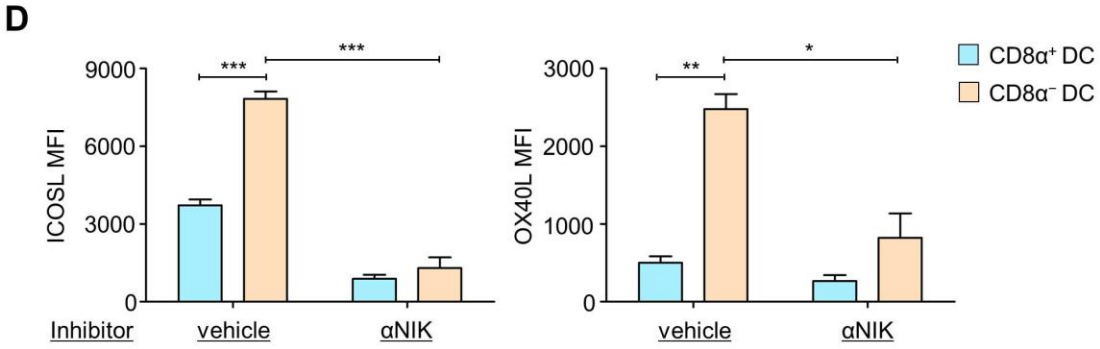

Figure 2-11. **CD8α$^-$ DCs induce high expressions of ICOSL and OX40L via enhanced non-canonical NF-κB signaling pathway.** (**A** and **B**) Sorted DC subsets were stimulated with either poly (I:C) or αCD40 for 2 hours *in vitro* followed by western blot analysis of non-canonical NF-κB-(**A**) or MAPK- (**B**) pathway related molecules. Phosphorylation (p), Total (T). (**C**) ChIP-PCR shows percent (%) input of p52 upstream of *Icosl* and *Ox40l* in the DC subsets in the absence or the presence of stimulation. Data are representative of three (**A** and **B**) or two (**C**) independent experiments (mean ± s.d.). (**D**) The two DC subsets were treated with either DMSO (vehicle) or a NIK inhibitor (αNIK) for 12 hours in the presence of poly (I:C) and the MFI of ICOSL or OX40L was analyzed. Data represent mean ± s.e.m. of three (ICOSL) or two (OX40L) independent experiments. * $P < 0.05$, ** $P < 0.01$, *** $P < 0.001$.

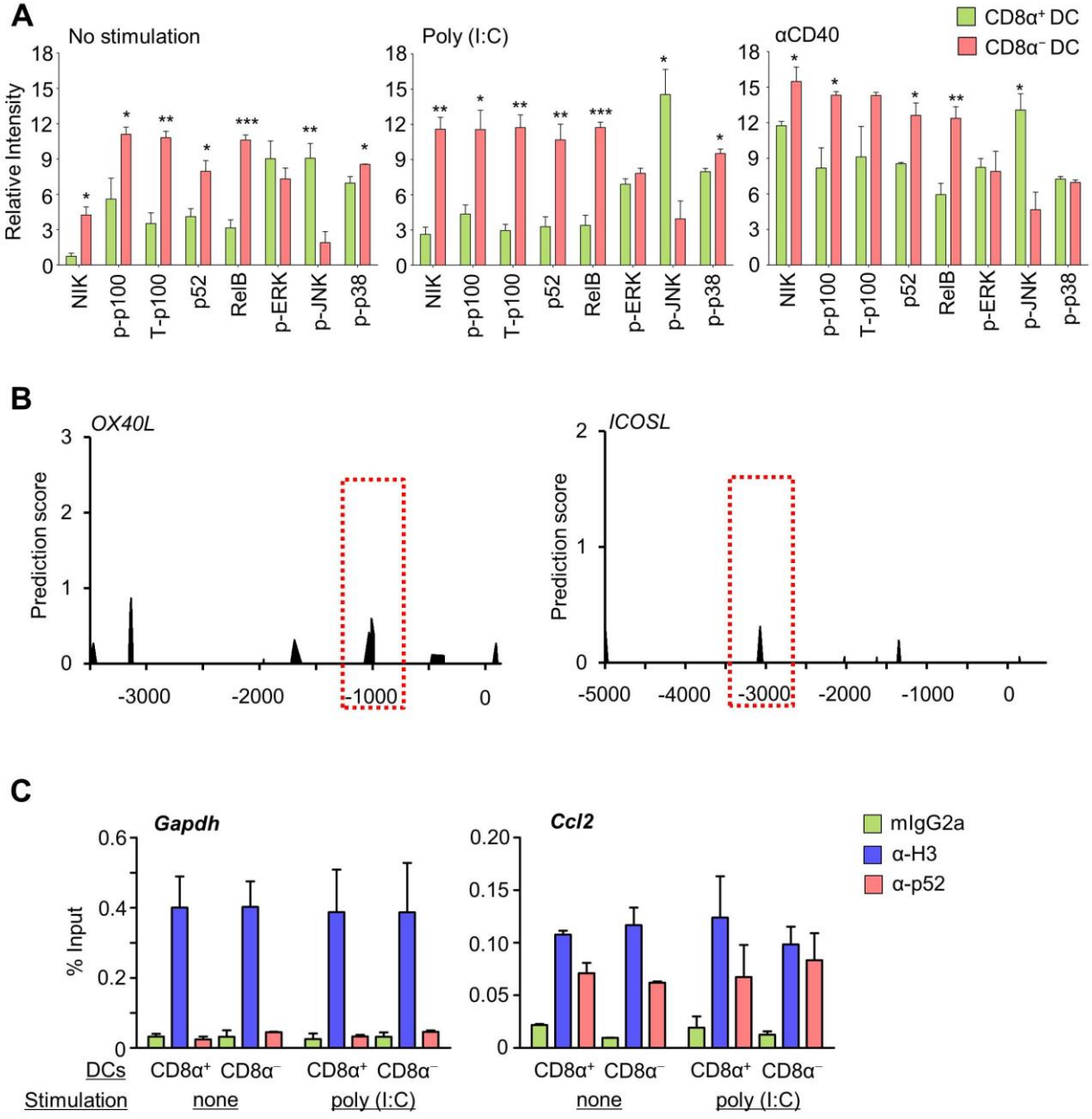

Figure 2-12. Western blot and chip analysis. (**A**) Quantitative and relative density of western blot analyses described in Figure 6A and 6B represent mean ± s.e.m. of three independent experiments. Phosphorylation (p), Total (T). (**B**) Predicted NF-κB complex binding site on the upstream regions of *OX40L* and *ICOSL* gene promoter. The predicted NF-κB complex binding sites were analyzed by NF-κB binding motif computation method (Britanova et al., 2008). Six major areas of NF-κB complex binding sites (-50, -500, -1000, -1700, -3200 and -3500) were identified on the upstream region of *OX40L* and three major areas of NF-κB complex binding sites (-1300, -3000 and -5000) were identified on the upstream region of *ICOSL*. Red dotted lines are the sites where are confirmed by Chip-qPCR. (**C**) ChIP-PCR shows percent (%) input of p52 upstream of *Gapdh* (negative control) and *Ccl2* (positive control) in the two DC subsets in the absence or the presence of stimulation. Data are representative of two independent experiments, mean ± s.d.

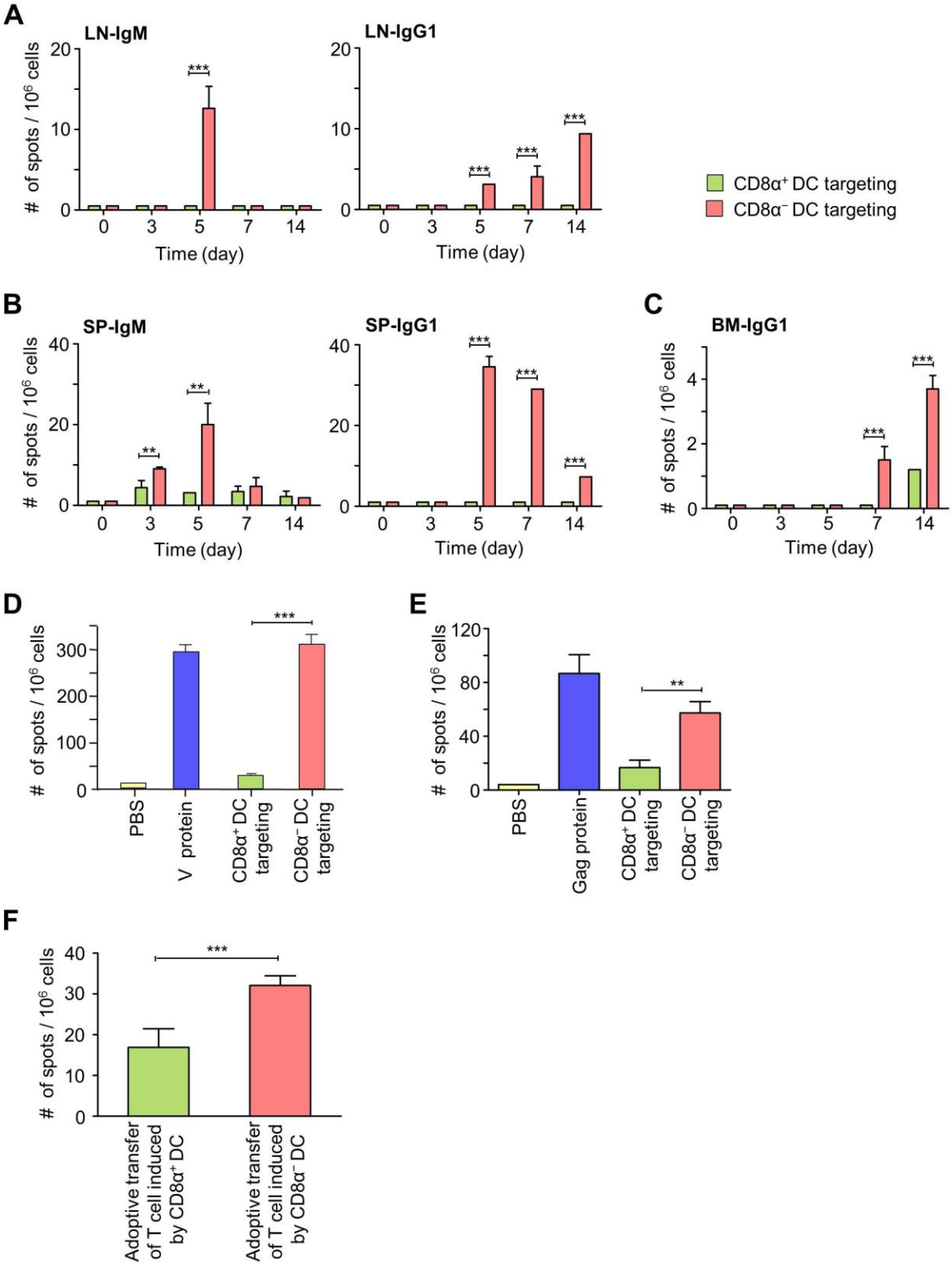

Figure 2-13. CD8α⁻ DCs enhance Tfh cell dependent-humoral immune responses against various human antigens. (**A**–**C**) BALB/c mice were immunized i.p. with either DEC:V ($CD8\alpha^+$ DC targeting) or DCIR2:V ($CD8\alpha^-$ DC targeting) conjugated mAbs in the presence of CD40 mAb and poly (I:C). At each indicated time point after the immunization, cells from the lymph nodes (LN) (**A**), spleen (SP) (**B**), or the bone marrow (BM) (**C**) were prepared and anti-V (IgM or IgG1) ASCs were analyzed. (**D**) BALB/c mice were primed and boosted with PBS, F1-V protein with alhydrogel (V protein), DEC:V ($CD8\alpha^+$ DC targeting), or DCIR2:V ($CD8\alpha^-$ DC targeting) conjugated mAbs in the presence of poly (I:C). Six months later, bone marrow cells were prepared and anti-V ASCs were analyzed. (**E**) B6 mice were primed and boosted i.p. with PBS, Gagp41 protein (Gag protein), DEC:gagp24 ($CD8\alpha^+$ DC targeting), or DCIR2:gagp24 ($CD8\alpha^-$ DC targeting) conjugated mAbs in the presence of poly (I:C). Two weeks after the boost, bone marrow cells were prepared and anti-gagp24 ASCs cells were analyzed. (**F**) Naive $CD4^+$ T cells co-cultured with each DC subset in the presence of poly (I:C) for 3 days were isolated and then adoptively transferred together with naïve $CD19^+$ B cells to RAG-1-deficient mice. Fourteen days after the boost immunization with soluble HBsAg, spleen cells were prepared and anti-IgG HBsAg ASCs were analyzed. ** $P < 0.01$, *** $P < 0.001$. All data represent mean ± s.d. of three or more independent experiments (**A**–**F,** n=3 per group).

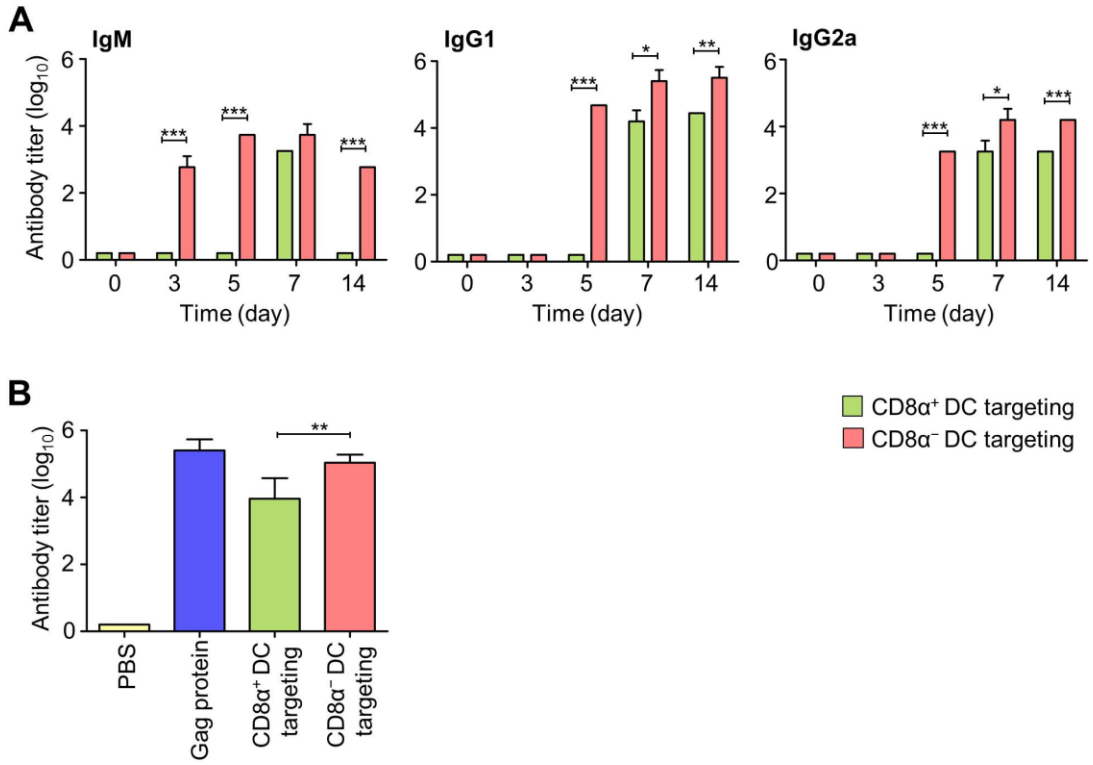

Figure 2-14. Induction of Tfh cell dependent-humoral immune responses by CD8α⁻ DCs. (**A**) ELISA analyses of V-specific serum antibodies collected from the mice described in Figure 7A. (**B**) ELISA of Gag-specific serum antibodies collected from the mice described in Figure 7E. * $P < 0.05$, ** $P < 0.01$, *** $P < 0.001$. All data represent mean ± s.d. of three or more independent experiments (**A** and **B,** n=3 mice per group).

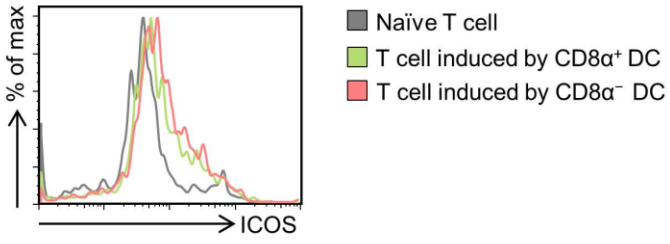

Figure 2-15. ICOS expression on the CD4$^+$ T cells induced by the two DC subsets with HBsAg. Representative histograms of the expression of ICOS on the CD4$^+$ T cells induced by the two DC subsets in the presence of HBsAg. Data are representative of three independent experiments.

References

AKIBA, H., TAKEDA, K., KOJIMA, Y., USUI, Y., HARADA, N., YAMAZAKI, T., MA, J., TEZUKA, K., YAGITA, H. & OKUMURA, K. 2005. The role of ICOS in the CXCR5+ follicular B helper T cell maintenance in vivo. *J Immunol,* 175**,** 2340-8.

BALLESTEROS-TATO, A. & RANDALL, T. D. 2013. Priming of T follicular helper cells by dendritic cells. *Immunol Cell Biol*.

BAUMJOHANN, D., OKADA, T. & ANSEL, K. M. 2011. Cutting Edge: Distinct waves of BCL6 expression during T follicular helper cell development. *J Immunol,* 187**,** 2089-92.

BAUQUET, A. T., JIN, H., PATERSON, A. M., MITSDOERFFER, M., HO, I. C., SHARPE, A. H. & KUCHROO, V. K. 2009. The costimulatory molecule ICOS regulates the expression of c-Maf and IL-21 in the development of follicular T helper cells and TH-17 cells. *Nat Immunol,* 10**,** 167-75.

BREITFELD, D., OHL, L., KREMMER, E., ELLWART, J., SALLUSTO, F., LIPP, M. & FORSTER, R. 2000. Follicular B helper T cells express CXC chemokine receptor 5, localize to B cell follicles, and support immunoglobulin production. *J Exp Med,* 192**,** 1545-52.

BRITANOVA, L. V., MAKEEV, V. J. & KUPRASH, D. V. 2008. In vitro selection of optimal RelB/p52 DNA-binding motifs. *Biochem Biophys Res Commun,* 365**,** 583-8.

BROCKER, T., GULBRANSON-JUDGE, A., FLYNN, S., RIEDINGER, M., RAYKUNDALIA, C. & LANE, P. 1999. CD4 T cell traffic control: in vivo evidence that ligation of OX40 on CD4 T cells by OX40-ligand expressed on dendritic cells leads to the accumulation of CD4 T cells in B follicles. *Eur J Immunol,* 29**,** 1610-6.

CANNONS, J. L., QI, H., LU, K. T., DUTTA, M., GOMEZ-RODRIGUEZ, J., CHENG, J., WAKELAND, E. K., GERMAIN, R. N. & SCHWARTZBERG, P. L. 2010. Optimal germinal center responses require a multistage T cell:B cell adhesion process involving integrins, SLAM-associated protein, and CD84. *Immunity,* 32**,** 253-65.

CHAKAROV, S. & FAZILLEAU, N. 2014. Monocyte-derived dendritic cells promote T follicular helper cell differentiation. *EMBO Mol Med,* 6**,** 590-603.

CHAPPELL, C. P., DRAVES, K. E., GILTIAY, N. V. & CLARK, E. A. 2012. Extrafollicular B cell activation by marginal zone dendritic cells drives T cell-dependent antibody responses. *J Exp Med,* 209**,** 1825-40.

CHOI, Y. S., KAGEYAMA, R., ETO, D., ESCOBAR, T. C., JOHNSTON, R. J., MONTICELLI, L., LAO, C. & CROTTY, S. 2011. ICOS receptor instructs T follicular helper cell versus effector cell differentiation via induction of the transcriptional repressor Bcl6. *Immunity,* 34**,** 932-46.

COOPE, H. J., ATKINSON, P. G., HUHSE, B., BELICH, M., JANZEN, J., HOLMAN, M. J., KLAUS, G. G., JOHNSTON, L. H. & LEY, S. C. 2002. CD40 regulates the processing of NF-kappaB2 p100 to p52. *EMBO J,* 21**,** 5375-85.

COURSAGET, P., YVONNET, B., CHOTARD, J., SARR, M., VINCELOT, P., N'DOYE, R., DIOP-MAR, I. & CHIRON, J. P. 1986. Seven-year study of hepatitis B vaccine efficacy in infants from an endemic area (Senegal). *Lancet,* 2**,** 1143-5.

CROTTY, S. 2011. Follicular helper CD4 T cells (TFH). *Annu Rev Immunol,* 29**,** 621-63.

CUBAS, R. A., MUDD, J. C., SAVOYE, A. L., PERREAU, M., VAN GREVENYNGHE, J., METCALF, T., CONNICK, E., MEDITZ, A., FREEMAN, G. J., ABESADA-TERK, G., JR., JACOBSON, J. M., BROOKS, A. D., CROTTY, S., ESTES, J. D., PANTALEO, G., LEDERMAN, M. M. & HADDAD, E. K. 2013. Inadequate T follicular cell help impairs B cell immunity during HIV infection. *Nat Med,* 19**,** 494-9.

CUCAK, H., YRLID, U., REIZIS, B., KALINKE, U. & JOHANSSON-LINDBOM, B. 2009. Type I interferon signaling in dendritic cells stimulates the development of lymph-node-resident T follicular helper cells. *Immunity,* 31**,** 491-501.

DEENICK, E. K., CHAN, A., MA, C. S., GATTO, D., SCHWARTZBERG, P. L., BRINK, R. & TANGYE, S. G. 2010. Follicular helper T cell differentiation requires continuous antigen presentation that is independent of unique B cell signaling. *Immunity,* 33**,** 241-53.

DEENICK, E. K., MA, C. S., BRINK, R. & TANGYE, S. G. 2011. Regulation of T follicular helper cell formation and function by antigen presenting cells. *Curr Opin Immunol,* 23**,** 111-8.

DEN HAAN, J. M., LEHAR, S. M. & BEVAN, M. J. 2000. CD8(+) but not CD8(-) dendritic cells cross-prime cytotoxic T cells in vivo. *J Exp Med,* 192**,** 1685-96.

DO, Y., KOH, H., PARK, C. G., DUDZIAK, D., SEO, P., MEHANDRU, S., CHOI, J. H., CHEONG, C., PARK, S., PERLIN, D. S., POWELL, B. S. & STEINMAN, R. M. 2010. Targeting of LcrV virulence protein from Yersinia pestis to dendritic cells protects mice against pneumonic plague. *Eur J Immunol,* 40**,** 2791-6.

DUDZIAK, D., KAMPHORST, A. O., HEIDKAMP, G. F., BUCHHOLZ, V. R., TRUMPFHELLER, C., YAMAZAKI, S., CHEONG, C., LIU, K., LEE, H. W., PARK, C. G., STEINMAN, R. M. & NUSSENZWEIG, M. C. 2007. Differential antigen processing by dendritic cell subsets in vivo. *Science,* 315**,** 107-11.

FILLATREAU, S. & GRAY, D. 2003. T cell accumulation in B cell follicles is regulated by dendritic cells and is independent of B cell activation. *J Exp Med,* 197**,** 195-206.

GOENKA, R., BARNETT, L. G., SILVER, J. S., O'NEILL, P. J., HUNTER, C. A., CANCRO, M. P. & LAUFER, T. M. 2011. Cutting edge: dendritic cell-restricted antigen presentation initiates the follicular helper T cell program but cannot complete ultimate effector differentiation. *J Immunol,* 187**,** 1091-5.

GOODNOW, C. C., VINUESA, C. G., RANDALL, K. L., MACKAY, F. & BRINK, R. 2010. Control systems and decision making for antibody production. *Nat Immunol,* 11**,** 681-8.

HADLER, S. C., FRANCIS, D. P., MAYNARD, J. E., THOMPSON, S. E., JUDSON, F. N., ECHENBERG, D. F., OSTROW, D. G., O'MALLEY, P. M., PENLEY, K. A., ALTMAN, N. L. & ET AL. 1986. Long-term immunogenicity and efficacy of hepatitis B vaccine in homosexual men. *N Engl J Med,* 315**,** 209-14.

HAMS, E., MCCARRON, M. J., AMU, S., YAGITA, H., AZUMA, M., CHEN, L. & FALLON, P. G. 2011. Blockade of B7-H1 (programmed death ligand 1) enhances humoral immunity by positively regulating the generation of T follicular helper cells. *J Immunol,* 186**,** 5648-55.

HAYNES, N. M., ALLEN, C. D., LESLEY, R., ANSEL, K. M., KILLEEN, N. & CYSTER, J. G. 2007. Role of CXCR5 and CCR7 in follicular Th cell positioning and appearance of a programmed cell death gene-1high germinal center-associated subpopulation. *J Immunol,* 179**,** 5099-108.

HU, H., WU, X., JIN, W., CHANG, M., CHENG, X. & SUN, S. C. 2011. Noncanonical NF-kappaB regulates inducible costimulator (ICOS) ligand expression and T follicular helper cell development. *Proc Natl Acad Sci U S A,* 108**,** 12827-32.

IYODA, T., SHIMOYAMA, S., LIU, K., OMATSU, Y., AKIYAMA, Y., MAEDA, Y., TAKAHARA, K., STEINMAN, R. M. & INABA, K. 2002. The CD8+ dendritic cell subset selectively endocytoses dying cells in culture and in vivo. *J Exp Med,* 195**,** 1289-302.

JOHNSTON, R. J., POHOLEK, A. C., DITORO, D., YUSUF, I., ETO, D., BARNETT, B., DENT, A. L., CRAFT, J. & CROTTY, S. 2009. Bcl6 and Blimp-1 are reciprocal and antagonistic regulators of T follicular helper cell differentiation. *Science,* 325**,** 1006-10.

KAPLAN, M. H., SCHINDLER, U., SMILEY, S. T. & GRUSBY, M. J. 1996. Stat6 is required for mediating responses to IL-4 and for development of Th2 cells. *Immunity,* 4**,** 313-9.

KLECHEVSKY, E., MORITA, R., LIU, M., CAO, Y., COQUERY, S., THOMPSON-SNIPES, L., BRIERE, F., CHAUSSABEL, D., ZURAWSKI, G., PALUCKA, A. K., REITER, Y., BANCHEREAU, J. & UENO, H. 2008. Functional specializations of human epidermal Langerhans cells and CD14+ dermal dendritic cells. *Immunity,* 29**,** 497-510.

LAHOUD, M. H., AHMET, F., KITSOULIS, S., WAN, S. S., VREMEC, D., LEE, C. N., PHIPSON, B., SHI, W., SMYTH, G. K., LEW, A. M., KATO, Y., MUELLER, S. N., DAVEY, G. M., HEATH, W. R., SHORTMAN, K. & CAMINSCHI, I. 2011. Targeting antigen to mouse dendritic cells via Clec9A induces potent CD4 T cell responses biased toward a follicular helper phenotype. *J Immunol,* 187**,** 842-50.

LINDQVIST, M., VAN LUNZEN, J., SOGHOIAN, D. Z., KUHL, B. D., RANASINGHE, S., KRANIAS, G., FLANDERS, M. D., CUTLER, S., YUDANIN, N., MULLER, M. I., DAVIS, I., FARBER, D., HARTJEN, P., HAAG, F., ALTER, G., SCHULZE ZUR WIESCH, J. & STREECK, H. 2012. Expansion of HIV-specific T follicular helper cells in chronic HIV infection. *J Clin Invest,* 122**,** 3271-80.

MA, C. S., DEENICK, E. K., BATTEN, M. & TANGYE, S. G. 2012. The origins, function, and regulation of T follicular helper cells. *J Exp Med,* 209**,** 1241-53.

MA, C. S., SURYANI, S., AVERY, D. T., CHAN, A., NANAN, R., SANTNER-NANAN, B., DEENICK, E. K. & TANGYE, S. G. 2009. Early commitment of naive human CD4(+) T cells to the T follicular helper (T(FH)) cell lineage is induced by IL-12. *Immunol Cell Biol,* 87**,** 590-600.

MOSMANN, T. R. & COFFMAN, R. L. 1989. TH1 and TH2 cells: different patterns of lymphokine secretion lead to different functional properties. *Annu Rev Immunol,* 7**,** 145-73.

NURIEVA, R. I., CHUNG, Y., HWANG, D., YANG, X. O., KANG, H. S., MA, L., WANG, Y. H., WATOWICH, S. S., JETTEN, A. M., TIAN, Q. & DONG, C. 2008. Generation of T follicular helper cells is mediated by interleukin-21 but independent of T helper 1, 2, or 17 cell lineages. *Immunity,* 29**,** 138-49.

NUSSENZWEIG, M. C., STEINMAN, R. M., WITMER, M. D. & GUTCHINOV, B. 1982. A monoclonal antibody specific for mouse dendritic cells. *Proc Natl Acad Sci U S A,* 79**,** 161-5.

QI, H., CANNONS, J. L., KLAUSCHEN, F., SCHWARTZBERG, P. L. & GERMAIN, R. N. 2008. SAP-controlled T-B cell interactions underlie germinal centre formation. *Nature,* 455**,** 764-9.

RANUNCOLO, S. M., PITTALUGA, S., EVBUOMWAN, M. O., JAFFE, E. S. & LEWIS, B. A. 2012. Hodgkin lymphoma requires stabilized NIK and constitutive RelB expression for survival. *Blood,* 120**,** 3756-63.

REINHARDT, R. L., LIANG, H. E. & LOCKSLEY, R. M. 2009. Cytokine-secreting follicular T cells shape the antibody repertoire. *Nat Immunol,* 10**,** 385-93.

SCHAERLI, P., WILLIMANN, K., LANG, A. B., LIPP, M., LOETSCHER, P. & MOSER, B. 2000. CXC chemokine receptor 5 expression defines follicular homing T cells with B cell helper function. *J Exp Med,* 192**,** 1553-62.

SHIN, C., HAN, J. A., KOH, H., CHOI, B., CHO, Y., JEONG, H., RA, J. S., SUNG, P. S., SHIN, E. C., RYU, S. & DO, Y. 2015. CD8alpha(-) Dendritic Cells Induce Antigen-Specific T Follicular Helper Cells Generating Efficient Humoral Immune Responses. *Cell Rep,* 11**,** 1929-40.

SHORTMAN, K. & LIU, Y. J. 2002. Mouse and human dendritic cell subtypes. *Nat Rev Immunol,* 2**,** 151-61.

SLIFKA, M. K., MATLOUBIAN, M. & AHMED, R. 1995. Bone marrow is a major site of long-term antibody production after acute viral infection. *J Virol,* 69**,** 1895-902.

STREECK, H., D'SOUZA, M. P., LITTMAN, D. R. & CROTTY, S. 2013. Harnessing CD4(+) T cell responses in HIV vaccine development. *Nat Med,* 19**,** 143-9.

SUN, S. C. 2011. Non-canonical NF-kappaB signaling pathway. *Cell Res,* 21**,** 71-85.

SWIGGARD, W. J., MIRZA, A., NUSSENZWEIG, M. C. & STEINMAN, R. M. 1995. DEC-205, a 205-kDa protein abundant on mouse dendritic cells and thymic epithelium that is detected by the monoclonal antibody NLDC-145: purification, characterization, and N-terminal amino acid sequence. *Cell Immunol,* 165**,** 302-11.

TANGYE, S. G., MA, C. S., BRINK, R. & DEENICK, E. K. 2013. The good, the bad and the ugly - TFH cells in human health and disease. *Nat Rev Immunol,* 13**,** 412-26.

TANGYE, S. G. & TARLINTON, D. M. 2009. Memory B cells: effectors of long-lived immune responses. *Eur J Immunol,* 39**,** 2065-75.

TRUMPFHELLER, C., LONGHI, M. P., CASKEY, M., IDOYAGA, J., BOZZACCO, L., KELER, T., SCHLESINGER, S. J. & STEINMAN, R. M. 2012. Dendritic cell-targeted protein vaccines: a novel approach to induce T-cell immunity. *J Intern Med,* 271**,** 183-92.

VINUESA, C. G. & CYSTER, J. G. 2011. How T cells earn the follicular rite of passage. *Immunity,* 35**,** 671-80.

YOO, J. K., FISH, E. N. & BRACIALE, T. J. 2012. LAPCs promote follicular helper T cell differentiation of Ag-primed CD4+ T cells during respiratory virus infection. *J Exp Med,* 209**,** 1853-67.

Chapter 3. Intrinsic features of the CD8α$^-$ dendritic cell subset in inducing functional T follicular helper cells

3.1. Introduction

T follicular helper (Tfh) cells have been identified as the true B cell helper and noted for their competence of regulating T cell dependent humoral immune responses (King, 2009, Crotty, 2011, McHeyzer-Williams et al., 2012). Once the major role of CXCR5 in Tfh cells was identified, leading its CXCL13 dependent migration into the germinal center (GC) (Breitfeld et al., 2000, Schaerli et al., 2000), where they help cognate B cells to induce antigen specific antibody responses, several distinct features of Tfh cells, high expressions of ICOS and PD1, low expression of CCR7, transcription factor Bcl6, and major cytokine IL-21 were identified to be distinguished from other CD4$^+$ T cell subsets (Ma et al., 2012). In addition, it has been reported that Tfh cells are involved in humoral immunity related diseases such as autoimmunity and humoral immunodeficiency (Tangye et al., 2013), suggesting understanding the initial induction of Tfh cell differentiation is vital and crucial. Although important features of Tfh cells have been identified by many researches, how naïve CD4$^+$ T cells receive initial signal to differentiate into Tfh cells is not clearly understood.

Dendritic cells (DCs), known as the most potent antigen presenting cell (APC), is the major regulator in inducing several CD4$^+$ effector T cell subsets (Steinman and Banchereau, 2007). Two major myeloid DC subsets in the secondary lymphoid organs such as the lymph nodes and spleen have been identified by the expression of CD8α, either CD11c$^+$CD8α$^+$ DCs which express the endocytic receptor DEC-205 or CD11c$^+$CD8$^-$ DCs that express the endocytic receptor DCIR2 (Iyoda et al., 2002, Dudziak et al., 2007). We recently reported that the conventional CD8α$^-$ DC subset specializes in inducing functional Tfh cells both *in vitro* and *in vivo* when compared with those induced by CD8α$^+$ DCs (Shin et al., 2015). We also demonstrated the importance of ICOSL and OX40L expressed on the CD8α$^-$ DC subset through the highly increased non-canonical signaling pathway in the induction of functional Tfh cells (Shin et al., 2015). However, several important and distinct features such as the proximal localization of the two conventional DC subsets to antigen specific CD4$^+$ T cells *in vivo*, potential cytokines secreted from the DC subsets and the possible involvement of other APCs, majorly cognate B cells, in inducing Tfh cells have not been elucidated. Therefore, the aim of this current study was to investigate the unknown intrinsic features of the two conventional DC subsets in the initiation of Tfh cell differentiation by utilizing DC subset targeting strategy and isolated DC subsets. In this study, we showed that the localization of the CD8α$^-$ DC subset in the marginal zone (MZ) bridging channels is closely related to the induction of CXCR5$^+$CCR7^{low} Tfh cells *in vivo*. We also demonstrated that that the major source of IL-6 cytokine in inducing Tfh cells is secreted from the antigen

specifically activated $CD4^+$ T cells induced by $CD8\alpha^-$ DCs, and those secreted by the two DC subsets seem minor. $CD8\alpha^-$ DCs were dominant in inducing Tfh cell dependent humoral immune responses over other antigen presenting cells including B cells. We here unveiled the undescribed important intrinsic features of the two DC subsets, suggesting the potential of utilizing $CD8\alpha^-$ DCs as a therapeutic vaccination tool to modulate T cell dependent humoral immune responses.

3.2. Experimental procedure

Mice

Naïve BALB/c (H-2^d) and C57BL/6 (H-2^b) mice were purchased from Taconic. OVA antigen specific transgenic OT-II and DO11.10 Thy 1.1 mice were purchased from The Jackson Laboratory. All mice were maintained under specific pathogen-free conditions and used at 6-8 weeks approved by Ulsan National Institute of Science and Technology Institutional Animal Care and Use Committee (approval number: UNISTIACUC-12-006-A).

Dendritic cell preparation

Total number of splenic dendritic cells was increased by Fms-like tyrosine 3 ligand (Flt3L) as previously described (Dudziak et al., 2007). In brief, 5×10^6 cells of Flt3L-melanoma cells were subcutaneously (s.c.) injected to naïve C57BL/6 mice. After 10-14 days, the expanded splenic $CD11c^+$ DCs were enriched with positive magnetic-activated cell sorting (MACS; Miltenyi Biotec, GmbH, Bergisch Gladbach, Germany) and were further sorted into the two DC subsets, $CD3^-B220^-CD11c^+CD8\alpha^+$ or $CD3^-B220^-CD11c^+CD8\alpha^-$ DCs by MoFlo XDP (Beckman Coulter, CA, USA). To analyze intrinsic differences in the two DC subsets, the DCs were stimulated with either 25 μg poly (I:C) or 100 ng/ml LPS for 0, 12 or 24 hours.

$CD4^+$ T cell preparation

OVA-specific transgenic $CD4^+$ T cells from the lymph nodes and the spleen of OT-II or DO11.10 Thy1.1 mice were negatively isolated using hybridoma supernatant cocktail of rat-anti mouse -CD8 (2.43), -MHC class II (T1B120), -Mφ (F4/80), -B220 (RA3-6B2), and -NK cell (NK1.1) antibodies followed by depletion with dynabeads sheep anti-rat IgG (Invitrogen, Carlsbad, CA, USA).

$CD4^+$ T cell priming by the DC subsets *in vitro*

Naive OVA-specific $CD4^+$ T (3×10^5) cells purified from OT-II mice were co-cultured either with sorted $CD8\alpha^+$ or $CD8\alpha^-$ DCs (0.3×10^5 each DCs, 1:10 ratio of DC to T cells) per well in the round bottom 96 well plate for 3 days in the presence of 25 μg/ml poly (I:C) or 100 ng/ml LPS with 2 μM OVA peptide (a.a. 323-339) (Genscript, Piscataway, NJ, USA). Then, cytokines in supernatants were detected by ELISA.

Induction of $CD4^+$ T cells by DC subset targeting *in vivo*

Isolated $CD4^+$ T cells from DO11.10 Thy 1.1 mice were adoptively transferred (3×10^6 cells per mouse) into naïve Thy 1.2^+ BALB/c mice intravenously (i.v.) at day -1. At day 0, PBS, 500 μg soluble OVA protein (endotoxin-free; Seikagaku Corp, Tokyo, Japan), or 5 μg of each distinct DC subset targeting monoclonal antibodies (anti-DEC-205 or anti-DCIR2 mAbs) genetically conjugated with OVA protein in the presence of 50 μg poly (I:C) were injected via the footpads of the mice. At indicated time points after the immunization, single cells from the lymph nodes or the spleen were prepared and analyzed for the expression of various molecules by flow cytometry. In some experiments, 5 μg of each distinct DC subset targeting mAbs conjugated with OVA protein + 50 μg soluble OVA protein with 50 μg LPS were injected via the footpads of the mice.

Production of DC subset-specific targeting antibodies conjugated with OVA protein

In this study, DC subset-specific targeting antibodies conjugated with OVA protein were used (Do et al., 2010, Trumpfheller et al., 2012). OVA protein were conjugated either to anti-mouse DEC-205 (for $CD8\alpha^+$ DC targeting) mAbs or to anti-mouse DCIR2 (for $CD8\alpha^-$ DC targeting) mAbs. All proteins used were free of endotoxin (<0.125 endotoxin units/mg) in a Limulus Amebocyte Lysate assay, QCL-1000 (Bio Whittaker, Chesterbrook, PA, USA).

ELISA for serum antibodies and cytokines

High binding ELISA plates (BD Bioscience, San Jose, CA, USA) were coated with 10 μg/ml OVA protein overnight at 4 ℃. Plates were washed 3 times with PBST (PBS with 0.1% of Tween 20) and blocked with PBST-BSA 5% for 1 hour at 37 ℃. Serial dilutions of mouse serum were added and incubated for 1 hour at 37 ℃. Various secondary goat anti-mouse Fc specific antibodies conjugated with horseradish peroxidase were added and developed with o-phenylenediamine (Sigma-Aldrich, St. Louis, MO, USA) tablets at room temperature for 15 minutes. Data are presented as log antibody titers, with the highest dilution showing OD_{450} >0.1. To detect cytokines in supernatants, we used CBA flex sets (BD Bioscience).

Immunohistochemistry

Briefly, tissue sections (10 μm) of the spleen were prepared by using Cryotome (Thermo Fisher scientific, Waltham, MA, USA) and then fixed with aceton on a slide. For localization images of DCs and T cells, samples were stained with BV-421 anti-mouse IgD (BioLegend, San Diego, CA, USA), PE anti-mouse DO11.10 (BD Biosciences), and APC anti-mouse DEC205 or 33D1 (BioLegend). Then, the stained samples were imaged with FV10i (Olympus, Southend-on-Sea, UK) confocal microscope.

Flow cytometry

Data were acquired by BD FACS Calibur or BD LSRfortessa and analyzed by FlowJo software (TreeStar, Ashland, OR, USA), shown on the log scale graph (from 10^1 to 10^4 or 10^5). All bar graph data values were shown after subtracting their corresponding isotype values. Median Fluorescence Intensity was abbreviated as MFI. Used antibodies in flow cytometry as follows: CD11c (HL3), CD8 (53-6.7), CD3 (145-2C11), B220 (RA3-6B2), Vα2 (B20.1), Thy1.1 (OX-7), DO11.10 (KJ1-26), CD4 (RM4-5), CD44 (IM7), CXCR5 (2G8), Bcl6 (K112-91), CCR7 (4B12), CD19 (1D3), IgD (11-26C.2A), FAS (Jo2), GL7 (GL7), CD80 (16-10A1), CD86(GL1), MHCII (M5/114), Rat IgG2a, κ (R35-95), and Rat IgG2b, κ (A95-1) were purchased from BD biosciences; PD1 (RMP1-30) and IL-21 (mhalx21) were purchased from eBioscience, San Diego, CA, USA.

Intracellular staining

Cells were stained with anti-mouse DO11.10, CD4, CD44 and CXCR5 for 30 minutes at room temperature. Following fixation and permeabilization with Cytofix/Cytoperm kit (BD Biosciences) according to the manufacturer's protocol, the cells were stained for intracellular Bcl6 or IL-21 along with their isotypes for 25 minutes at 4 ℃. Data were analyzed by flow cytometry.

Statistics

Results are expressed as mean ± s.e.m. We used PRISM 4.0 program (GraphPad Prism, La Jolla, CA, USA) and performed nonparametric Mann-Whitney U test when appropriate. The *P* values < 0.05 were considered significant.

3.3. Results

$CD4^+$ T cells primed by $CD8\alpha^-$ DCs are localized proximal to $CD8\alpha^-$ DCs in the marginal zone (MZ) bridging channels

To specifically deliver ovalbumin (OVA) antigens to each DC subset *in vivo*, we utilized two DC subset targeting monoclonal antibodies (mAbs) genetically conjugated with OVA protein, αDEC-205:OVA (for $CD8\alpha^+$ DCs targeting) or αDCIR2:OVA (for $CD8\alpha^-$ DCs targeting) mAbs. Then, we observed the localizations of each DC subset together with OVA antigen specifically primed $DO11.10^+CD4^+$ T cells by each DC subset. We confirmed the distinct locations of the two DC subsets in the spleen; $CD8\alpha^+$ DCs predominantly localize in the T cell enriched arear whereas $CD8\alpha^-$ DCs localize in the MZ bridging channels (**Figure 3-1**), consistent with the previous report (Dudziak et al., 2007). Interestingly, the $CD4^+$ T cells primed by $CD8\alpha^-$ DCs tended to localize in the MZ bridging channels, proximal to the localization of the $CD8\alpha^-$ DC subset as early as 1 day after the immunization, and 3 and 5 days after the immunization, the $CD4^+$ T cells induced by $CD8\alpha^-$ DCs predominantly localized in the MZ bridging channels. In contrast, the $CD4^+$ T cells primed by $CD8\alpha^+$ DCs remained in the T cell enriched arear at all-time points tested (**Figure 3-1**).

$CD4^+$ T cells primed by $CD8\alpha^-$ DCs express high levels of CXCR5 and low levels of CCR7

Consistent to the previous study (Shin et al., 2015), we here again confirmed that $CD8\alpha^-$ DCs efficiently induce Tfh cells based on the highly expressed feature factors of Tfh cells such as ICOS, PD1, Bcl6 and IL-21 (**Figures 3-2A-D**; **Figures 3-3A-B**). Given the fact that pre-Tfh cells up-regulate CXCR5 and down-regulate CCR7 to migrate into the inter-follicular region/MZ bridging channels (Hardtke et al., 2005, Haynes et al., 2007), where the development of Tfh cell initiates (Kerfoot et al., 2011), we examined the relations of the expressions of CXCR5 and CCR7 on the antigen specifically activated $CD44^+CD4^+$ T cells primed by the two distinct DC subsets. Interestingly, we found high expressions of CXCR5 on the $CD4^+$ T cells primed by $CD8\alpha^-$ DCs compared with those induced by $CD8\alpha^+$ DCs at 5 and 7 days after the immunization both in the lymph node and the spleen (**Figures 3-4A** and **B**), and the percentage of $CCR7^{low}CD4^+$ T cells induced by $CD8\alpha^-$ DCs was dramatically increased (**Figures 3-4C** and **D**), indicating that the pre-Tfh cells primed by $CD8\alpha^-$ DCs tend to locate in the MZ bridging channels through CXCR5-CXCL13 interaction. In contrast, $CXCR5^{low}CCR7^{high}$ $CD4^+$ T cells primed by $CD8\alpha^+$ DCs remained in the T cell enriched area via CCR7-CCL19/21 interaction (**Figures 3-4A-D**). Although the $CD4^+$ T cells induced by $CD8\alpha^-$ DCs were slightly more proliferative than those by $CD8\alpha^+$ DCs, the

proliferation of $CD4^+$ T cells induced by OVA protein was similar to those induced by $CD8\alpha^+$ DCs *in vivo* (**Figure 3-5**), indicating that the inefficacy of $CD8\alpha^+$ DCs in inducing Tfh cells are not due to the defected $CD4^+$ T cell proliferation.

IL-6 cytokine level secreted from the two DC subsets is dependent on an adjuvant type

Despite previous reports showing the significance of interleukin-6 (IL-6) for the induction of Tfh cells (Eto et al., 2011, Choi et al., 2013), its source, together with the potential of its secretion from the DC subsets, were not clearly reported. In order to investigate the level of IL-6 and other cytokines secreted from the two DC subsets, we purified each DC subset, $CD3^-B220^-CD11c^+CD8\alpha^+$ DCs or $CD3^-B220^-CD11c^+CD8\alpha^-$ DCs. Each isolated DC subset was treated either with poly (I:C) or LPS for 12 or 24 hours *in vitro*. Unexpectedly, significantly enhanced IL-6 secretion from $CD8\alpha^+$ DCs compared with that from $CD8\alpha^-$ DCs was observed upon poly (I:C) stimulation (**Figure 3-6A**). However, in the presence of LPS stimulation, the level of IL-6 secretion was comparable between the two DC subsets 12 hours after the stimulation and its level secreted from $CD8\alpha^-$ DCs was higher 24 hours after the stimulation (**Figure 3-6B**). Notably, significantly higher level of IL-6 cytokine secreted from the $CD4^+$ T cells primed by $CD8\alpha^-$ DCs was observed in both poly (I:C) and LPS stimulations (**Figure 3-6C**), demonstrating the minor role of IL-6 secreted from $CD8\alpha^-$ DCs in the induction of Tfh cells. We observed higher levels of pro-inflammatory cytokines such as IL-1β and TNF-α secreted from $CD8\alpha^+$ DCs both in poly (I:C) and LPS stimulations (**Figures 3-6A** and **B**). The expression levels of co-stimulator CD80 or CD86 and MHCII were similar between the two DC subsets (**Figure 3-7**).

$CD8\alpha^-$ DCs specialize in inducing functional Tfh cells

It has been reported that $CD8\alpha^-$ $DCIR2^+$ DCs have a unique capacity to initiate extra-follicular B cell responses via rapid activation of Ag-specific B cells *in vivo* (Chappell et al., 2012), indicating the probability that each DC subset is differentially able to deliver antigens to cognate B cells in the induction of T cell dependent and antigen specific humoral immune responses. To examine the effect of different antigen accessibility of APCs, majorly B cells, on the induction Tfh cells via DC subset targeting, we designed one experiment to provide antigens to all APCs equivalently in the both $CD8\alpha^+$ and $CD8\alpha^-$ DC targeted groups. When mice were immunized with 5 μg of each DC subset specific targeting mAbs conjugated with OVA protein (each immunization contains approximately ~1.6 μg OVA protein), 50 μg soluble OVA protein was given together to the mice to ensure that B cells and other APCs have equivalent access to antigens. Five days after the immunization, significantly higher percentages of $CXCR5^+PD1^+$, $CXCR5^+Bcl6^+$ and $CXCR5^+IL\text{-}21^+$ Tfh cells were observed both in the lymph nodes

(**Figures 3-8A** and **B**) and the spleen (**Figures 3-8C** and **D**) from the $CD8\alpha^-$ DC targeted group compared with those from the $CD8\alpha^+$ DC targeted group. Moreover, we observed higher percentage of $CD19^+IgD^-GL7^+FAS^+$ GC B cells in splenocytes from the $CD8\alpha^-$ DC targeted group (**Figures 3-9A** and **B**). The titers of IgM were comparable between $CD8\alpha^+$ and $CD8\alpha^-$ DCs targeted groups at day 3. At day 5, higher IgM and IgG titers from the $CD8\alpha^-$ DC targeted group were observed when compared with those induced by $CD8\alpha^+$ DCs (**Figure 3-9C**).

3.4. Discussion

Modulating the induction of Tfh cell differentiation is the major step to potentially treat dysfunctional humoral immune responses. However, the induction of Tfh cells by DCs has not been clearly understood. In the present study, we examined the unknown intrinsic features of the two myeloid DC subsets important for the initiation of Tfh cell induction.

The localization of DCIR2$^+$CD4$^+$ DCs (equivalent to CD8α$^-$ DCs in this study) in the MZ bridging channel/inter-follicular region has been reported to be mediated via the chemotactic receptor EBI2 (Yi and Cyster, 2013, Gatto et al., 2013), which has an important function in inducing blood-borne particulate antigen specific CD4$^+$ T cell and B cell immune responses. Supported by these previous reports, we demonstrate that the localization of DCIR2$^+$ CD8α$^-$ DCs may provide advantages in the initiation of Tfh cell differentiation given the fact of the early recruitment of antigen specific CD4$^+$ T cells primed by CD8α$^-$ DCs into MZ bridging channels 1 day after the immunization. Moreover, the migration of these CD4$^+$ T cells into the MZ bridging channels was presumably mediated via the high level of CXCR5 and the low level of CCR7 expressions, consistent with the previous reports (Hardtke et al., 2005, Haynes et al., 2007). CD8α$^+$ DC primed CD4$^+$ T cells expressed low level of CXCR5 and high level of CCR7, which may make them be retained in the localization of the T cell enriched region, resulting in the differentiation to IFN-γ secreting Th1 cells (Shin et al., 2015).

Secretory cytokines often determine the fate of various effector CD4$^+$ T cell subsets (Ottenhoff, 2012), and IL-6 has been reported as a major cytokine in inducing Tfh cell differentiation (Ballesteros-Tato and Randall, 2014). We demonstrated that CD8α$^-$ DCs properly induced Tfh cells as well as Tfh cell dependent humoral immune responses both in the presence of poly (I:C) and LPS (**Figure 3-10A** and **B**) (Shin et al., 2015). However, the two myeloid DC subsets showed opposites in the level of IL-6 secretion in the presence of poly (I:C) and LPS stimulation, indicating the insignificance of IL-6 secreted from the DC subsets in inducing Tfh cells. Instead, the high levels of autocrine IL-6 (**Figure 3-6C**) secreted from the antigen specifically activated CD4$^+$ T cells induced by CD8α$^-$ DCs, regardless of the adjuvant types, seem to be important in inducing Tfh cell differentiation. The pro-inflammatory cytokines IL-1β and TNF-α highly secreted from CD8α$^+$ DCs in the presence of both poly (I:C) and LPS, may be involved in inducing other effector CD4$^+$ T cell subsets (Ottenhoff, 2012).

The advantageous localization of CD8α$^-$ DCs in MZ bridging channels to encounter antigen specific B cells (Chappell et al., 2012) and their slow rate of antigen internalization for prolonged antigen presentation (Dudziak et al., 2007) have been reported, which may help B cells to uptake antigens easily,

resulting in highly activated antigen specific B cells. However, the dominance of CD8α⁻ DCs over other APCs including B cells in the initiation of functional Tfh cells with excess OVA antigens has been confirmed. Nonetheless, given the previous reports demonstrating that the deficiency of functional B cells resulted in the decreased number of Tfh cells (Haynes et al., 2007, Johnston et al., 2009) and other DC subsets such as late activator antigen-presenting cells (Yoo et al., 2012) or monocyte-derived DCs (Chakarov and Fazilleau, 2014) induced Tfh cell differentiation through different types of immune responses, further studies are required to understand how other APCs interplay each other in the induction of Tfh cell differentiation.

Together with highly enhanced ICOSL and OX40L expressed on CD8α⁻ DCs in inducing Tfh cells (Shin et al., 2015), supported by the previous reports demonstrating the significant role of ICOSL and OX40L on dendritic cells or APCs in Tfh cell differentiation (Choi et al., 2011, Jacquemin et al., 2015), the localization of the CD8α⁻ DC subset in MZ bridging channels may deliver synergic effects in Tfh cell induction. The difference in antigen processing (Dudziak et al., 2007) and the duration of antigen presentation (Deenick et al., 2010, Lahoud et al., 2011) are other factors in DC subsets that may need to be considered for Tfh cell differentiation.

In conclusion, we demonstrate the unknown intrinsic features of CD8α⁻ DCs, proposing its specialty in inducing functional Tfh cells. Based on the results we showed so far, we present a rationale to find the counterpart of CD8α⁻ DCs in humans to develop efficient DC-based vaccines for improved T cell dependent humoral immune responses.

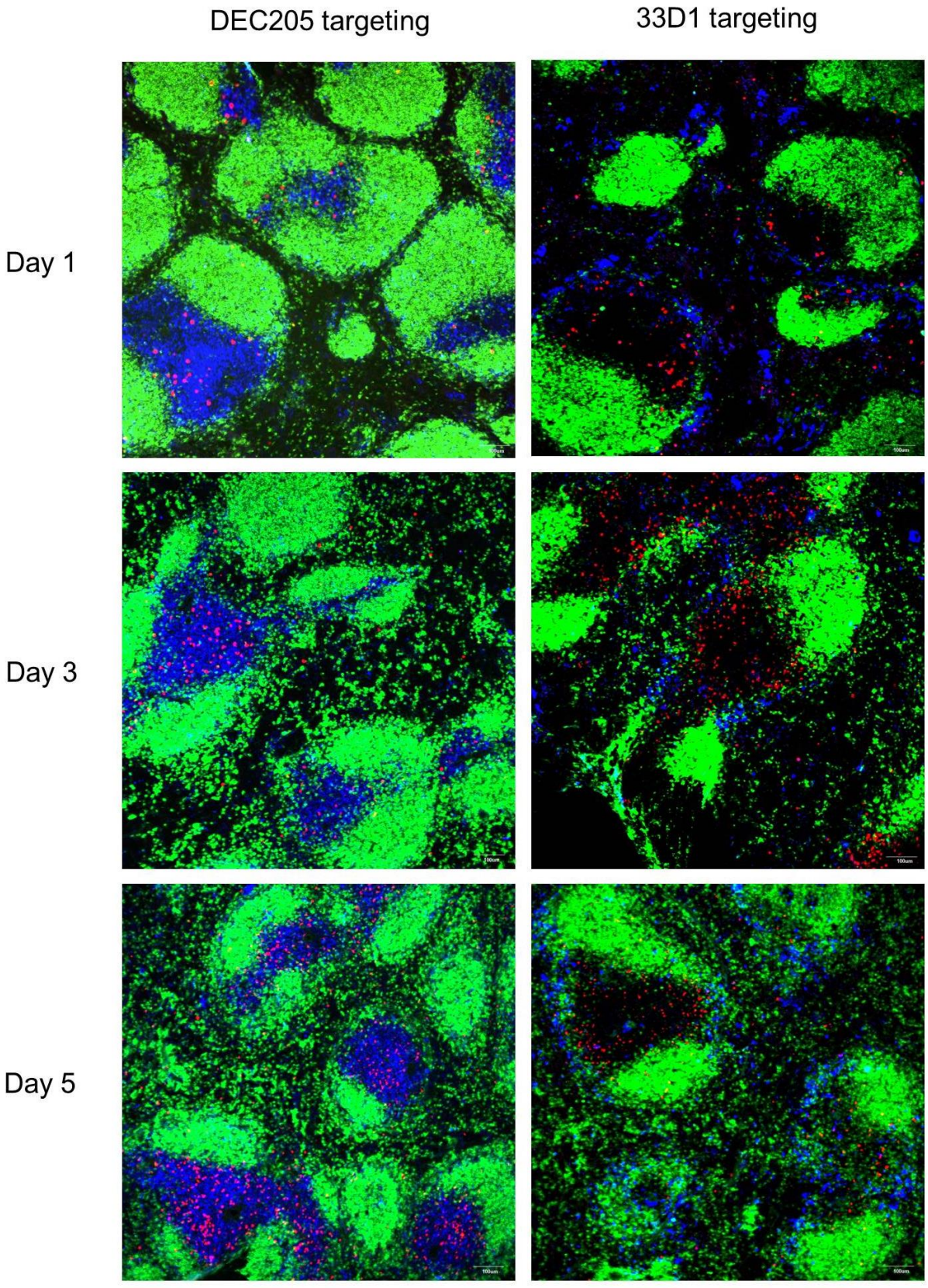

Figure 3-1. $CD4^+$ T cells primed by $CD8\alpha^-$ DCs localized in the MZ bridging channels. OVA specific $DO11.10^+CD4^+$ T cells were adoptively transferred to naive BALB/c mice at day -1, and were immunized subcutaneously (s.c.) either with αDEC:OVA ($CD8\alpha^+$ DC targeting) or αDCIR2:OVA ($CD8\alpha^-$ DC targeting) conjugated monoclonal antibodies (mAbs) in the presence of poly (I:C) at day 0. At each indicated time point after the immunization, immunohistochemical staining of spleen sections from each group was prepared and detected by fluorescence confocal microscopy. IgD, green; DO11.10, red; DEC205 (for DEC205 targeted group) or 33D1 (for 33D1 targeted group), blue. Data are representative of three or more independent experiments (n > 10 per group).

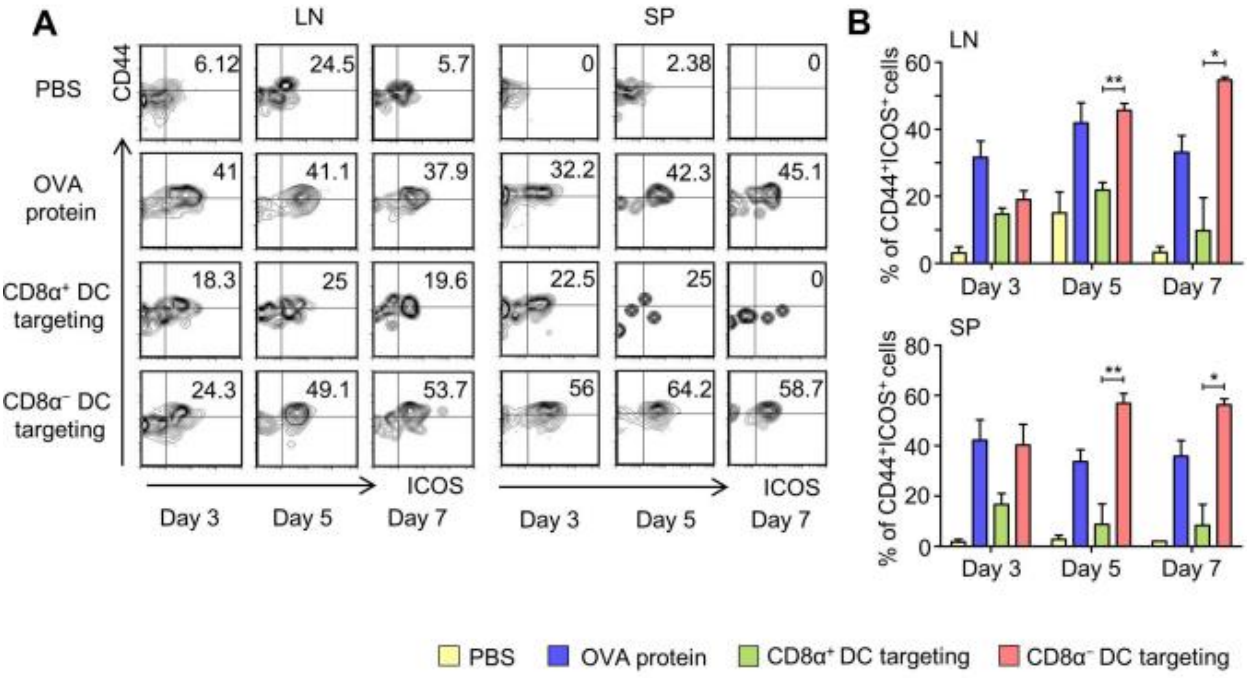

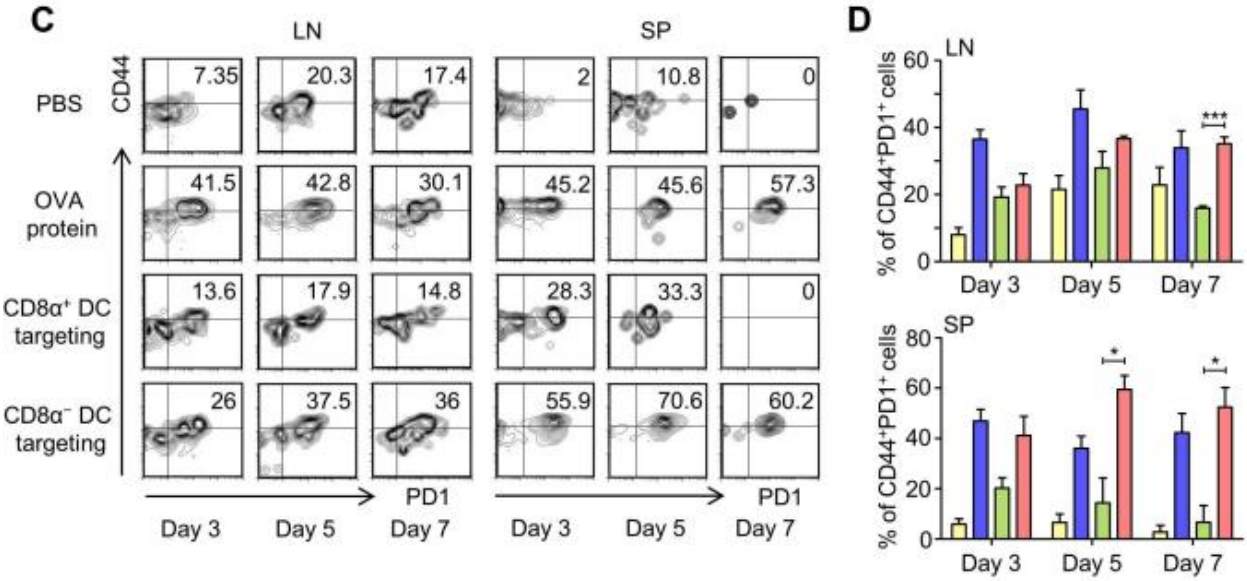

Figure 3-2. Induction of ICOS$^+$PD1$^+$ Tfh cells by CD8α^- DCs *in vivo*. (**A**–**D**) OVA specific DO11.10$^+$Thy1.1$^+$CD4$^+$ T cells were adoptively transferred to naive Thy1.2$^+$ BALB/c mice at day -1, and were immunized s.c. with PBS, soluble OVA protein (OVA protein), or either αDEC:OVA (CD8α$^+$ DC targeting) or αDCIR2:OVA (CD8α$^-$ DC targeting) conjugated mAbs in the presence of poly (I:C) at day 0. At each indicated time points after the immunization, lymph node (LN) or spleen (SP) cells were prepared and Tfh cells gated from the Thy1.1$^+$CD4$^+$ T cells were analyzed. (**A** and **C**) Representative flow cytometry plots of CD44$^+$ICOS$^+$ (**A**) or CD44$^+$PD1$^+$ (**C**) Tfh cells. (**B** and **D**) Data represent mean ± s.e.m. of three independent experiments described in (A) or (C), respectively. * $P < 0.05$, ** $P < 0.01$, *** $P < 0.001$. (**A**–**D**, n=3 per group).

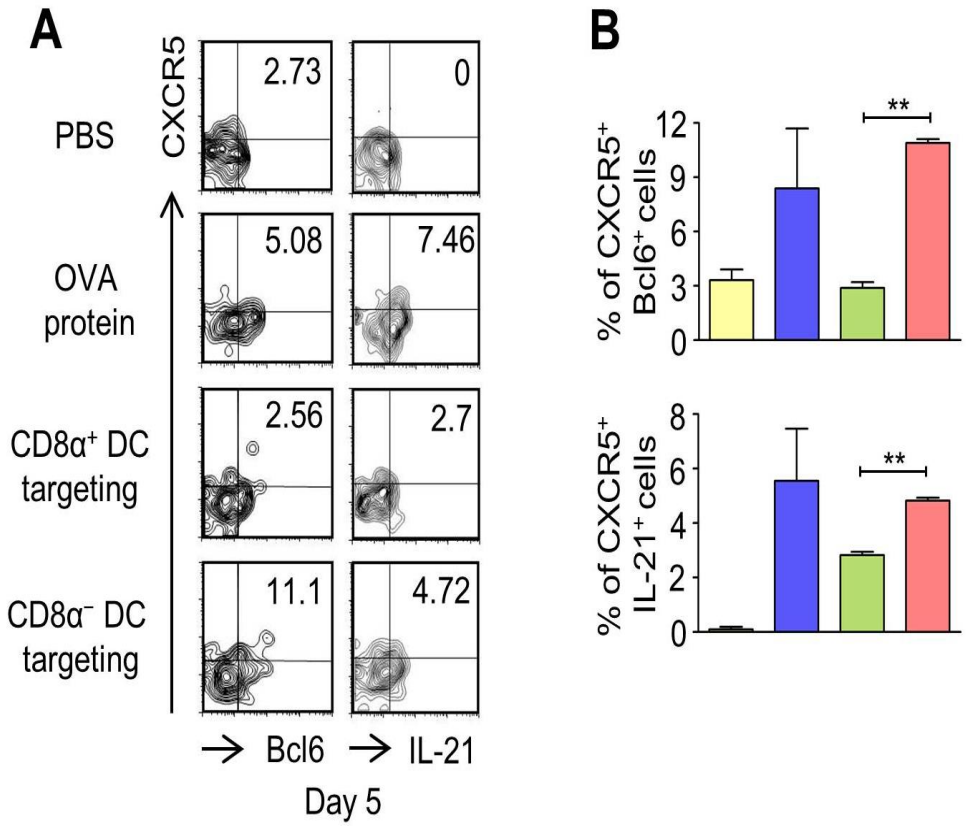

Figure 3-3. Induction of CXCR5$^+$Bcl6$^+$ or CXCR5$^+$IL-21$^+$ Tfh cells by CD8α$^-$ DCs *in vivo*. (**A** and **B**) OVA specific DO11.10$^+$Thy1.1$^+$CD4$^+$ T cells were adoptively transferred to naive Thy1.2$^+$ BALB/c mice at day -1, and were immunized s.c. with PBS, soluble OVA protein (OVA protein), or either αDEC:OVA (CD8α$^+$ DC targeting) or αDCIR2:OVA (CD8α$^-$ DC targeting) conjugated mAbs in the presence of poly (I:C) at day 0. 5 days after the immunization, lymph node cells were prepared and Tfh cells gated from the Thy1.1$^+$CD4$^+$ T cells were analyzed. (**A**) Representative flow cytometry plots of CXCR5$^+$Bcl6$^+$ or CXCR5$^+$IL-21$^+$ Tfh cells. (**B**) Data represent mean ± s.e.m. of two independent experiments described in (A). ** $P < 0.01$. (n=3 per group).

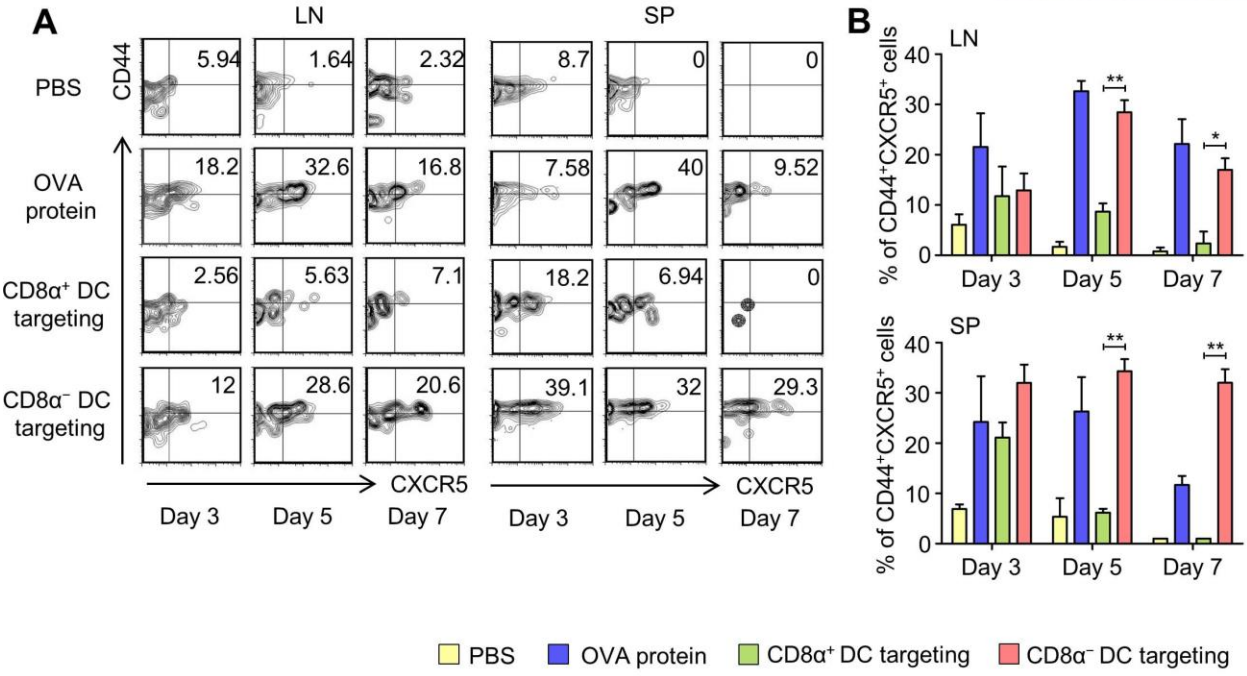

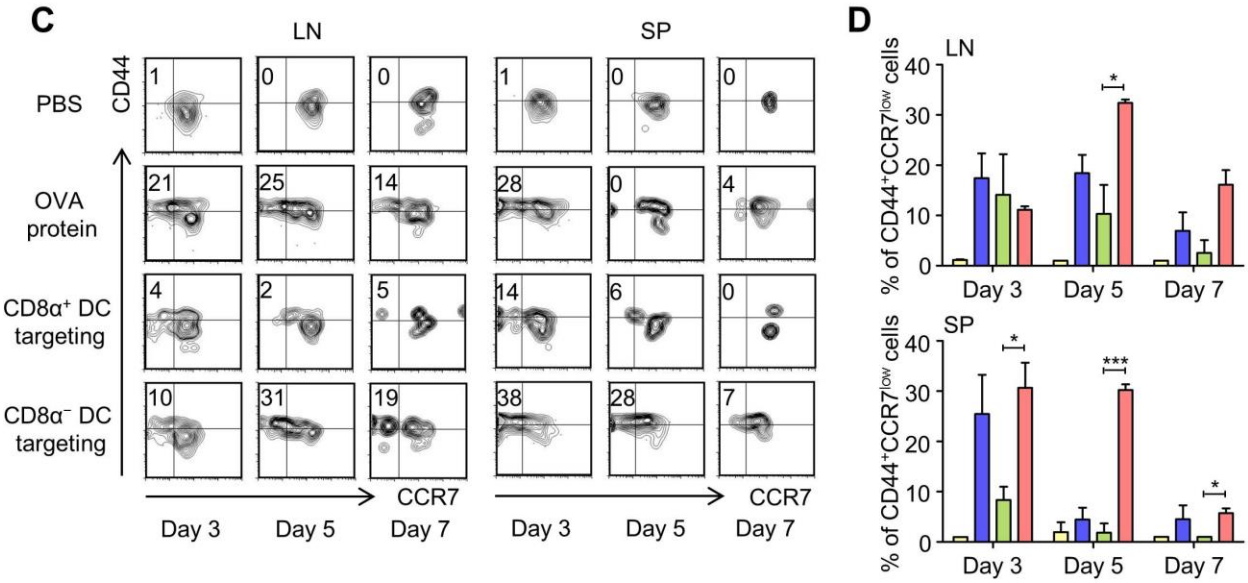

Figure 3-4. Induction of CXCR5^{+}CCR7^{low} Tfh cells by CD8α^{-} DCs *in vivo*. (**A**–**D**) OVA specific DO11.10^{+}Thy1.1^{+}CD4^{+} T cells were adoptively transferred to naive Thy1.2^{+} BALB/c mice at day -1, and were immunized s.c. with PBS, soluble OVA protein (OVA protein), or either αDEC:OVA (CD8α^{+} DC targeting) or αDCIR2:OVA (CD8α^{-} DC targeting) conjugated mAbs in the presence of poly (I:C) at day 0. At each indicated time points after the immunization, lymph node (LN) or spleen (SP) cells were prepared and Tfh cells gated from the Thy1.1^{+}CD4^{+} T cells were analyzed. (**A** and **C**) Representative flow cytometry plots of CD44^{+}CXCR5^{+} (**A**) or CD44^{+}CCR7^{low} (**C**) Tfh cells. (**B** and **D**) Data represent mean ± s.e.m. of three independent experiments described in (A) or (C), respectively. * $P < 0.05$, ** $P < 0.01$, *** $P < 0.001$. (**A**–**D**, n=3 per group).

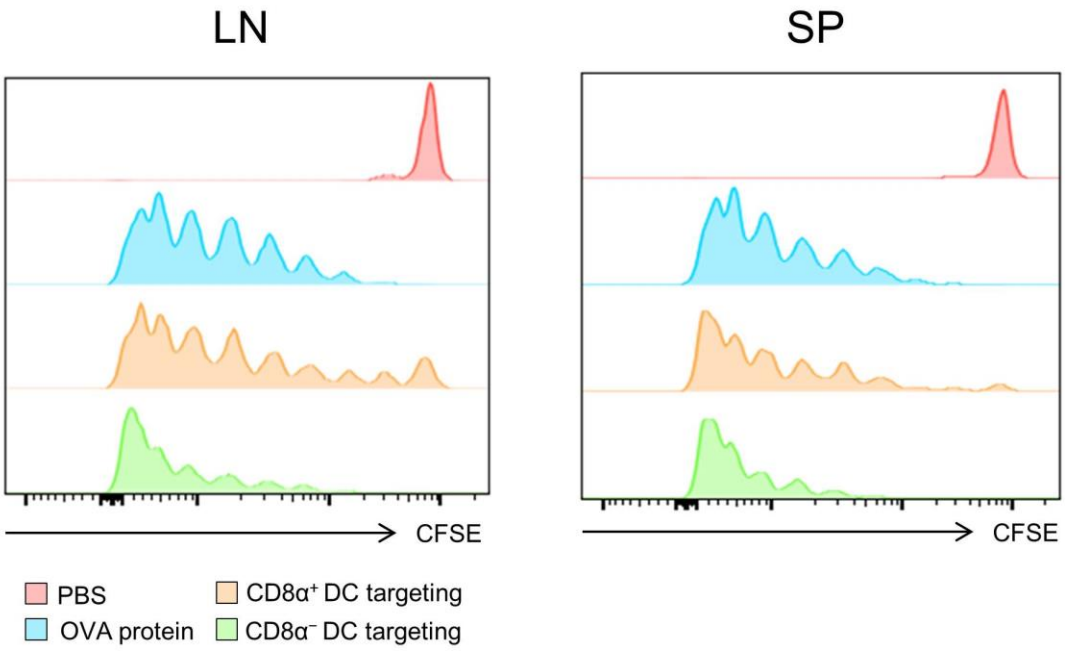

Figure 3-5. The proliferation of CD4$^+$ T cells induced by the two DC subsets *in vivo*. OVA specific DO11.10$^+$Thy1.1$^+$CD4$^+$ T cells were adoptively transferred to naive Thy1.2$^+$Balb/c mice at day -1, s.c. immunized with PBS (PBS), OVA protein (OVA protein), αDEC:OVA (CD8α$^+$ DC targeting), or αDCIR2:OVA (CD8α$^-$ DC targeting) conjugated antibodies in the presence of LPS at day 0. At each indicated time point after the immunization, lymph node (LN) or spleen (SP) cells were prepared and Tfh cells gated from the DO11.10$^+$CD4$^+$CD44$^+$ T cells were analyzed. Proliferation of OVA specific DO11.10$^+$Thy1.1$^+$CD4$^+$ T cells was analyzed by CFSE dilution assay. Data are representative of two independent experiments. (n=3-4 per group).

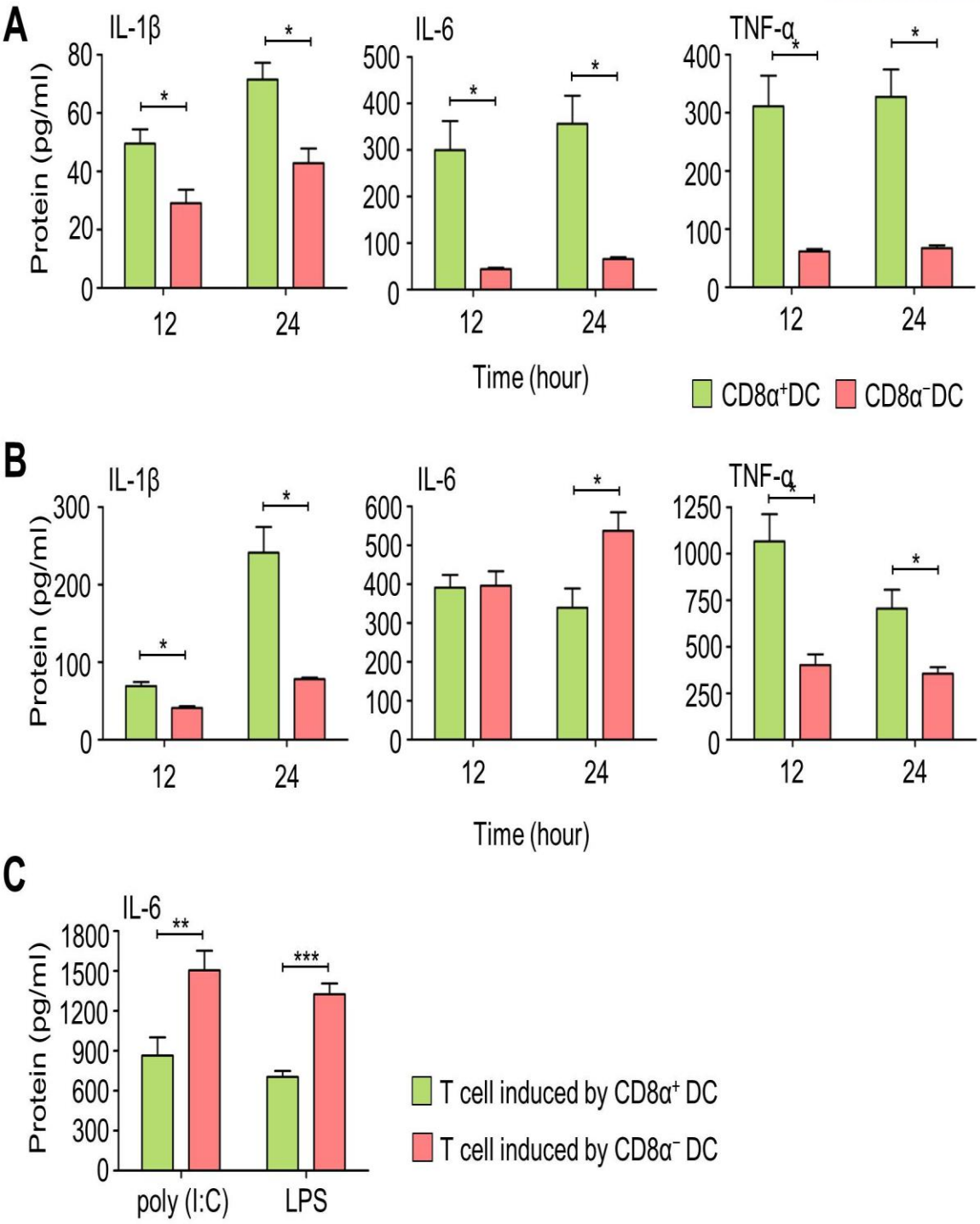

Figure 3-6. IL-6 cytokine from the DC subsets or the DC subset induced CD4$^+$ T cells. (**A** and **B**) ELISA analysis of the cytokines, IL-1β, IL-6, TNF, secreted from the two DC subsets stimulated either with poly (I:C) (**A**) or LPS (**B**) for 12 or 24 hours. * $P < 0.05$. Data represent mean ± s.e.m. of three independent experiments (**A** and **B**). (**C**) OT-II OVA specific Vα2$^+$CD4$^+$ T cells were co-cultured with each DC subset in the presence of OVA peptide (323-339) either with poly (I:C) or LPS. After 3 days of the co-culture, the level of IL-6 cytokine in the supernatant was measured by ELISA. ** $P < 0.01$.

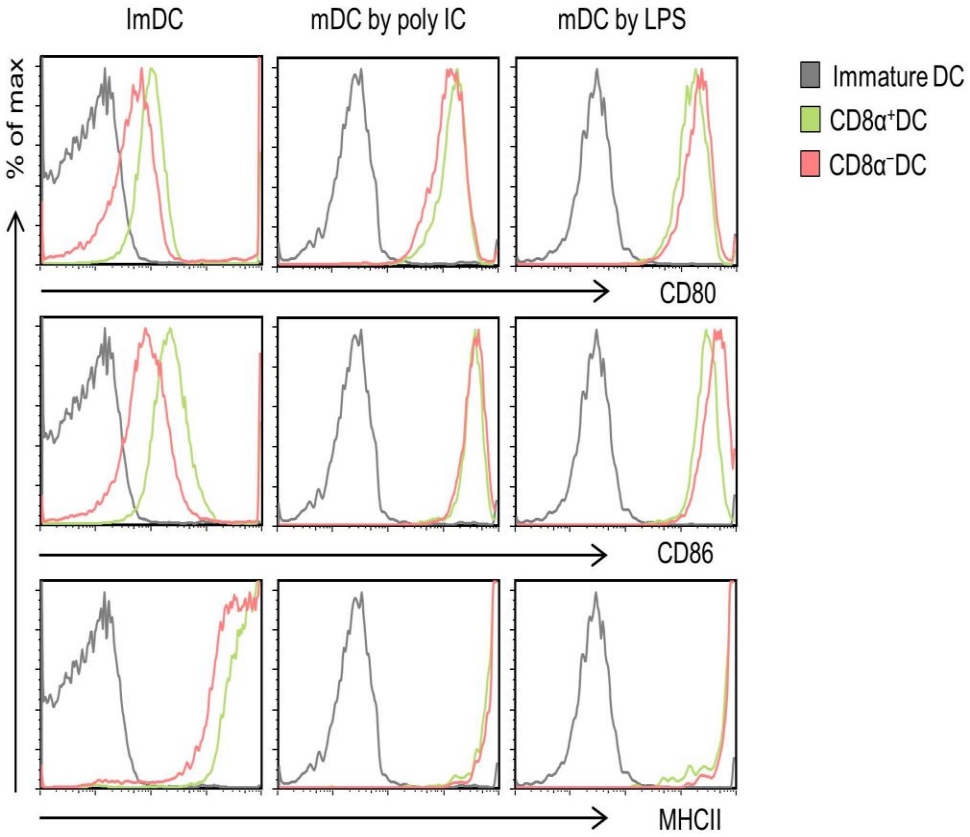

Figure 3-7. Maturation markers on the DC subsets. Maturation markers on the two DC subsets. The two DC subsets were stimulated either with poly (I:C) or LPS for 0 (immature) or 24 hours (mature). Representative histograms of CD80, CD86 or MHCII on the DC subsets. Data are representative of three independent experiments.

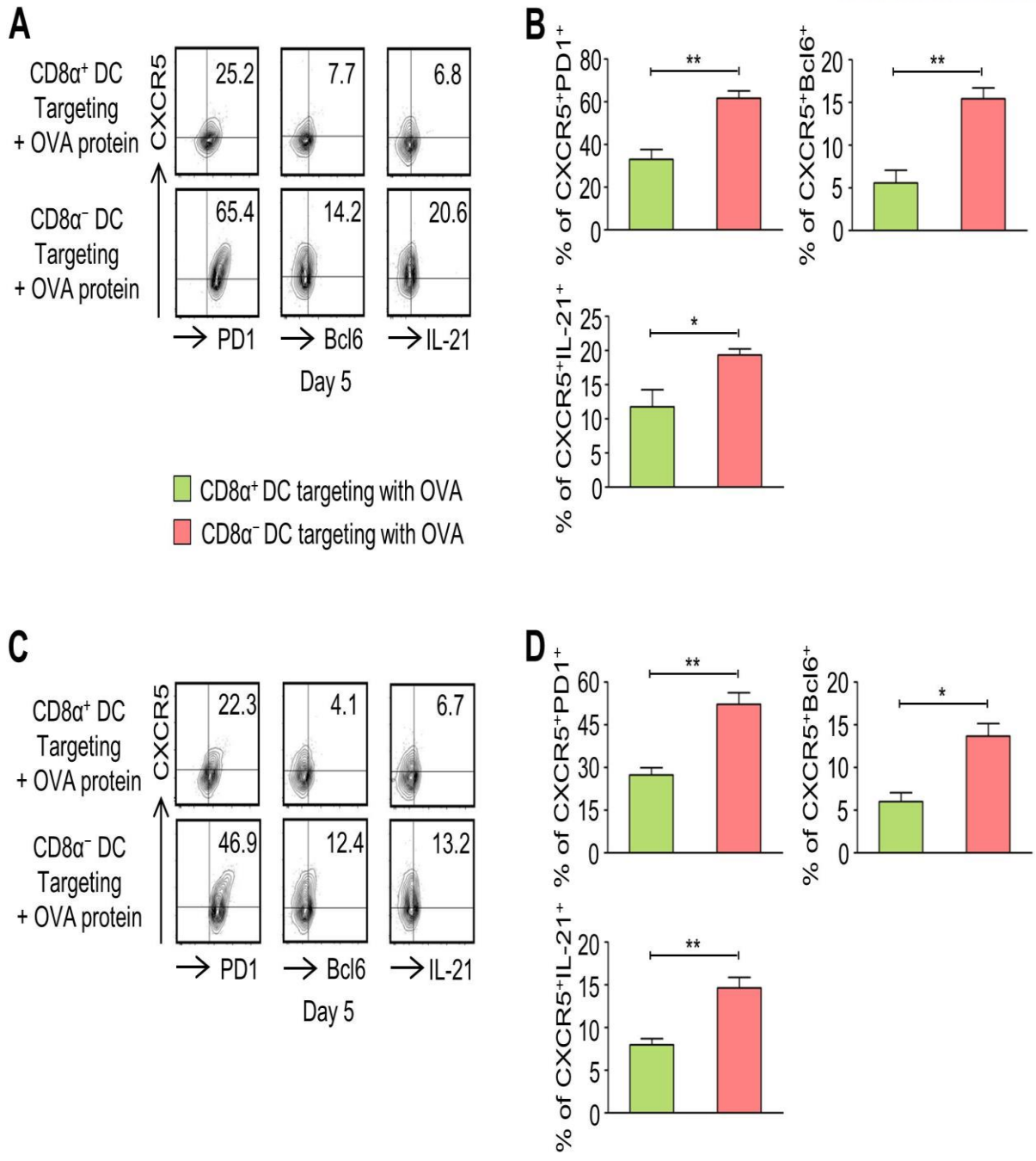

Figure 3-8. **CD8α$^-$ DCs specialize in inducing Tfh cells *in vivo***. OVA specific DO11.10$^+$CD4$^+$ T cells were adoptively transferred to naive Balb/c mice at day -1, and were immunized s.c. either with αDEC:OVA (CD8α$^+$ DC targeting) or αDCIR2:OVA (CD8α$^-$ DC targeting) conjugated mAbs in the presence of soluble OVA protein + LPS. 5 days after the immunization, lymph node cells (**A** and **B**) or spleen cells (**C** and **D**) were prepared and Tfh cells gated from the DO11.10$^+$CD4$^+$CD44$^+$ T cells were analyzed. (**A** and **C**) Representative FACS plots of CXCR5$^+$PD1$^+$, CXCR5$^+$Bcl6$^+$, or CXCR5$^+$IL-21$^+$ Tfh cells. (**B** and **D**) Data represent mean ± s.e.m. of three independent experiments described in (**A** and **C**), respectively. * $P < 0.05$, ** $P < 0.01$. (n=3 per group).

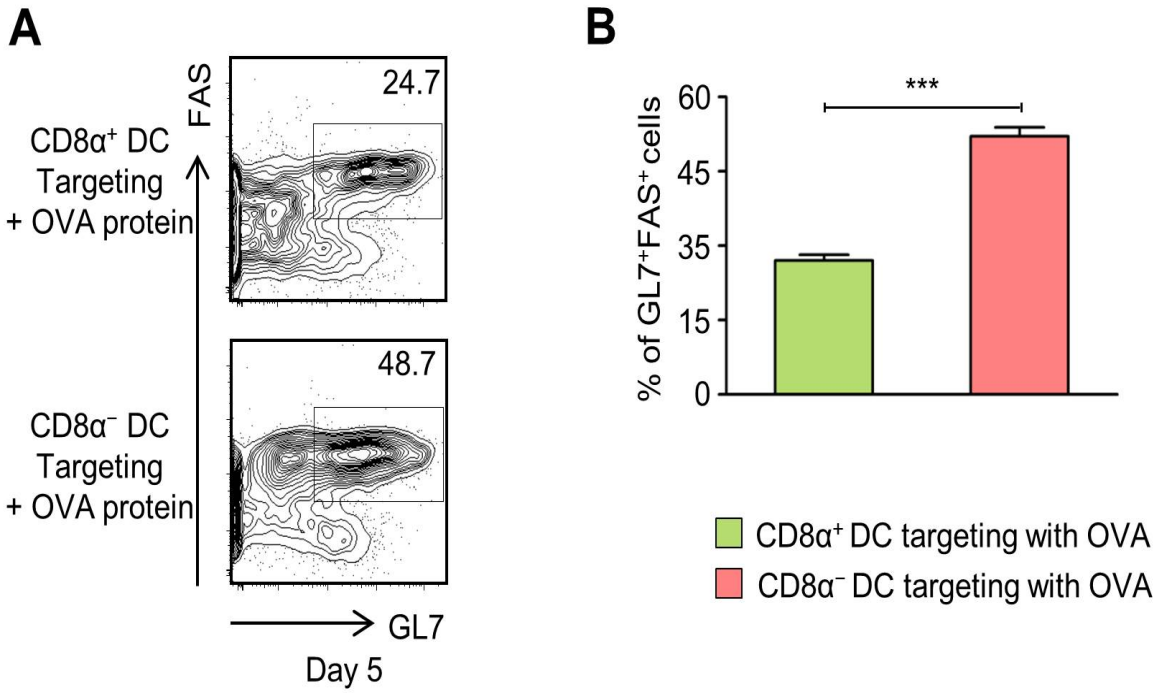

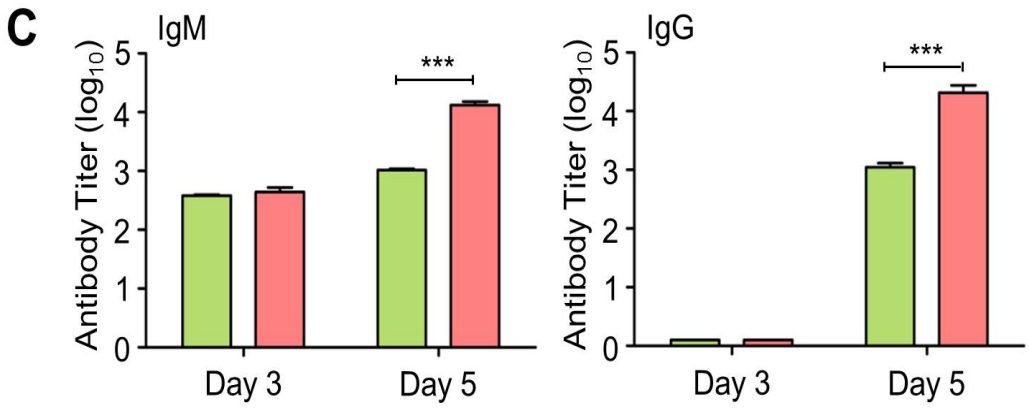

Figure 3-9. **CD8α^- DCs are superior in generating efficient humoral immune responses *in vivo***. OVA specific DO11.10$^+$CD4$^+$ T cells were adoptively transferred to naive Balb/c mice at day -1, and were immunized s.c. either with αDEC:OVA (CD8α$^+$ DC targeting) or αDCIR2:OVA (CD8α$^-$ DC targeting) conjugated mAbs in the presence of soluble OVA protein + LPS. At each indicated time point after the immunization, data were analyzed. (**A**) Representative FACS plots of GL7$^+$FAS$^+$ GC B cells gated from CD19$^+$IgD$^-$ splenocytes. (**B**) Data represent mean ± s.e.m. of three independent experiments described in (A). (**C**) ELISA analyses of OVA-specific serum IgM or IgG antibodies. Data represent mean ± s.e.m. of three independent experiments. *** $P < 0.001$. (n=3 per group).

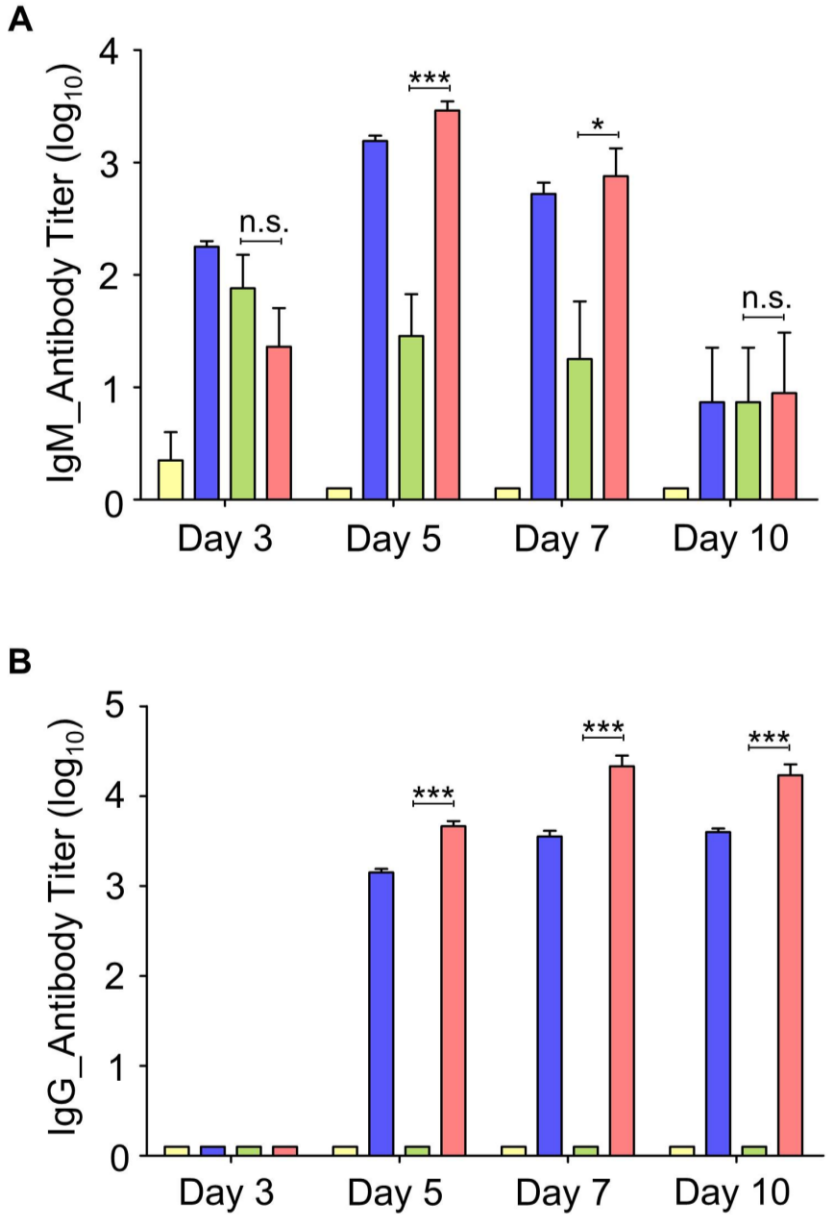

Figure 3-10. Efficient humoral immune responses are induced by CD8α$^-$ DCs *in vivo*. (**A** and **B**) OVA specific DO11.10$^+$Thy1.1$^+$CD4$^+$ T cells were adoptively transferred to naive Thy1.2$^+$ Balb/c mice at day -1, ans were immunized s.c. either with PBS, OVA protein (OVA protein), αDEC:OVA (CD8α$^+$ DC targeting), or αDCIR2:OVA (CD8α$^-$ DC targeting) conjugated mAbs in the presence of LPS. At the indicated time point, ELISA analyses of OVA−specific serum IgM antibodies were performed. Data represent mean±s.e.m. of four independent experiments. * $P < 0.05$, *** $P < 0.001$, n.s. (not significant). (n=4 per group).

References

BALLESTEROS-TATO, A. & RANDALL, T. D. 2014. Priming of T follicular helper cells by dendritic cells. *Immunol Cell Biol,* 92**,** 22-7.

BREITFELD, D., OHL, L., KREMMER, E., ELLWART, J., SALLUSTO, F., LIPP, M. & FORSTER, R. 2000. Follicular B helper T cells express CXC chemokine receptor 5, localize to B cell follicles, and support immunoglobulin production. *J Exp Med,* 192**,** 1545-52.

CHAKAROV, S. & FAZILLEAU, N. 2014. Monocyte-derived dendritic cells promote T follicular helper cell differentiation. *EMBO Mol Med,* 6**,** 590-603.

CHAPPELL, C. P., DRAVES, K. E., GILTIAY, N. V. & CLARK, E. A. 2012. Extrafollicular B cell activation by marginal zone dendritic cells drives T cell-dependent antibody responses. *J Exp Med,* 209**,** 1825-40.

CHOI, Y. S., ETO, D., YANG, J. A., LAO, C. & CROTTY, S. 2013. Cutting edge: STAT1 is required for IL-6-mediated Bcl6 induction for early follicular helper cell differentiation. *J Immunol,* 190**,** 3049-53.

CHOI, Y. S., KAGEYAMA, R., ETO, D., ESCOBAR, T. C., JOHNSTON, R. J., MONTICELLI, L., LAO, C. & CROTTY, S. 2011. ICOS receptor instructs T follicular helper cell versus effector cell differentiation via induction of the transcriptional repressor Bcl6. *Immunity,* 34**,** 932-46.

CROTTY, S. 2011. Follicular helper CD4 T cells (TFH). *Annu Rev Immunol,* 29**,** 621-63.

DEENICK, E. K., CHAN, A., MA, C. S., GATTO, D., SCHWARTZBERG, P. L., BRINK, R. & TANGYE, S. G. 2010. Follicular helper T cell differentiation requires continuous antigen presentation that is independent of unique B cell signaling. *Immunity,* 33**,** 241-53.

DO, Y., KOH, H., PARK, C. G., DUDZIAK, D., SEO, P., MEHANDRU, S., CHOI, J. H., CHEONG, C., PARK, S., PERLIN, D. S., POWELL, B. S. & STEINMAN, R. M. 2010. Targeting of LcrV virulence protein from Yersinia pestis to dendritic cells protects mice against pneumonic plague. *Eur J Immunol,* 40**,** 2791-6.

DUDZIAK, D., KAMPHORST, A. O., HEIDKAMP, G. F., BUCHHOLZ, V. R., TRUMPFHELLER, C., YAMAZAKI, S., CHEONG, C., LIU, K., LEE, H. W., PARK, C. G., STEINMAN, R. M. & NUSSENZWEIG, M. C. 2007. Differential antigen processing by dendritic cell subsets in vivo. *Science,* 315**,** 107-11.

ETO, D., LAO, C., DITORO, D., BARNETT, B., ESCOBAR, T. C., KAGEYAMA, R., YUSUF, I. & CROTTY, S. 2011. IL-21 and IL-6 are critical for different aspects of B cell immunity and

redundantly induce optimal follicular helper CD4 T cell (Tfh) differentiation. *PLoS One,* 6**,** e17739.

GATTO, D., WOOD, K., CAMINSCHI, I., MURPHY-DURLAND, D., SCHOFIELD, P., CHRIST, D., KARUPIAH, G. & BRINK, R. 2013. The chemotactic receptor EBI2 regulates the homeostasis, localization and immunological function of splenic dendritic cells. *Nat Immunol,* 14**,** 446-53.

HARDTKE, S., OHL, L. & FORSTER, R. 2005. Balanced expression of CXCR5 and CCR7 on follicular T helper cells determines their transient positioning to lymph node follicles and is essential for efficient B-cell help. *Blood,* 106**,** 1924-31.

HAYNES, N. M., ALLEN, C. D., LESLEY, R., ANSEL, K. M., KILLEEN, N. & CYSTER, J. G. 2007. Role of CXCR5 and CCR7 in follicular Th cell positioning and appearance of a programmed cell death gene-1high germinal center-associated subpopulation. *J Immunol,* 179**,** 5099-108.

IYODA, T., SHIMOYAMA, S., LIU, K., OMATSU, Y., AKIYAMA, Y., MAEDA, Y., TAKAHARA, K., STEINMAN, R. M. & INABA, K. 2002. The CD8+ dendritic cell subset selectively endocytoses dying cells in culture and in vivo. *J Exp Med,* 195**,** 1289-302.

JACQUEMIN, C., SCHMITT, N., CONTIN-BORDES, C., LIU, Y., NARAYANAN, P., SENESCHAL, J., MAUROUARD, T., DOUGALL, D., DAVIZON, E. S., DUMORTIER, H., DOUCHET, I., RAFFRAY, L., RICHEZ, C., LAZARO, E., DUFFAU, P., TRUCHETET, M. E., KHORYATI, L., MERCIE, P., COUZI, L., MERVILLE, P., SCHAEVERBEKE, T., VIALLARD, J. F., PELLEGRIN, J. L., MOREAU, J. F., MULLER, S., ZURAWSKI, S., COFFMAN, R. L., PASCUAL, V., UENO, H. & BLANCO, P. 2015. OX40 Ligand Contributes to Human Lupus Pathogenesis by Promoting T Follicular Helper Response. *Immunity,* 42**,** 1159-70.

JOHNSTON, R. J., POHOLEK, A. C., DITORO, D., YUSUF, I., ETO, D., BARNETT, B., DENT, A. L., CRAFT, J. & CROTTY, S. 2009. Bcl6 and Blimp-1 are reciprocal and antagonistic regulators of T follicular helper cell differentiation. *Science,* 325**,** 1006-10.

KERFOOT, S. M., YAARI, G., PATEL, J. R., JOHNSON, K. L., GONZALEZ, D. G., KLEINSTEIN, S. H. & HABERMAN, A. M. 2011. Germinal center B cell and T follicular helper cell development initiates in the interfollicular zone. *Immunity,* 34**,** 947-60.

KING, C. 2009. New insights into the differentiation and function of T follicular helper cells. *Nat Rev Immunol,* 9**,** 757-66.

LAHOUD, M. H., AHMET, F., KITSOULIS, S., WAN, S. S., VREMEC, D., LEE, C. N., PHIPSON, B., SHI, W., SMYTH, G. K., LEW, A. M., KATO, Y., MUELLER, S. N., DAVEY, G. M., HEATH, W. R., SHORTMAN, K. & CAMINSCHI, I. 2011. Targeting antigen to mouse dendritic cells via

Clec9A induces potent CD4 T cell responses biased toward a follicular helper phenotype. *J Immunol,* 187**,** 842-50.

MA, C. S., DEENICK, E. K., BATTEN, M. & TANGYE, S. G. 2012. The origins, function, and regulation of T follicular helper cells. *J Exp Med,* 209**,** 1241-53.

MCHEYZER-WILLIAMS, M., OKITSU, S., WANG, N. & MCHEYZER-WILLIAMS, L. 2012. Molecular programming of B cell memory. *Nat Rev Immunol,* 12**,** 24-34.

OTTENHOFF, T. H. 2012. New pathways of protective and pathological host defense to mycobacteria. *Trends Microbiol,* 20**,** 419-28.

SCHAERLI, P., WILLIMANN, K., LANG, A. B., LIPP, M., LOETSCHER, P. & MOSER, B. 2000. CXC chemokine receptor 5 expression defines follicular homing T cells with B cell helper function. *J Exp Med,* 192**,** 1553-62.

SHIN, C., HAN, J. A., KOH, H., CHOI, B., CHO, Y., JEONG, H., RA, J. S., SUNG, P. S., SHIN, E. C., RYU, S. & DO, Y. 2015. CD8alpha(-) Dendritic Cells Induce Antigen-Specific T Follicular Helper Cells Generating Efficient Humoral Immune Responses. *Cell Rep,* 11**,** 1929-40.

STEINMAN, R. M. & BANCHEREAU, J. 2007. Taking dendritic cells into medicine. *Nature,* 449**,** 419-26.

TANGYE, S. G., MA, C. S., BRINK, R. & DEENICK, E. K. 2013. The good, the bad and the ugly - TFH cells in human health and disease. *Nat Rev Immunol,* 13**,** 412-26.

TRUMPFHELLER, C., LONGHI, M. P., CASKEY, M., IDOYAGA, J., BOZZACCO, L., KELER, T., SCHLESINGER, S. J. & STEINMAN, R. M. 2012. Dendritic cell-targeted protein vaccines: a novel approach to induce T-cell immunity. *J Intern Med,* 271**,** 183-92.

YI, T. & CYSTER, J. G. 2013. EBI2-mediated bridging channel positioning supports splenic dendritic cell homeostasis and particulate antigen capture. *Elife,* 2**,** e00757.

YOO, J. K., FISH, E. N. & BRACIALE, T. J. 2012. LAPCs promote follicular helper T cell differentiation of Ag-primed CD4+ T cells during respiratory virus infection. *J Exp Med,* 209**,** 1853-67.

Conclusion

Rapidly accumulating data on T follicular helper (Tfh) cells for the last 10 years has enlightened our understanding on T cell-dependent humoral immunity. However, how dendritic cells (DCs) polarize antigen-specific Tfh cells differently from various other $CD4^+$ effector T cell subsets still remain unclear. Here we investigated the unknown intrinsic features of the two distinct myeloid DC subsets, $CD8\alpha^+$ DCs and $CD8\alpha^-$ DCs, and demonstrated an unexplored role of cellular and molecular mechanisms of $CD8\alpha^-$ DCs to promote antigen-specific functional Tfh cell differentiation. In addition, we showed that efficient humoral immune responses were induced by utilizing $CD8\alpha^-$ DCs against various human pathogenic antigens such as *Y. pestis* LcrV, human immunodeficiency virus (HIV) Gag, and hepatitis B surface antigen (HBsAg). This study proposes a new paradigm on Tfh cell research field by elucidating how DCs influence Tfh cell fate providing rationale to enhance humoral immunity. This study suggests that even a small amount of antigen delivered directly to $CD8\alpha^-$ DCs is sufficient to induce fully functional Tfh cells, providing a rationale for targeting the $CD8\alpha^-$ DC subset for efficient DC-based therapies, which will be of great interest to broad readership - including basic scientists and clinicians - interested in regulating humoral immunity for improved vaccine and novel therapy development.

Acknowledgments

석박통합 과정으로 유니스트에 입학하여 벌써 6년하고도 반절이 지났습니다. 막상 이렇게 박사를 졸업하면서 감사의 글을 쓰려고 하니 많은 일들이 주마등처럼 스쳐 지나쳐 갑니다. 그 무엇보다 모든 상황, 환경 속에서 나와 항상 함께 하시며 나의 인생을 인도해 나가시는 하나님께 감사 드립니다. 박사학위를 마치기에 있어서 너무도 감사한 분들이 많습니다. 부족한 저에게 한없이 든든한 버팀목이 되어주신 아버지와 어머니, 저를 항상 응원해주고 격려해 주는 제 반쪽 영지, 이제 막 백일이 지난 너무나 예쁜 아들 주윤이, 미국에서 동생을 열심히 응원하고 있는 형과 형수님, 부족한 사위지만 항상 응원하고 격려해 주시는 장인어른 장모님 참 감사합니다. 비록 지금은 조금 멀리 계시지만, 2009년 가을 처음으로 이 학교에 와서 고 도윤경 교수님을 만나고, 6년여 동안 교수님의 첫 제자로서 참 많은 가르침을 받았던 기억이 스쳐 지나갑니다. 지병에도 불구하고 제자들을 자식처럼 아끼시며 참된 과학자로서 성장 할 수 있도록 사랑과 조언을 아끼지 않으셨던 교수님이 그리워 지는 순간 입니다. 고 도윤경 교수님은 본인의 지병이 악화 됨에도 불구하고 끝까지 제자들의 걱정을 앞서 하셨던 그런 스승님 이셨습니다. 저에게 주셨던 인생의 가르침을 잊지 않는 과학자가 되도록 노력 하겠습니다. 저와 같이 한 실험실의 대학원생으로서 동거 동락했던 한재아 와 최봉서 후배들 에게도 참 고맙습니다. 조금은 부족하고 고집스러운 형을 의지하고 따라와 주었던 동생들에게 참 감사합니다. 같이 실험하고, 밤늦게 통닭과 라면 김밥을 즐겨 먹었던 기억도 머리 속에서 스쳐 지나갑니다. 비록 우리 DISNI Lab의 이름은 사라졌지만, 재아와 봉서도 교수님의 가르침을 이어받아 부끄럽지 않는 제자로, 과학자로 성장하기를 기도합니다. 제가 학위논문을 잘 마무리 하게 도와주시고, 저의 든든한 후견인이 되어 주신 류성호 교수님께도 감사의 말씀을 드립니다. 같은 실험실에서 연구원으로 계시면서 여러 도움을 주셨던 라재선, 김아라 선생님 에게도 감사의 말을 전하고 싶습니다. 그리고, 제가 박사과정을 잘 마무리 할 수 있게 저를 실험실에 받아주시고 연구를 지속하게 도와주신 현재 저의 지도교수님이신 조윤경 교수님의 배려와 지원에도 진심으로 감사 드립니다. 또한 제가 박사졸업을 잘 하기까지 조언을 아끼지 않으신, 강세병 교수님, 강병헌 교수님, 고명곤 교수님께도 감사의 말씀을 드립니다. 실험실에 선배가 없어 실험적으로 어려워하고 있을 때 많은 조언과 도움을 아끼지 않으신 박혜경 박사님께도 참 고맙다는 말을 전하고 싶습니다. 그리고 갑자기 조윤경 교수님

실험실 들어왔음에도 불구하고, 선배라고 불러주며 많은 도움을 주웠던 현 실험실 사람들에게도 많은 감사의 말씀을 전하고 싶습니다. 비록 일일이 언급은 못했지만, 제가 박사학위를 하며 지냈던 7 년여 동안 만난 많은 고마운 사람들에게도 감사의 말씀을 전하고 싶습니다. 이제 막 박사를 졸업하여 앞으로 배우고 헤쳐 나가야 할 일이 더 많겠지만, 유니스트 에서 받은 가르침을 잊지 않고 전달할 수 있는 과학자가 되도록 노력하겠습니다. 감사합니다.